THESIS ERRATA

Page 4 Line 20, " ... where $Z > 0$ fluid α and $Z < 0$ outside fluid α ... "

should read: " ... where $Z < 0$ in fluid α and $Z > 0$ outside fluid α ... "

Page 12 Line 3,

$$"V^{\beta} = \frac{1}{3}\omega[a^3 - (R^{\beta})^3]" \qquad (2.21)$$

should read:

$$"V^{\beta} = \frac{1}{3}\omega[(R^{\beta})^3 - a^3]" \qquad (2.21)$$

Page 38

$$"a = (a_o^3 + 3a_o \sum_{n=1}^{N} (2_n + 1)^{-1} \; a_n^2)^{1/3}"$$

and

$$"a \simeq a_o(1 + \sum_{n=1}^{N} (2_n + 1)^{-1} \; \frac{a_n^2}{a_o^2})" \qquad (3.6)$$

$"(2_n + 1)^{-1}"$

should read: $"(2n + 1)^{-1}"$

Page 51

$$"P_E = -\frac{Q_2}{8\pi a_o}" \qquad (3.34)$$

should read:

$$"P_E = \frac{-Q^2}{8\pi a_o}"$$

Page 123 Equation (B-7) should read:

$$\frac{t_{n-2,\,1-\gamma} S}{\sqrt{\sum_{j=1}^{N} (x_j - \bar{x})^2}} \qquad (B\text{-}7)$$

SURFACE TENSION MEASUREMENTS ON PURE LIQUID IRON AND NICKEL

SURFACE TENSION MEASUREMENTS ON PURE LIQUID IRON AND NICKEL BY THE OSCILLATING DROP TECHNIQUE

By

MICHAEL FRASER, B.Sc.

A Thesis

Submitted to the School of Graduate Studies

in Partial Fulfilment of the Requirements

for the Degree

Master of Science

McMaster University

May 1970

MASTER OF SCIENCE (1970)
(Metallurgy)

McMASTER UNIVERSITY
Hamilton, Ontario.

TITLE: Surface Tension Measurements on Pure Liquid Iron and Nickel by the Oscillating Drop Technique

AUTHOR: Michael Edward Fraser, B.Sc. (McMaster University)

SUPERVISOR: Professor W-K Lu

NUMBER OF PAGES: xi, 130

SCOPE AND CONTENTS:

The theory which relates the natural frequency of oscillation of a drop and its surface tension was investigated. Based on this, a new experimental technique of measuring surface tension was developed. The surface tension of pure iron and pure nickel were measured over the temperature ranges, 1550-1650°C and 1475-1625°C, respectively.

ACKNOWLEDGEMENTS

The author wishes to express his gratitude to Dr. W.K. Lu for his supervision and for his helpful and patient assistance during the course of this study.

The author wishes also to express his appreciation of the generous financial support which was provided by the American Iron and Steel Institute and to the National Research Council for the award of an N.R.C. Scholarship.

Grateful acknowledgments are due to the technical staff and graduate students of the Department of Metallurgy and Material Science at McMaster whose help has been invaluable.

Many thanks are given to Mrs. Barbara O'Connor for the excellent typing of this thesis and to Mr. Martin van Oosten and Mr. Don Wilson for their capable assistance with the technical drawings and photographs.

TABLE OF CONTENTS

TABLE OF APPENDICES

LIST OF TABLES

LIST OF ILLUSTRATIONS

CHAPTER I

INTRODUCTION

The surface tension of liquid metals has been found to be very susceptible to small amounts of adsorbed oxygen and sulphur. It is thought, then, that surface tension can be used as a tool in studies of the initial rates of oxidation of iron if changes in surface tension with concentration can be successfully monitored. It is the purpose of this thesis to develop a technique for measuring surface tension of liquid metals at high temperatures which will be suitable for the above purpose.

The measurement of surface tension of liquid metals at high temperatures (1500-2000°C) has always been a difficult task and was achieved only with extremely careful design and control of the experiments. The most reliable measurements to date have been made with static methods, notably the sessile drop technique. Nevertheless, experimental difficulties have limited investigation and most workers have been content with high temperature surface tension measurements at a single temperature.

The method to be proposed and developed in this thesis is a dynamic method of measuring surface tension. The oscillations of a vibrating drop of molten metal suspended in an electromagnetic field are recorded by means of high

speed motion pictures and the frequency determined from these films. This frequency is then related to surface tension through an equation developed by Rayleigh. The materials studied are pure iron and pure nickel.

Surface tension is defined in terms compatible with the proposed experimental conditions. The existing methods of high temperature surface tension measurements are reviewed and a literature survey concerning previous measurements of the surface tension of pure liquid iron and nickel has been made. The theory of oscillating fluid drops is also discussed in detail with specific reference to the proposed levitation melting system.

The experimental apparatus and techniques are described and results of experiments from 1550°C to 1650°C for iron and, from 1475°C to 1625°C for nickel, are reported. By means of statistical analysis of the experimental results certain conclusions are made about the validity of some of the assumptions in the theory of oscillating fluid drops as applied to this system. The experimental errors are evaluated and the measured values of surface tension compared to previously measured values within the limits of these errors.

CHAPTER II.

LITERATURE REVIEW

2.1 DEFINITION OF SURFACE TENSION

2.1.1 INTRODUCTION

Surface tension, γ, is a parameter associated with the interface defined by applying fundamental principles to a system consisting of coexisting fluid phases. It may be defined in terms of force balance (or mechanical equilibrium), energy balance (or first law of thermodynamics) or in terms of the second law of thermodynamics. The units of surface tension are force per unit length (or energy per unit area), internal energy per unit area, and Helmholtz free energy per unit area, respectively. Although the physical meaning of surface tension can be conceptually different, the experimental values evaluated and based on different definitions are indistinquishable under practical conditions.

2.1.2 NATURE OF THE INTERFACE BETWEEN TWO FLUID PHASES

For any system composed of two or more phases, there exists an interface region between any two phases which contributes an important factor to the mechanical and thermodynamic behaviour of the system. The most important phenomenon associated with this interface is the surface tension. In order to actually define the surface tension, however, the nature of the interface must be established.

From a simple and rather intuitive point of view the interface may be considered as a uniformly stretched membrane, having no thickness and separating two fluid phases. This definition is however, based on the model that there is a sharp discontinuity of fluid properties at the interface. From the molecular point of view, there is no such discontinuity, but a continuous change in structure across an extremely small interface region or boundary zone[1]. In order to avoid the necessity of assigning some thickness to the interface region, it has been found useful to relate the properties of this region to an imaginary surface called the dividing surface (Gibb's Surface)[1]. This is placed in the interface zone such that it is normal to the density gradient in the zone and is of constant density and under isothermal conditions. The dividing surface is constructed in such a way, that, if the change in density across the interface was discontinuous, the mean number of molecules in the interface region is unchanged from the actual physical situation. Letting Z be the direction normal to the dividing surface (which may be planar or spherical) where $Z>0$ in fluid α and $Z<0$ outside fluid α (as per Fiqure 1) we can define the dividing surface such that[1]

$$\int_{-a}^{b} n\,dz = a\,n_i^{\alpha} + b n_i^{\beta} \qquad (2.1)$$

where n_i^{α} is the molecular density of species i (molecules per unit volume) for $z<-a$ and n_i^{β} is the corresponding quantity for $z>b$.

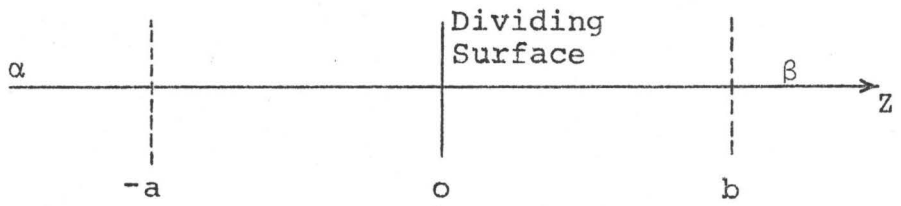

Figure 1. Liquid Surface Model[1]

Another way of looking at this is to let N_i^α and N_i^β be the number of molecules in the bulk phases α and β respectively[2]. Thus N_i^α is the product of n_i^α and V^α, the volume of the bulk phase α and similarly N_i^β is equal to $n_i^\beta V^\beta$. In general, however, N_i, the total number of molecules of species i in the system does not always equal the sum of N_i^α and N_i^β but rather[3]

$$N_i = N_i^\alpha + N_i^\beta + N_i^s \qquad (2.2)$$

where N_i^s is the contribution due to molecules adsorbed at the interface.

For a single component system, the dividing surface may be chosen so that N_i^s vanishes, this particular choice of dividing surface being called the equimolecular dividing surface. This is identical to the dividing surface defined by (2.1).

N_i^s is not always zero since its value will depend on the location of the imaginary dividing surface. It is the number of molecules of species i adsorbed at the interface and is designated a superficial quantity. All such superficial

quantities associated with a particular choice of dividing surface will be given the superscript s in the following text.

It can be shown, in much the same fashion, that there is a similar contribution of the interface associated with all thermodynamic quantities describing the complete system for a given choice of dividing surface. Hence, we may have the following equations to define the superficial quantities associated with the dividing surface

$$F = F^{\alpha} + F^{\beta} + F^{s} \tag{2.3}$$

$$U = U^{\alpha} + U^{\beta} + U^{s} \tag{2.4}$$

$$S = S^{\alpha} + S^{\beta} + S^{s} \tag{2.5}$$

where F, U and S are the Helmholtz free energy, internal energy and entropy, respectively of the system and since $F = U - TS$, also we have for isothermal conditions in the system,

$$F^{s} = U^{s} - TS^{s} \tag{2.6}$$

2.1.3 THERMODYNAMIC DEFINITION OF SURFACE TENSION FOR A PLANAR INTERFACE

The system shown in Figure 2 consists of a rectangular vessel containing two phases, α and β separated by a planar interface which is normal to one of the edges of the container[3].

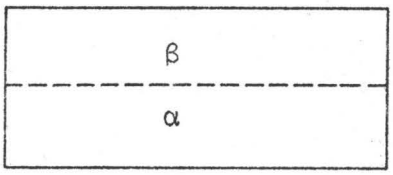

Figure 2. Two phase System with Planar Interface

If the area A is changed via a reversible and isothermal displacement of the side walls of the vessel(walls perpendicular to the interface) by the amount dA and the system is in mechanical equilibrium with pressure p, then the work done in this process involves two components. These are the pdV work to increase the volume by dV and the additional work required to increase the interfacial area by dA. The latter work term will be denoted by $-\gamma dA$. The total reversible work done by the system is thus $pdV-\gamma dA$. The system is then returned reversibly to its original volume by moving the walls parallel to the interface, the work done in this case being $-pdV$, with no change in interfacial area. At the finish of this cycle, the system is at its original volume, pressure, temperature, and composition with the only change being in the area A, which has been enlarged by the amount of dA. The work done, therefore, on the system to increase the area by dA is equal to γdA, where γ is the proportionality constant denoting the work done per unit interfacial area on the system and we shall call γ, the surface tension[3].

The defining equation for surface tension is given in the expression for the work done by the system, dW, for a volume increment, dV and interfacial area increment, dA. Thus,

$$dW = pdV - \gamma dA \qquad (2.7)$$

No mention has been made so far of the location of a dividing surface and it is seen from (2.7) that the surface tension of a

planar interface as defined here is independent of the arbitrary positioning of such a surface. It is also evident that, as defined in (2.7), surface tension must be greater than zero or the interface would increase its' area spontaneously. That is to say, a planar interface is stable only when γ is positive[3].

Since the internal energy, U, of a system must increase interfacial area, we may write the first law of thermodynamics and equation (2.7) as

$$dQ = dU + pdV - \gamma dA \tag{2.8}$$

from which it is easily seen that

$$\gamma = \left(\frac{\partial Q}{\partial A}\right)_{U,V} \tag{2.9}$$

or

$$\gamma = \left(\frac{\partial U}{\partial A}\right)_{V,\ \text{adiabatic}} \tag{2.10}$$

where dQ is the heat absorbed by the system for the infinitesimal interfacial area change, dA, under constant temperature and volume in a closed system. These relations hold even if the system is not in thermodymanic equilibrium so long as it is maintained in mechanical equilibrium with pressure p.

It is possible to arrive at another definition of surface tension for the same system as above if thermodynamic equilibrium is assumed, in terms of the second law of thermodynamics, dQ becomes TdS for a reversible transformation, where dS is the entropy change of the system. Equation (2.8) now becomes

$$dE = TdS - pdV + \gamma dA \tag{2.11}$$

or in terms of the Helmholtz free energy, F,

$$dF = -pdV - SdT + \gamma dA \tag{2.12}$$

and for an open system

$$dF = -pdV - SdT + \gamma dA + \sum_{i=1}^{x} \mu_i dN_i \tag{2.13}$$

where x is the number of species, μ_i is the chemical potential per molecule of species i and is constant throughout the system since chemical equilibrium has been assumed.

Assuming the free energy, F, is a known function of volume, temperature, interface area and number of molecules of each species and the surface tension, γ. One of the ways to define γ in terms of (2.13) is

$$\gamma = \left(\frac{\partial F}{\partial A}\right)_{T,\ V,\ N'} \tag{2.14}$$

where N' is the set of numbers $N_1, N_2, \ldots, N_x$.

The relationship between the superficial quantities associated with the interface (Sec. 2.1.2) and surface tension can now be developed. At constant temperature, pressure, composition and vessel height, the Helmholtz free energy, F, is a homogeneous function of the first degree in V, N, and A.[3] Applying Euler's Theorem we find

$$F = \sum_{i=}^{x} \mu_i N_i - pV + \gamma A \tag{2.15}$$

and for each of the two bulk phases, α and β , (Fig. 2)

$$F^{\alpha} = \sum_{i=1}^{x} \mu_i N_i^{\alpha} - pV^{\alpha} \tag{2.16}$$

$$F^{\beta} = \sum_{i=1}^{x} \mu_i N_i^{\beta} - pV^{\beta} \tag{2.17}$$

Subtracting (2.16), and (2.17) from (2.15) and using (2.2), (2.3) and the additivity of volumes, we get

$$F^s = \sum_{i=1}^{x} \mu_i N_i^s + \gamma A \qquad (2.18)$$

It has been shown (2.1.2) that N_i^s and hence F^s are dependent upon the placement of the dividing surface. Thus we choose the dividing surface to make $\sum_{i=1}^{x} \mu N_i^s$ vanish and (2.18) becomes

$$F^s = \gamma A \qquad (2.19)$$

This choice of dividing surface is identical with the equimolecular dividing surface described in 2.1.2 for a single component system. Thus we have a new definition of surface tension as given in (2.19) such that surface tension is equal to the superficial density of the Helmholtz free energy[4]. This applies only for this choice of dividing surface and only for the system maintained in thermodynamic equilibrium.

2.1.4 THERMODYNAMIC DEFINITION OF SURFACE TENSION FOR A SPHERICAL INTERFACE

In this thesis, we shall be concerned with the measurement of the surface tension of a droplet of molten metal under constant total pressure and constant vapour pressure. Thus, it is necessary to look at the difference in the definition of surface tension for a spherical interface separating two phases. The development of the definition after Ono and Kondo[6] follows the same fundamental line of argument as that described in 2.1.3 but the definition for the case of mechanical equilibrium is somewhat different.

The system shown in Figure 3 is a closed system consisting of two phases contained in a conical vessel (in order to simplify the mathematical treatment) separated by a spherical interface layer. The vessel extends from $r = R^{\alpha}$ to $r = R^{\beta}$ ($R^{\beta} > R^{\alpha}$) the extremities of the vessel being the solid line in Figure 3[5]. W and r are the solid

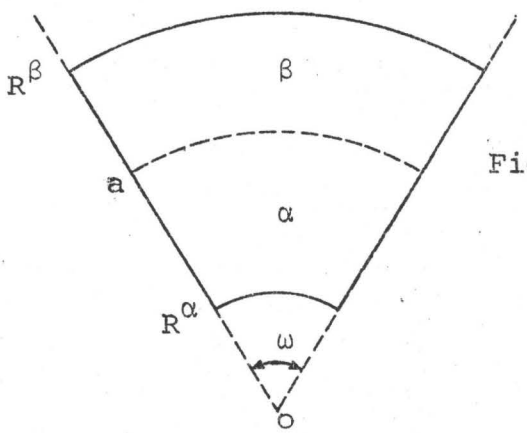

Figure 3. Two phase System with Spherical Interface

angle of the cone and the radial coordinate of the cone, respectively. The origin of r is at the apex of the cone which is also the centre of curvature of the spherical interface and the extremities of the vessel. As in 2.1.3, the system is composed of x independent components and is under the influence of no external fields. The intensive properties are thus dependent upon r, i.e. temperature need not be a constant throughout the system in the present case of mechanical equilibrium.

Letting r = a be the location of the dividing surface we have the total volume V composed of two parts, namely,

V^{α} and V^{β} where[5]

$$V^{\alpha} = \frac{1}{3}\omega\,[a^3 - (R^{\alpha})^3] \tag{2.20}$$

$$V^{\beta} = \frac{1}{3}\omega\,[a^3 - (R^{\beta})^3] \tag{2.21}$$

The dividing surface has an area A where

$$A = \omega\, a^2 \tag{2.22}$$

However, unlike the planar case, the pressure in the interior of phase α, p^{α} can not equal the pressure in the interior of phase β, p^{β} , under the assumption of mechanical equilibrium. p^{α} and p^{β} must, however, be uniform within their respective phases. This restriction is valid as long as the spherical droplet is sufficiently large to have homogeneous bulk properties, i.e., the interface region must not be a large proportion of the total radius of the drop[5].

In a manner similar to that used for the planar case, we will suppose that the solid angle ω is increased infinitesimally by $d\omega$ through a reversible and isothermal displacement of the side walls of the vessel, all other factors being kept constant. The work done by the system to affect this change may be said to be equal to $-\eta d\omega$. As in 2.1.3 this work involves two components : the pdV work, which is $p^{\alpha}dV^{\alpha} + p^{\beta}dV^{\beta}$ and the additional work, $-\gamma dA$, to increase the interfacial area by dA. Thus the total work dW is given by[5]

$$dW = -\eta d\omega = p^{\alpha}dV^{\alpha} + p^{\beta}dV^{\beta} - \gamma dA \tag{2.23}$$

Mathematically speaking, the $-\gamma dA$ term in (2.23) can be considered as a correction term added to the effects of the volume change to make up dW. $-\gamma dA$ thus may be said to account

for the unknown effects arising out of the existence of the interface region. The coefficient γ of this work term may be regarded as that work done on the system associated with a unit increase in area of the dividing surface of a given curvature, as done in 2.1.3. This suggests that the dividing surface may be looked at as if it were a simple membrane of zero thickness and radius, a, separating the phases α and β with a uniform tension, γ, in all directions on the membrane. Thus, γ, as defined by (2.23) can be considered as the surface tension of a spherical interface.

Differentiating (2.20), (2.21), (2.22) and substituting into (2.23) we find[6]

$$\gamma = \frac{1}{3} a (p^{\alpha} - p^{\beta}) + \frac{K}{a^2} \tag{2.24}$$

where $$K = \eta + \frac{1}{3} p^{\beta} (R^{\beta})^3 - \frac{1}{3} p^{\alpha} (R^{\alpha})^3 \tag{2.25}$$

and where[8]

$$\eta = (\frac{\partial F}{\partial \omega})_{R^{\alpha}, R^{\beta}, T, N} \tag{2.26}$$

Differentiating (2.24) with respect to a,[6]

$$\gamma + \frac{1}{2} a [\frac{\partial \gamma}{\partial a}] = \frac{1}{2} a (p^{\alpha} - p^{\beta}) \tag{2.27}$$

On differentiating (2.27), we would obtain an expression containing the quantity $[\frac{\partial \gamma}{\partial a}]da$. This represents the change in surface tension due to the mathematical displacement of the dividing surface by da, maintaining all physical quantities in the system and all external constraints constant. This is not equivalent to the change in γ due to an increase in the radius of curvature of the physical interface layer since a

in this case refers to the radius of curvature of the dividing surface. The surface tension of a spherical interface as defined by (2.23) is, therefore, not independent of the choice of dividing surface[7].

The particular dividing surface to be chosen here is that which will result in the disappearance of the term $[\frac{\partial \gamma}{\partial a}]$ from (2.27). The radius of this surface is denoted as a^s (where the subscript s refers to any quantity associated with this surface) and is defined by[6]

$$[\frac{\partial \gamma}{\partial a}]_{a=a^s} = 0 \qquad (2.28)$$

This dividing surface is termed the surface of tension. Equation (2.27) reduces, now, to

$$p^\alpha - p^\beta = \frac{2\gamma_s}{a_s} \qquad (2.29)$$

Equation (2.29) is a familar relation for any system containing a spherical interface, and in fact may be derived from a very simple model, that of a uniformly stretched membrane, having no thickness and representing the interface separating two fluid phases. We then define a spherical interface of radius a, separating a fluid, α, exerting a pressure p^α, inside the membrane and a fluid, β, exerting a pressure p^β, outside the membrane. Assuming mechanical equilibrium, (that is to say, the net force acting on the membrane is zero), the equation (2.29) is easily derived[8].

Substituting (2.24) into (2.29) and eliminating K, we obtain[7]

$$\gamma = \frac{a_s^2 \gamma_s}{3a^2} + \frac{2\gamma_s a}{3a_s} \qquad (2.30)$$

It can be shown from (2.30), that, for any dividing surface located within the interface layer, γ is very nearly equal γ^s (γ_s is the minimum value of γ, as seen from (2.30), $\gamma = \gamma_s$ at $a = a_s$) the minimum value of γ, as long as a_s is large compared to interface thickness. White[13] also derives the surface curvature dependence and shows there is no significant effect on surface tension until the radius of curvature approaches the value of interface thickness. Thus, macroscopically, surface tension is virtually independent of the choice of dividing surface. The preceding analysis is valid for a system such that the subsystems are not necessarily in thermodynamic equilibrium with one and other since no such restriction has been assumed.

The assumption of thermodynamic equilibrium leads to an exactly parallel development of the relationship between superficial Helmholtz free energy per unit area and surface tension as that done in 2.1.3. Recalling (2.19) we have

$$F^s = \gamma A \qquad (2.19)$$

This relation, then, holds true for any system in thermodynamic equilibrium containing a planar or spherical interface as long as the dividing surface is the equimolecular dividing surface.

Ono and Kondo[10] and White[13] also deal extensively with surface tension on a molecular basis using the methods

of irreversible thermodynamics, statistical mechanics and quantum statistical mechanics. However, the definitions given above are the most appropriate to the problem at hand, that of actually measuring the surface tension of molten iron with a specimen of macroscopic size.

2.1.5 TEMPERATURE DEPENDENCE OF SURFACE TENSION

The Helmholtz free energy for the bulk phases, α and β (Figure 2) for the case of a planar interface are given by

$$dF^{\alpha} = -pdV^{\alpha} - S^{\alpha}dT + \sum_{i=1}^{x} \mu_i \, dN_i^{\alpha} \tag{2.31}$$

$$dF^{\beta} = -pdV^{\beta} - S^{\beta}dT + \sum_{i=1}^{x} \mu_i \, dN_i^{\beta} \tag{2.32}$$

Subtracting (2.31), and (2.32) from (2.13) and employing (2.2), (2.3) and (2.13) a corresponding relation for the interface is found to be

$$dF^{s} = -S^{s}dT + \gamma dA + \sum_{i=1}^{x} \mu_i \, dN_i^{s} \tag{2.33}$$

Differentiating (2.18) and using (2.33), we arrive at the Gibbs adsorption equation (2.34) for a planar interface in its general form.

$$Ad\gamma + S^{s}dT + \sum_{i=1}^{x} N_i^{s} \, d\mu_i = 0 \tag{2.34}$$

Dividing by A and noting that N_i^{s}, S^{s} and U^{s} are proportional to area, (2.34) may be written as[11]

$$d\gamma + \sigma \, dT + \sum_{i=1}^{x} \Gamma_i' \, d\mu_i = 0 \tag{2.35}$$

where σ is the superficial density of entropy $(\frac{S^{s}}{A})$ and Γ_i is the superficial number density of the molecules of species i.

Since by definition,

$$\left(\frac{\partial \mu i}{\partial T}\right)_{x^\alpha} = -s_i^\alpha + v_i^\alpha \left(\frac{\partial P}{\partial T}\right)_{x^\alpha} \tag{2.36}$$

where x^α refers to the set of mole fractions of species i; $x_1, x_2, x_3 \ldots, x_x$ we can obtain from (2.35) and (2.36),

$$\left(\frac{\partial \gamma}{\partial T}\right)_{x^\alpha} = -\sigma + \sum_{i=1}^{x} \Gamma_i \left(s_i^\alpha - v_i^\alpha \left(\frac{\partial p}{\partial T}\right)_{x^\alpha} \right) \tag{2.37}$$

The temperature dependence of surface tension is thus a function of the superficial density of the entropy, σ, and the superficial number density of molecules of species i adsorbed at the interface. It can be shown[12] that a similar temperature dependence exists for the spherical interface.

In the case of pure liquids, it can be shown[11, 12] that, for both planar and spherical interface, if the equimolecular dividing surface is selected, then (2.37) reduces to

$$\frac{\partial \gamma}{\partial T} = -\sigma \tag{2.38}$$

It will be noted that the equimolecular dividing surface is identical to the choice of dividing surface chosen under the conditions of thermodynamic equilibrium (2.1.3) and thus the simplification for temperature dependence given by (2.38) is only valid for systems in thermodynamic equilibrium. Thus, although (2.37) is valid for any choice of dividing surface, under conditions of the thermodynamic equilibrium the magnitude and the sign of the temperature dependence, $\frac{\partial \gamma}{\partial T}$, are functions of the choice of dividing surface.

As pointed out previously, the mechanical definition of surface tension is expressed in terms of energy per unit area rather than free energy per unit area as above. Recalling Equation (2.8)

$$dQ = dU + pdV - \gamma dA \tag{2.8}$$

the following relation is seen to hold

$$\gamma = -\left(\frac{\partial Q}{\partial A}\right)_{U,V} \tag{2.39}$$

However, by the second law of thermodynamics $dQ = TdS$ and hence, by differentiation of (2.39) with respect to T we obtain

$$\frac{\partial \gamma}{\partial T} = -\left(\frac{\partial S}{\partial A}\right)_{U,V} \tag{2.40}$$

where the right hand side is the superficial density of the entropy, σ. Thus the situation for mechanical equilibrium is entirely analogous to the previous case discussed above provided that the restrictions imposed by the second law are obeyed. This involves, essentially, a reversible heat exchange of the system with the surroundings, a restriction that in practice can, at best, be only approximated.

2.2 THE MEASUREMENT OF SURFACE TENSION OF LIQUID METALS

2.2.1 STATIC METHODS

The designation of certain methods of measuring surface tension of liquids as static methods, as opposed to dynamic methods, arises from the fact that the liquid is at rest with respect to its surroundings. The applications of static methods to the surface tension of liquid metals has been thoroughly reviewed by White[13] and Semenchenko[14].

The major static methods can be placed in two general categories. The first of these relates the pressure to force a bubble of gas through a capillary tube immersed in a liquid metal to the surface tension (the maximum-bubble-pressure method). A variation of this is the maximum-drop-pressure technique in which a liquid metal is forced very slowly through a capillary tube to form a drop of liquid metal. By use of a semi-empirical formula, the surface tension may be calculated from this pressure data[13, 14].

Apart from certain difficulties shared by all surface tension measurement techniques, these "pressure" methods, have a unique shortcoming; namely, that surface tension is not independent of the contact angle between the liquid and the wall of the capillary tube. Because liquid metals are neither completely wetting nor completely non-wetting with respect to a typical capillary tube material, the bubble (or drop) does not always locate itself consistently at the internal or external diameter of the end of the capillary tube.

Since the pressure required to place a bubble (or drop) at either of these locations is not the same[13], a variety of values for surface tension will occur. If the top of the capillary has a wall thickness less than 0.001 mm, this effect is overcome. However, in practice, when using refractory material for capillary tubing at high temperatures, this is clearly an impossibility.

The other general type of static method is the drop-shape method. Drops may be classified either as sessile drops, those resting freely on a flat horizontal surface or as pendant drops which are suspended from a vertical support. The surface tension is determined by measuring certain parameters on the outline of a vertical section through the drop centre. The shape itself is determined by the balance between gravitational and surface tension forces and this is a function of size, density and surface tension. Having measured certain critical dimensions of the drop shape, usually from blown-up photographs, surface tension is found with the aid of numerical solutions to the fundamental differential equations for a large variety of drop shapes as tabulated by Bashforth and Adams[13, 14] or with the aid of other related formulae[13, 14].

The difficulties in finding the critical dimensions of the drop shape are very great indeed (for instance, the accurate location of the line through the maximum diameter and measurement of contact angle[14, 16]) especially since the

use is often made of enlarged photographs. As a result empirical formulae (eg. 15) have been developed for use in conjunction with the Bashforth and Adams tables. Some of the more difficult measurements are thus eliminated.

The pendant drop method is treated in a similar[13, 14] fashion and finds its usefulness in the measurement of surface tension of high melting point and refractory metals due to less contact with a support device.

The accuracy of any of the above methods, is of course, largely dependent on the experimenter himself, but with proper care and attention, values of surface tension are generally with $\pm$ 1%.

2.2.2 DYNAMIC METHODS

Dynamic measurements of surface tension rely on the cause-effect relation between surface tension, γ, and certain characteristics of a disturbed liquid surface. Such a feature might be the length of capillary waves spreading on the surface of a liquid. Kelvin (Thomson 1871)[17] has shown that if the influence of surface tension is taken into account, then in addition to the force of gravity per unit mass, g, a force $\frac{4\pi^2\gamma}{\rho\lambda^2}$ acts on a unit mass, where ρ is the density and λ the wavelength of the capillary wave. The velocity of propagation v, of a wave is related to the wavelength and the total force, f, by the simple formula

$$v^2 = \frac{\lambda}{2\pi} f \qquad (2.41)$$

With this basic information, Kelvin, then showed that for small values of λ, the velocity of propagation is determined by the value of γ and for large λ, by the value of g, the gravitational force per unit mass. The working equation to find the surface tension is found to be[17]

$$\gamma = \frac{\rho\tau v^2}{2\pi}\left(v - \frac{g\tau}{2\pi} \right) \qquad (2.42)$$

where τ is the period of oscillation of the capillary waves.

Another technique that has been used in connection with liquid metals is the vibrating jet method. The original theory was first derived by Rayleigh[19] and was subsequently improved by Bohr[20]. This theory relates the surface tension of vibrating jet issuing from an elliptical orifice to the length of the jet (the distance between two nodes), the flow velocity of the jet, the fluid density and the density of the surrounding medium. One obvious problem that is encountered here is selection of a suitable material to construct an orifice that will not be eroded. Contamination of the liquid metal will be discussed in 2.2.3.

As is easily seen from (2.42), the velocity, v and the period, τ, must be very accurately determined since γ is a function of v^3 and τ^2. Any error in these quantities will be greatly magnified in the final value of surface tension. A similar criticism applies to the vibrating jet method. Before the advent of ultra high speed cinematography, the accuracy with which such quantities, such as velocity, could be found was somewhat limited and depended on elaborate

optical and photographic techniques[18]. Unlike the measurement problems associated with the static methods, those considered here must be measured quite directly. The accuracy of the above dynamic methods is slightly less than one per cent but vibrating jet experiments always result in values which are slightly lower than the accepted values established by a variety of static methods[18]. The theory which relates the surface tension of droplet and its natural frequency of oscillation will be reviewed in a separate chapter to follow.

2.2.3 GENERAL EXPERIMENTAL PRECAUTIONS

Although each technique for measuring surface tension will have its own unique experimental problems, there are many common difficulties. Perhaps the most critical concern is the experimenter himself. Every leading worker in the field of surface tension measurement emphasizes the point repeatedly, that systematic attention must be given to every experimental detail, whether it is seemingly trivial or not[13, 14, 16]. The following is a summary of the particular aspects of this work which one must constantly be aware of.

For accurate surface tension measurements, the liquid under consideration must be free of extraneous electrical, mechanical and chemical effects. Taking first the electrical effects, it is a well known fact that any electrostatic charge present in a conductor resides on the surface of that conductor[21]. Furthermore, this surface charge will have an effect on

measured values of surface tension[22] if the precaution of grounding the liquid metal is not taken. The effects of electron bombardment and induction heating when using the pendant drop or drop weight methods have been investigated by Peterson et al[23]. Various coil configurations resulted in varying values of surface tension for titanium due to different magnetic field distributions within the coil. For example, certain coils tended to lift the molten drop, thereby changing its shape and also affecting the maximum weight before the drop detaches itself. Also, vertical vibrations set up in the suspended drops contributed greatly to experimental difficulty and thus were a great source of error.

In static system, the need for absolute quiesence in the liquid is important. Photographic images are obscured if vibration occurs and premature falling of drops or busting of bubbles, as the case may be, will result[13] if the system is not completely still.

In dynamic systems, however, there is no such necessity, since usually it is some mechanical phenomenon such as a vibration which is being measured and related to surface tension.

Chemical reaction (including adsorption and desorption) with the liquid metal will result in contamination and, for surface active impurities, often a sharp reduction in surface tension, even for trace quantities. The group VI elements, for example, tend to reduce the surface tension of otherwise

pure iron from 1780 dyn/cm at 1550°C to as low as 950 dyn/cm (Fe-Se) where the impurity level is only .05 atomic percent. Generally, this decrease in γ is expressed [13] by

$$\left(\frac{\partial \gamma}{\partial x_2}\right)_{x_2 \to 0} < 0 \qquad (2.43)$$

The three main sources of contamination result from impurities within the metal, physical contact with the apparatus and impurities in the experimental environment.

Much early surface tension data, as will be seen in 2.3 was low compared to presently accepted values and in many cases this may be attributed to use of impure specimens. White[13] shows that by increasing the purity of zinc from 99.99^{+}% to 99.9999% pure, the surface tension rises from 757 ± 5 dyn/cm to 767.5 ± 5 dyn/cm at 420°C.

In static methods, there is danger of chemical reaction and, hence, contamination from the support material, whether it be a refractory plate or capillary tube, especially at high temperatures. Much care must be taken in selection of a suitable material with due respect paid to thermochemical data and even more important, to impurity levels in the proposed material. For non carbide formers, high purity, dense graphite is a good choice but, unfortunately, most other high temperature refractories are not so free from contamination. For high temperature work the pendant drop method, where the solid metal provides support for the liquid metal is the only real choice in the majority of cases. For dynamic methods, such as

those discussed in 2.2.2, the same care must be exercised in materials selection for such parts of the apparatus as an orifice.

The major environmental contaminants are oxygen and water vapour. These come into the system via leaks in the apparatus, impurities in gas flowing into the system or are present in the apparatus itself.

Evacuation and degassing of the apparatus removes adsorbed gases after opening to the atmosphere. The metal charge may be cleaned up by passing pure hydrogen over it at elevated temperatures to remove oxide film and adsorbed oxygen and some adsorbed sulfur.

Air will readily diffuse through even tiny pinhole leaks in spite of the lack of pressure gradient since there is a negative fugacity gradient between the air and the highly purified internal environment[13]. This pure environment is obtained by use of purification train suitable to the gas being cleaned. A typical set up for hydrogen and helium consists of a series of a copper furnace at 500°C, a ferrochrome furnace to 800°C and various cold traps of activated charcoal and molecular sieves in liquid nitrogen[13].

In order to have thermodynamic equilibrium, there should be no net loss of atoms from the liquid through the vapour to a sink[13] since continuous vapourization has a randomizing effect on the liquid surface. The absolute

magnitude of the surface entropy S^s is increased. From 2.33, it is seen that $\frac{\partial \gamma}{\partial T}$ is proportional to $-S^s$, a fact which has been corroborated by White[25] who was able to change the temperature coefficient of surface tension for zinc from positive to negative by inducing vapourization. For liquid metals vapourization rates are not neglible[28] and precautions must be taken to ensure thermodynamic equilibrium. The Russians[26] have cleverly devised a technique immerse the critical parts of a maximum bubble pressure apparatus in a thermostatically controlled closed environment. Measurements should never be attempted under conditions of a dynamic vacuum.

As noted, however, in 2.1.2 and 2.1.3, surface tension may be well defined under conditions of non-equilibrium, as long as mechanical equilibrium exists. On this basis, the condition becomes one of maintaining a constant pressure of gaseous phase with respect to the liquid and, more important, reducing vapour diffusion rates in the presence of a cold spot, by having gas in the system at sufficient high total pressure (eg. 1 atm.)This condition, then, results in mechanical equilibrium at the interface. This condition has been verified in the case of levitated droplets on molten metals in a variety of environments at 1 atmosphere[27].

The density of liquid metals is a quantity which must be measured experimentally at any given temperature and is therefore subject to error. Virtually, every formula used

in calculation of surface tension is a function of density and hence the accuracy of surface tension data can be no more accurate than the density data from which it is calculated. In the past, apparent discrepencies in surface tension measurements have been at least partially cleared up by normalizing the densities quoted by the authors[16] where possible. In the technique to be developed in this work, the density problem is overcome by combining density and drop radius to get the mass, which can be readily measured in this case.

These then are the basic pitfalls to be avoided in the experimental determination of surface tension of liquid metals and as such were the guiding principles behind the design of the present apparatus and experimental technique as given in Chapter 4.

2.3 EXPERIMENTAL RESULTS REPORTED IN LITERATURE

2.3.1 THE SURFACE TENSION OF LIQUID IRON

One of the major reasons for undertaking this study was the existance of great discrepancies in the literature for the surface tension of liquid metals at high temperatures. The surface tension of liquid iron is no exception.

Kozakevitch and Urbain[28] discount all surface tension measurements made prior to 1955. Without exception these are all lower (by 12 to 40 per cent) than presently accepted values. In light of 2.2.3, the reasons may seem obvious, but this is with the benefit of considerable hindsight. First, the effects of oxygen and sulfur on surface tension were not fully appreciated before 1955[28]. Also, the techniques of density measurement of liquid metals at high temperatures had not produced values with sufficient accuracy, that, for a given metal at a given temperature, any one value was in general acceptance. The early work of Kingery and Humenik[29] also shows that metals of fairly low purity, such as Armco iron and electrolytic iron were considered adequate for surface tension work. The results of Kingery and Humenik gave the surface tension of "pure" iron, γ_{fe}, at 1550°C values ranging from 1230 to 1560 dyn/cm.

Once more was known about the problems involved in measuring surface tension at high temperatures, Kingery and Halden[30] found the first "acceptable" results. Using Ferrovac

E (a vacuum melted iron containing, in their case, 0.0006% O_2, 0.027% C, and 0.005% S) in purified helium, they found γ_{fe} to be 1717 dyn/cm at 1570°C using the sessile drop technique. The errors were estimated to be ± 2% with the maximum deviation in a number of experiments never exceeding 3%.

In 1960, Samarin et al[31] found γ_{fe} at 1550°C to be 1865 dyn/cm. Unfortunately, this work was not supported by any data, save that the iron contained 0.001% O_2. Kozakevitch[28] supposed, however, that these workers had used the most widely accepted value of the density of liquid iron, 7.21 gm/cc,and recalculated the results for this sessile drop work assuming the density of iron to be 7.01 gm/cc,a more recently established value. This returned a value of 1813 dyn/cm which is much more acceptable, especially in the light of his own work discussed below.

Again using the sessile drop method, Kozakevitch and Urbain[28] measured the surface tension of pure liquid iron to be 1788 dyn/cm ± <1%. Iron with less than 0.001% O_2 and no detectable sulfur was used. Also, no effect was noticed in changing support materials (Al_2O_3, C_aO, BeO and ThO_2 were all tried) or changing the environment from argon to hydrogen. Previously both these factors had affected the results of Kingery and Humenik[29]. Kozakevitch and Urbain estimate that their value is within 1% of the value that might be obtained

for iron completely free of oxygen. There apparently has been no serious attempt made to date to study the temperature dependence of γ_{fe}.

2.3.2 THE SURFACE TENSION OF LIQUID NICKEL

The surface tension of liquid nickel has not been studied to the same extent as that of iron. Following the approach of disregarding pre-1955 results as in 2.3.1 we have the following data to consider.

Using both the sessile drop and maximum bubble pressure methods, a Russian team[32] found γ_{Ni} at 1520°C to range from 1490 to 1770 dyn/cm. These results, however, were obtained on nickel with a total impurity level of 0.01% but with no estimates of oxygen or sulfur concentrations. Also the results varied widely with composition of the support material and with the composition of the gaseous environment (hydrogen, argon and vacuum).

This is in sharp contrast with the values obtained by Kozakevitch and Urbain[24] who used the sessile drop method with high purity nickel. They obtained a value of γ_{Ni} of 1934 dyn/cm at 1550°C and no detectable effects arising from either changes in atmosphere (hydrogen or argon) or changes in support material. Certainly, it is evident that surface tension values should not be a function of the support material if they are to be useful and thus the Russian results are suspect. Monma and Suto[34] obtained a value of 1600 dyn/cm

at 1600°C for γ_{Ni} and correcting their value using the more widely accepted density of nickel of 7.64 gm/cc instead their quoted value of 8.1 gm/cc, this becomes still lower at 1509 dyn/cm[28]. This result seems extraordinarily low and oxygen and sulfur contamination are thus suspected.

CHAPTER III

THE THEORY OF OSCILLATING FLUID DROPS

3.1 INTRODUCTION

The phenomenon of oscillating liquid droplets is observed in drops formed from the breaking up of an oscillating jet of liquid issuing, under pressure, from a small orifice. The detached droplets, once formed from the jet, do not immediately assume a constant spherical shape, but rather begin to vibrate[36], being alternately compressed and elongated in the direction of the axis of symmetry of the original jet. Not only this, but also each drop is in the same phase of vibration at a given point in space. It appeared then to observers such as Kelvin[35] and Rayleigh[36] that this phenomenon involved a fundamental and natural frequency of oscillation, which was a function of the nature of the fluid (it's surface tension, γ, and it's density, ρ) and of the drop size.

The following sections are intended to outline the basis of calculation and to discuss the results in the light of the problem at hand, the measurement of the surface tension of liquid metals.

3.2 MATHEMATICAL DEVELOPMENT

3.2.1 BASIC ASSUMPTIONS

The mathematical development of the theory of oscillating fluid drops is based on small vibrations of the liquid mass about its spherical figure of equilibrium[35, 36]. In other words, the surface displacement is small compared to drop radius. The sphere is considered to be made of an incompressible liquid of density, ρ and zero viscosity, surrounded by an infinite mass of another fluid of density , ρ'. For the case of liquid drops as opposed to bubbles, ρ' approaches zero. The fluid which the oscillating drop is made of is assumed to be completely elastic and hence no damping of the natural oscillations will occur.

Motion within the drop is assumed completely irrotational. Also, only modes of vibration which are symmetrical about an axis will be considered. These modes can be expressed in terms of Legendre polynomials as will be shown later. The final, and perhaps most far reaching assumption with respect to this work is that, as observed by Lamb[37] p. 639-41, the results (i.e. frequencies) obtained are valid regardless of the nature of the forces which are tending to keep the drop spherical, whether they be due to self-gravitation (e.g. in the case of a liquid globe of the size of the earth) or due

to surface tension. The former situation has been solved completely by Lamb[38] and by Chandrasekhar[39], the latter by Reid[40]. In a levitation melting system there is no net gravitational force on the liquid drop[42] and hence the tendency to spherical form is due entirely to surface tension.

With these assumptions, then the relationship between surface tension and natural oscillation frequency can be developed.

3.2.2 DERIVATION

The relationship between drop radius, surface tension and oscillation frequency was first developed by Rayleigh[36], who made use of Legendre polynomials in dealing with the spherical surface, as will be discussed below. Subsequent authors[37, 38, 39, 40, 41] have tended to use a more sophisticated approach involving spherical harmonics although the basic principles followed in either case are identical. It is the original work of Rayleigh that will be followed in this derivation.

The curved surface of a nearly spherical body may best be described in terms of spherical coordinates r, θ, ϕ as shown in Figure 20(a). In the present case, however, we are concerned with a sphere deformed slightly, compressed or elongated, in the z-direction, and thus independence of ϕ. The coordinates of the system are then reduced to those shown in Figure 20(b) in which the radius, r, of the point p on the surface is a function of its colatitude, θ, for a given configuration.

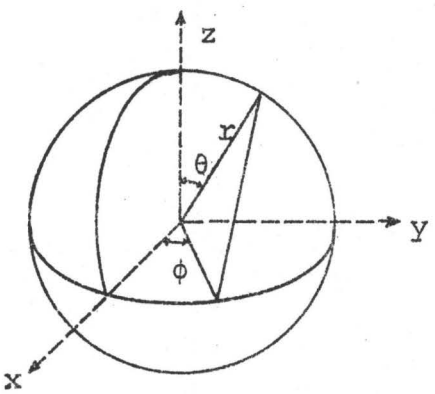

Figure 20 (a)
Curved Surface Showing
Spherical Coordinates

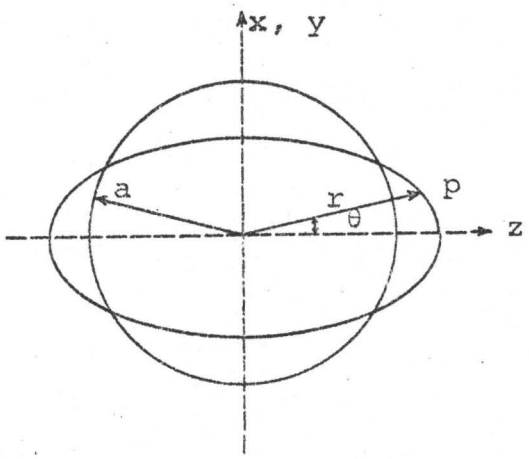

Figure 20 (b)
Surface Showing Spherical symmetry with coordinates r, θ. a is radius of sphere.

It can be shown that if a function is single valued and continuous except for a finite number of finite discontinuities (i.e., piecewise continuous) and has a finite number of maxima and mimima, then that function may be represented by a linear combination of Legendre polynomials[43]. Such a function is the polar equation of the surface bounding a liquid drop and is assumed to satisfy the aforementioned mathematical requirements. This equation may be expanded, then at any time t, in the series

$$r = a_o + a_1 P_1(\mu) + \ldots + P_n(\mu)$$

or

$$r = \sum_{n=1}^{N} a_n P_n(\mu) \qquad (3.1)$$

where a's are the coefficients of the Legendre polynomials, $P_n(\mu)$, and are functions of time, t; $\mu = \cos\theta$ and $P_o(\mu) = 1$. Also, $a_1, a_2, \ldots a_n$ are small compared to a_o.

We now assume that the volume, V_s, of the liquid contained by the surface, as defined by (3.1), is a constant for all time. If the average value of f (x) of any function, f (x) over the range between x_2 and x_1 is given by[45]

$$f(x) = \frac{1}{x_2 - x_1} \int_{x_1}^{x_2} f(x)\, dx \qquad (3.2)$$

then, knowing that r is a function of μ and, hence, that V_s is also a function of μ. But physically V_s is a constant and independent of the configuration. The constant value of V_s may be obtained by eliminating its dependence on μ in the following way:

$$V_s = \left(\frac{4}{3}\pi\right)\left(\frac{1}{2}\right) \int_{-1}^{+1} \left[a_o + \sum_{n=1}^{N} a_n P_n(\mu) \right]^3 d\mu \qquad (3.3)$$

The limits of integration are found(Figure 20(b))to be 0 to π for the integrand involving sinθ dθ and, upon transforming sinθ dθ to dμ (d(cosθ)), become -1 to 1. Expanding the cubic term in the integrand of (3.3) and integrating term by term, and considering the facts that Legendre polynomials are orthoganal and odd in μ then we have

$$V_s = \frac{4}{3}\pi a_o^3 + 3a_o \sum_{n=1}^{N} a_n^2 \int_{-1}^{+1} [P_n(\mu)]^2\, d\mu \qquad (3.4)$$

and using the known relation, $\int_{-1}^{+1} [P_n(x)]^2\, dx = \frac{2}{2n+1}$ [43], the average volume becomes

$$V_s = \frac{4}{3}\pi a_o^3 \left[1 + 3 \sum_{n=1}^{N} (2n+1)^{-1} \frac{a_n^2}{a_o^2}\right] \qquad (3.5)$$

Assuming the equilibrium configuration to be a sphere of volume, V_s, the radius, a, of the sphere of equilibrium if found from $V_s = \frac{4}{3}\pi a^3$. Hence from (3.5)

$$a = \left(a_o^3 + 3a_o \sum_{n=1}^{N} (2_n + 1)^{-1} a_n^2 \right)^{\frac{1}{3}}$$

or by neglecting high order terms

$$a \simeq a_o \left(1 + \sum_{n=1}^{N} (2_n+1)^{-1} \frac{a_n^2}{a_o^2} \right) \tag{3.6}$$

The potential energy of capillarity is defined as the potential energy due to surface curvature[37]. The definition of surface tension is taken to be the mechanical definition as given by (2.23) with units of energy/unit area. γ is also assumed constant. The zero of potential energy will correspond to that given by the surface configuration of the sphere of equilibrium.

To calculate S, we have from consideration of Figure 20 (b),

$$S = 2\pi \int_{-1}^{+1} r \sin\theta \left\{ r^2 + \left(\frac{dr}{d\theta}\right)^2 \right\}^{\frac{1}{2}} d\theta \tag{3.7}$$

Integrating by parts[36] we obtain

$$S = 4\pi a_o^2 + 2\pi \sum_{n=1}^{N} (2_n+1)^{-1} (n^2+n+2) a_n^2 \tag{3.8}$$

and substituting (3.6)

$$S = 4\pi a^2 + 2\pi \sum_{n=1}^{N} (n-1)(n+2)(2_n+1)^{-1} a_n^2 \tag{3.9}$$

where $4\pi a^2$ is the surface area of the sphere of equilibrium. The potential energy, P, thus becomes

$$P = 2\pi\gamma \sum (n-1)(n+2)(2n+1)^{-1} a_n^2 \qquad (3.10)$$

taking the sphere of equilibrium as the zero point for potential energy.

We now turn to the development of the equation for the kinetic energy of the motion. With any motion of a fluid there is associated a velocity potential, ψ, where $u = -\nabla\psi$, u being the velocity vector. The velocity potential is a single valued function and continuous throughout the fluid and thus, satisfying the Dirichlet conditions, may be expanded in the series

$$\psi = \beta_o + \sum_{n=1}^{N} \beta_n r^n P_n(\mu) \qquad (3.11)$$

The velocity potential is related to the kinetic energy, K, through the following expression[37]

$$K = \frac{1}{2} \rho \iint \psi (\partial\psi/\partial n)\, dS \qquad (3.12)$$

where $-\partial\psi/\partial n$ denotes the normal velocity of the fluid inwards and $\rho\psi$ is the impulsive pressure necessary to generate the motion, where ρ is the fluid density. Hence, by integrating over the surface, the right hand side of (3.12) is the work done on the surface to cause the liquid to flow and is, thus, equal to the kinetic energy of the motion. For the system at hand (3.12) becomes

$$K = \frac{1}{2} \rho \iint \psi(d\psi/dr)\, a^2\, d\phi d\mu \tag{3.13}$$

which, after integrating, reduces to[36]

$$K = 2\pi \rho a^3 \sum_{n=1}^{N} (2n^2 + n)^{-1} \left(\frac{da_n}{dt}\right)^2 \tag{3.14}$$

We now wish to find a relationship between the potential energy, P and the kinetic energy, K. One of the basic assumptions made in 3.2.1 was that the motion consisted of small oscillation about the spherical position. We shall now further assume that the spherical position is one of stable equilibrium, that is to say, a small disturbance of the system from equilibrium results only in small bounded motion about the rest position and hence, there are no uncontrolled forces of inertia[44]. By definition, the system is said to be in equilibrium when the generalized forces acting on the system vanish. Thus,

$$\left(\frac{\partial P}{\partial q_n}\right)_o = 0 \tag{3.15}$$

where q_n represents the generalized coordinates and the subscript o denotes the equilibrium position. P is a function of $(a, a_1, a_2 \ldots, a_n)$ with n degrees of freedom (since a is constant with time) as seen from (3.9). Hence the generalized coordinates q_n for the potential energy function become

$$q_n = a_n \tag{3.16}$$

Expanding P about the equilibrium position as a Taylor's series (low order terms only since we assume small oscillations) we obtain[44]

$$P\ (a,\ a_1,\ \ldots,\ a_n) = P\ (a,\ o,\ \ldots,\ o) + \sum_n \left(\frac{\partial P}{\partial a_n}\right)_o a_n + \frac{1}{2} \sum_{n,m} \left(\frac{\partial^2 P}{\partial a_n \partial a_m}\right)_o a_n a_m + \ldots \tag{3.17}$$

The first term in the series is the potential energy of the equilibrium position, P (a, o, ...,o), and is made to vanish by shifting the arbitrary zero of potential to coincide with the equilibrium potential as was done previously. The second term has been shown to be zero also by (3.15). Therefore, we are left with

$$P = \frac{1}{2} \sum_{n,m} \left(\frac{\partial^2 P}{\partial a_n \partial a_m}\right)_o a_n\ a_m \tag{3.18}$$

By substituting (3.10) for P in the right hand side it can be shown that (3.18) becomes

$$P = \frac{1}{2} \sum_n \left(\frac{\partial^2 P}{\partial a_m^2}\right) a_n^2 \tag{3.19}$$

where $\sum_n \left(\frac{\partial^2 P}{\partial a_m^2}\right) = 4\ \pi\gamma \sum (n-1)\ (n+2)\ (2_n+1)^{-1}$

Similarly it can be shown[44] that

$$K = \frac{1}{2} \sum_n \left(\frac{\partial^2 K}{\partial \dot{a}_n}\right) \dot{a}_n^2 \tag{3.20}$$

where $\dot{a}_n = \frac{da_n}{dt}$ and $\sum_n \left(\frac{\partial^2 K}{\partial \dot{a}_n^2}\right) = 4\pi \rho a^3 \quad \Sigma(2n^2 + n)^{-1}$

The potential and kinetic energies, as expressed by (3.19) and (3.20) respectively contain no terms with products of a_n and da_n/dt and may be related to one another via the Lagrangian, L, where[44]

$$L = K - P \tag{3.21}$$

Substituting (3.19) and (3.20) into (3.21) we obtain

$$L = \frac{1}{2} \sum_n \left[4\pi \rho a^3 \sum_{n=1}^{N} (2n^2 + n)^{-1} \dot{a}_n^2 - 4\pi\gamma \sum_{n=1}^{N} (n-1)\right.$$

$$\left.(n+2)\ (2n+1)^{-1}\ a_n^2\ \right] \tag{3.22}$$

Taking the a_n's as generalized coordinates, the Lagrangian of (3.22) leads to the following n equations of motion[44].

$$\frac{d}{dt}\left(\frac{\partial L}{\partial \dot{a}_n}\right) - \left(\frac{\partial L}{\partial a_n}\right) = 0;\ n=1,\ 2,\ \ldots N \tag{3.23}$$

or simplifying with the aid of (3.22), (3.23) becomes

$$\frac{d^2 a_n}{dt^2} + n\ (n-1)\ (n+2)\ \frac{\gamma}{\rho a^3}\ a_n = 0 \tag{3.24}$$

(3.24) has the solution of the form

$$a_n \propto \cos\ (pt + \varepsilon) \tag{3.25}$$

where

$$p^2 = n\ (n-1)\ (n+2)\ \frac{\gamma}{\rho a^3} \tag{3.26}$$

and where $p/2\pi$ is the frequency of oscillation, ω , and ε is the phase angle. n is taken as the mode of vibration.

For n=0, the surface displacements would be spherically symmetrical and independent of θ and ϕ. Since the fluid is incompressible, such oscillations are not possible[46]. For n=1, the type of motion created is not oscillatory, but rather translational due to external forces. Again such a case does not exist in the system at hand. Finally, for n=2, the motion is oscillatory (as it is for n>2) and the deformation is ellipsoidal[35]. Taking n=2, then, to be the lowest fundamental frequency of oscillation for this system, replacing ρa^3 by the corresponding term involving the mass of the sphere (m), and solving for surface tension, γ, we find

$$\gamma = 3/8\pi \; m \; \omega^2 \qquad (3.27)$$

This is, therefore, the fundamental relationship between oscillation frequency and surface tension, bearing in mind the initial assumptions. The following sections in this chapter will discuss the validity of some of these assumptions with relationship to a drop of liquid metal and also, later, these assumptions will be reexamined in the light of the experimental observations.

3.3 FACTORS AFFECTING RAYLEIGH EQUATION

3.3.1 VISCOSITY

In the original work by Rayleigh[30], the effects of viscosity of both the drop and the surrounding fluid were assumed neglible. By its very nature, viscosity, being the resistance of a fluid to change shape (or the "elasticity" of a fluid) would intuitively seem to have some damping effect on the amplitude of vibration.

If the equations of motion for the drop are rederived including, now, the viscosity, it can be shown[37, 38, 41] that this results in the addition of a term describing the damping due to viscous effects in the drop, where this term is $\frac{2(n-1)(2n+1)\mu}{a^2\rho}\frac{da_n}{dt}$ and where μ is the drop viscosity in gm/cm-sec. Equation (3.24) becomes

$$\frac{d^2a_n}{dt^2} + \frac{2(n-1)(2n+1)}{a^2\rho}\mu\frac{da_n}{dt} + \frac{n(n-1)(n+2)\gamma}{\rho a^3}a_n = 0 \tag{3.28}$$

Furthermore, it can be shown[37, 38] that the coefficient of da_n/dt is related to the decay factor (decay time), τ, such that

$$\tau = \frac{1}{(n-1)(2n+1)}\frac{a^2}{\nu} \tag{3.29}$$

where ν $(=\mu/c)$ is the kinematic viscosity and a is, as before the radius of the spherical drop.

The decay factor is the time for vibration caused by a single perturbation to virtually cease. Thus if τ is less than the period of oscillation, a continuous vibratory motion will be non-existant and the oscillations are said to become aperiodic. Taking values for the parameters of (3.29) typical of those expected in a levitation melting system for a 1/2 gm specimen of pure iron, we find that τ = 3.5 seconds for a = 0.23 cm, ν = 0.003 cm^2/sec[50] and n=2. Comparing τ to the expected period of oscillation from (3.27) (γ = 1788 dyn/cm[28]) of 2 x 10^{-2} seconds, we see, for the case iron (and typically of many liquid metals), that the decay time is considerably greater than the period of oscillation.

Taking a different approach, now, we note that surface tension varies as a^{-3} (3.27) and that the damping forces vary as a^{-2} (3.28). Since these two forces oppose one another, there exists a critical drop size below which damping is predominant and aperiodic motion is found. Chomiak[41] shows this to be

$$r_c = \frac{(n-1)(2n+1)^2 \nu^2 \rho}{n(n+2)\gamma} \qquad (3.30)$$

where r_c is the critical drop radius above which aperiodic motion disappears. Using the same values for ν, ρ, γ and n as above, the critical drop radius is approximately 10^{-8}cm for liquid iron. This very small value is due primarily to the very low kinematic viscosity, $3x10^{-3}cm^2/sec$. For the system to be used in this work, we will be concerned with

drop radii eight orders of magnitude greater.

These two calculations show, therefore, that, for liquid metal drops of the type to be used for this study, the effects of viscosity in damping the oscillations in liquid metal drops are not significant since we are very far removed from the conditions of aperiodic motion.

The viscous effects of the surrounding medium are also not to be overlooked and, in fact, a fair amount of effort has been spent studying this aspect of oscillating fluid drop systems[41, 47, 48]. Chomiak[41] shows the effects most explicitly and relates the influence of viscosity of the surrounding medium to an increase in effective mass of the drop. If ρ_o is the density of the surrounding medium, μ_o, its viscosity, and if $\beta = \left(\frac{p\rho_o}{2\mu_o}\right)^{\frac{1}{2}}$ where p $(=2\pi\omega)$ is the circular frequency of oscillation from 3.26, then viscosity increases the mass by the amount

$$\frac{10}{3} \frac{\rho o}{\rho} \frac{1 + \beta a}{1 + 2\beta a + 2\beta^2 a^2} m \qquad (3.31)$$

where m is the mass of the drop. If the gas surrounding the drop is helium with 6% hydrogen ($\rho_o \simeq 2\times10^{-4}$ gm/cc, $\mu_o \simeq 10^{-5}$ gm/cm-sec)[50], then the increase in effective mass for the liquid metal systems used here is less than one thousandth of one percent, a neglible amount.

It is thus very reasonable to assume, as we have done at the outset, that neither the viscosity of the drop or

surrounding medium have any influence on the damping of oscillation for the present study.

Another effect of viscosity is the tendency to split the oscillation frequency into two modes, one higher and one lower than the Rayleigh frequency[47], the lower frequency being energetically favourable. Subramanyam[47], however, points out that, in the limiting case of a drop oscillating in free space, the deviation from the frequency expected from 3.26 is very small (<.1%). This condition is virtually identical to that considered here, as was shown above, and hence, we shall consider for this work, that all the effects of viscosity are neglible and the original assumption of zero viscosity remains valid.

3.3.2 INERTIAL EFFECTS

One of the main criticisms of dynamic methods of measuring surface tension is that in all flowing systems there will be uncontrolled inertia effects[13, 36]. These are due to interaction of the fluid with its surroundings. For a spherical (or nearly spherical) drop moving relative to its surroundings (translation not oscillation), it has been shown by consideration of the normal stresses on the drop surface due to flow past the surface, that deformation of the drop will occur and that this is caused entirely by inertial effects[49]. Expressing this deformation in terms of drop radius, we have[49]

$$r = 1 + \xi(\mu) \qquad (3.32)$$

where r is the dimensionless radius and $\xi(\mu)$ determines the deviation of the drop from the spherical shape due to inertia ($\mu = \cos\theta$ as above). For the case of interest here; namely, that fluid viscosity/gas viscosity ratio $\to\infty$, it can be shown that $\xi = -.25\ We\ P_2(\mu)$ where We $(=\frac{\rho a u^2}{\gamma}$; where u is the drop velocity) is the Weber number and $P_2(\mu)$ is Legendre polynomial.

In the experimental setup to be used in this study, a liquid metal droplet will be suspended in an electromagnetic field (levitation coil, Chapter 4) and will be stationary with respect to its surroundings. Although gas flows in this system, it does so at a very slow rate (~1l/hr) and into a large chamber (~0.5 ft^3). It is evident, then, that deformation caused by inertial effects related to drop translation will not occur in this system since such deformation is proportional to the square of the velocity of the drop motion, which is near zero.

Although the drop is not in translation, it will oscillate and one might anticipate inertial effects arising out of the latter motion. Miller and Scriven[48] have shown, however, that when the surrounding medium is a gas of low density and low viscosity, there is no appreciable boundary-layer flow, provided the interface is free (clean). Hence no "viscous dissipation"[48] of the oscillations will occur in the boundary layer near the interface for drops where radius is large compared to interface thickness.

We may come to the conclusion, therefore, that a liquid metal drop of the size to be considered here (~2.5mm), oscillating in a helium, 6% hydrogen gas mixture ($\rho_{gas} \simeq 2 \times 10^{-4}$ gm/cc, $\mu_{gas} = 10^{-5}$ gm/cm-sec), is free of extraneous and uncontrolled inertial effects.

3.3.3 TEMPERATURE

Recalling the Rayleigh equation of the form of 3.26, we have

$$p^2 = n\,(n-1)\,(n+2)\,\frac{\gamma}{\rho a^3} \qquad (3.26)$$

No attempt has been made in this relationship to demonstrate any temperature dependance that may exist among the variables.

The temperature dependance of density[51,52] is accomodated by a corresponding change in radius, since the mass remains constant. Thus, any temperature dependance of surface tension, γ, must be reflected in the frequency term, p^2. The nature of this dependance, however, is not specified and will depend mainly on the definition of surface tension applicable to any given system, as discussed in 2.1.5.

3.3.4 ELECTRIC CHARGE

In the absence of any other forces such as surface tension, the spherical equilibrium position of a mass of liquid is unstable if there is any electric charge on the liquid. This is due to the repulsive nature of the electrostatic forces. Under the influence of an attractive force

such as surface tension, a small disturbance from the equilibrium position will result only in small bounded motion about the equilibrium, whereas in the case of only electrostatic forces acting on the system, a small disturbance from the equilibrium causes a shift in equilibrium to some undefined non-spherical shape[36, 56].

Assuming that we have a spherical mass of liquid in the equilibrium position of radius a_o and with charge Q. The potential of this configuration, P_{E_o} is Q/a_o. However, if the mass is deformed slightly, the polar equation of the surface may be expressed in the following series;[56]

$$r = a_o (1 + F_1 + F_2 + \ldots + F_n) \qquad (3.33)$$

where the terms $F_1, \ldots, F_n$ are determined from the partial solution of Laplace's equation[58, 59] ($\nabla^2\psi = 0$) for the case of the potential, ψ, being independent of the coordinate ϕ under the assumption of axial symmetry as in 3.2.1. The evaluation of these terms is not of any importance in this instance since the electrostatic potential, P_E, will be compared to the potential energy due to capillarity which will also be derived in terms of (3.33). The mathematical development of these two potential energies follows the method of Lamb[37] which is just a more mathematically sophisticated variation of the original Rayleigh work described in 3.2.2.

The electrostatic potential of the system, taking the equilibrium position as zero can be shown[56] to be

$$P_E = -\frac{Q_2}{8\pi a_o} \sum_{i=1}^{N} (n-1) \iint F_n^2 \, d\sigma \qquad (3.34)$$

where $d\sigma$ denotes an element of area of the spherical surface. Using Lamb's approach[37], the potential energy of capillarity becomes

$$P_c = \frac{1}{2} a_o^2 \gamma \sum_{i=1}^{N} (n-1)(n+2) \iint F_n^2 \, d\sigma \qquad (3.35)$$

(3.35) is equivalent to (3.10) as derived in (3.2.2) using Rayleigh's method.

To find the effect of P_E on P_c, (3.34) and (3.35) are added. The value of the integral parts of (3.34) and (3.35) are equal at any time and, in fact, $\iint F_n^2 \, d\sigma$ is the only time dependent part of both of these equations. Choosing n=2 as per 3.2.2, the following expression results from the combination of (3.34) and (3.35)

$$A = \gamma \left(1 - \frac{Q^2}{16\pi a_o^3} \frac{1}{\gamma} \right) \qquad (3.36)$$

where A is a constant of any given point of time. The part in parenthesis may be regarded as a correction factor applied to the value of γ, as a result of the presence of an electrostatic charge, Q, on the drop surface. It is evident that if $\gamma > Q^2/16\pi a_o^3$, the spherical form remains the equilibrium position for any small displacement of the drop surface. The potential, Q/a_o, necessary to create an unstable equilibrium is found, in electrostatic units, to be

$$Q/a_o = (16\pi a_o \gamma)^{\frac{1}{2}} \qquad (3.37)$$

Using typical values for a_o and γ, as might be expected in the levitated metal drop system, of 0.25 cm and 2000 dyn/cm respectively, and, converting from statvolts to volts, the drop must have a potential of 45,000 volts before the onset of instability of the spherical equilibrium shape. Using the same values for a_o and γ, it is easily shown that to introduce at 1% error in γ the drop must have a potential of 180 volts.

CHAPTER IV

4.1 INTRODUCTION

The purpose of this study is to establish a technique for the measurement of the surface tension of molten metals by determination of the frequency of oscillation of a droplet of the liquid metal. The technique of levitation melting[42] is well suited for this purpose since it enables a molten drop of metal to remain suspended in contact only with a gaseous atmosphere for long periods of time. The purity of the atmosphere is easily controlled and hence droplet contamination is prevented. The temperature is easily controlled by power input to the levitation coil and is readily monitored with an optical pyrometer. The levitated specimen may be photographed with a high speed movie camera and the frequency of oscillation of the drop determined from the film. The effects of drop size, material of the specimen and temperature on the surface tension of iron and nickel were investigated.

4.2 APPARATUS

A general view of the complete apparatus used for the photography of an oscillating drop of molten metal is shown in Figure 4. The apparatus as a whole was designed according to the principles laid down in Chapter 2.

In the upper left hand part of the photograph is the levitation chamber (see Figure 5, 6) containing the levitation coil. At the bottom of this chamber are the leads connecting the coil to the high frequency generator through a step-down transformer, both of the latter being partially obscured by the high speed camera and its supporting tripod. The top of the table contains, from left to right, the camera speed control, the remote power control for the generator and part of the gas purification system. Behind the latter is a Vacustat connected to the levitation chamber by a series of three-way stop cocks. These may be adjusted so that gas passes freely through the system or the system is linked directly to a mechanical vacuum pump and the Vacustat. Behind the levitation chamber is the two-colour optical pyrometer, its temperature indicator and the vacuum pump. On the lower level of the table is a titanium furnace at 900°C with its temperature controller (partially hidden by a gas cylinder), a two-stage bubbler vented to the air and a constant voltage supply to run the camera. Not seen in this picture is a pulse generator

which acts as an independent timer for the determination of the frame rate (film speed).

4.2.1 LEVITATION CHAMBER

The levitation chamber is shown diagrammatically in Figure 5 and in a photograph in Figure 6.

The design of the apparatus as a large chamber of controlled internal atmosphere containing a levitation coil was chosen over the system more commonly used in levitation work for thermodynamic and kinetic studies (in which the reaction chamber is a narrow tube inserted along the vertical axis of the levitation coil[54]) in order to have simultaneous temperature measurement and photography of the droplet incorporating both top and side views in one frame on the film. The tube-within-the-coil design could not be suitably adapted to photograph the side view of the drop as the spacing between the top and bottom windings of the coil was too narrow to permit the insertion of the optical flat necessary to obtain an undistorted view.

The chamber is 12" high and 8" in diameter, made of 1/4" plexiglas enclosing a levitation coil of 1/8" insulated copper tubing and a prism for photographing the top view of the droplet. The top and bottom of the chamber are made of 1/2" plexiglas, necessary to withstand repeated evacuation. Each plate is bolted separately in six places onto a flange and the seal between the flange and the plate is made with an 1/8" O ring.

A sliding quartz tube, 1/4" in diameter, is used for passing gas into the chamber, for lowering samples into the coil and for retrieving the quenched droplets. When the system is to be placed under vacuum, a seal about this tube is made with an O ring in a Swagelok fitting and a stopcock between the gas purification train and the gas inlet is closed. During a run, the Swagelok is released and an oil bath (vacuum pump oil) is moved up around the top of the fitting to prevent diffusion of air into the system.

Two observation ports, 3" in diameter, covered with glass are placed opposite each other at the level of the coil. One is used for pyrometry, the other for photography. The sides of the ports are painted flat black to reduce extraneous reflections into the camera. The prism (45°, 45°, 90°) is cemented to a horizontal glass rod which is placed through a vertical swivel. The prism is swung into position from outside the chamber by means of a magnet acting on a piece of iron attached to the horizontal rod near the chamber wall.

The leads to the coil pass through base plate where they are brazed into Swagelok fittings which are in turn cemented to the base providing a vacuum tight seal. The ends of the coil are then inserted into these Swageloks. This has the advantage of providing a fairly rugged system which can be easily dismantled for maintenance. Finally the base of the apparatus is protected from falling drops of molten metal, which burn through plexiglas, by an asbestos plate. This is

the hard asbestos board, not the asbestos fibre which makes evacuation more difficult.

4.2.2 GAS PURIFICATION

The gas used in this work is a commercially available 6% hydrogen-balance helium mixture. This mixture was chosen since it is highlyreducing and will remove any oxygen from the drop surface (below limits of detection). It is also a non-combustible mixture. Originally pure hydrogen was used but this was discontinued after an explosion which destroyed the levitation chamber.

The purification train for this gas mixture is shown in Figure 7. It contains first a platinum-palladuim catalyst cylinder, then ascarite (KOH) for removal of CO/CO_2. Next are Drierite (anhydrous $CaSO_4$) and silica gel, followed by a cold trap of activated charcoal in liquid nitrogen. The gas is then passed through a furnace containing spirally wound titanuim foil ribbons at 900°C. At sufficiently low flow rates the Po_2 of the gas entering the chamber will be of the order of 10^{-30} atmosphere.

Prior to each run the chamber is sealed off as described in 4.2.1 and evacuated to 0.1 mm Hg, backfilled with the purified gas mixture and reevacuated. The atmosphere in the chamber was tested for oxygen content by levitating a small sample of aluminum. If no oxide remained on the molten aluminum drop surface a few minutes after melting, the gas mixture was considered satisfactory; i.e. the Po_2

was about 10^{-30} atmosphere. Completing the gas flow system was a two stage bubbler containing low-vapour pressure dibutyl-phthalate vented to the air. This is to prevent back diffusion of air into the chamber.

The gas was also of very low sulphur content. The bottle of gas used was tested by bubbling it through sodium hypochlorite (NaOCl) solution for a considerable time (1 day). No trace of sulphur was found in the solution afterwards and since NaOCl is used in the collection of sulphur from gases for the purposes of analysis, it was taken that there was no sulphur in the gas. It is necessary, however, to check each new bottle of gas as there is always the possibility of sulphur contamination of the drop.

4.3 EXPERIMENTAL TECHNIQUES

4.3.1 COIL DESIGN

Besides the purification of the chamber atmosphere, the most important part of the apparatus is the levitation coil. It is only with a coil constructed with great care that stable levitation of a drop of metal will occur. Often each metal studied with require a modification in one or other of the coil design parameters in order to have successful levitation. Such parameters are coil diameter, number of turns in the coil and spacing between top and bottom windings. The characteristics and design of levitation coils have been discussed in a review by Peifer[53].

The levitation coil used for the surface tension measurements of iron and nickel is shown schematically in Figure 8 and photographically in Figure 9. The coil was wound out of 1/8" copper tubing, insulated with fibreglass sleeving, on a conical former with a semi-angle of 30°. The bottom windings consisted of two coplanar turns followed by two more turns while the top reverse winding consisted of two turns wound on the same former. This number of turns was selected by trial and error on the basis of which configuration levitated a molten droplet of iron in the temperature range 1550°C to 1700°C[53]. This design is used to promote a high degree of lateral stability in the confined area within the coil.

It was observed, however, that frequently the droplet appeared to spin and to precess about the coil axis. On viewing a film taken either of the top or the side view of a drop, it was very difficult to distinquish between any rotation and any oscillation of the drop that might be occurring. In order to facilitate this distinction films were taken which recorded the top and side views simultaneously as shown in Figure 10 (also 4.3.5). This revealed that, in fact, rotation of the specimens was occurring. The difference can be observed best on viewing the film as shown by a movie projector, but some indication of the problem is given in Appendix A, by means of a blown up sequence of a rotating droplet and a similar sequence of an oscillating droplet. To check that the rotation phenomena was not unique to iron, samples of copper and nickel were filmed with the same results, showing that rotation was due to coil design and not unique to a given metal.

It was found that the stability of the levitated specimens is influenced by several factors in coil design. First, the coil must be precision wound so as to be perfectly circular and so that both top and bottom windings are coaxial. Next, to counteract the field reducing effects of the leads carrying the current and water cooling to and from the coil, the reverse wound top coil must be tilted slightly down on the side opposite the leads as shown in Figure 8 (b).

This results in a vertical electromagnetic field vector. If this vector is even slightly off the vertical, the droplet will begin to precess about the coil axis. Any precession makes film analysis very difficult as described above. The redesigned coil was checked out by filming a series of droplets and comparing the simultaneous shape changes of top and side views. It is extremely doubtful that any meaningful results could be obtained without this modification which will give a stable levitated droplet that will exhibit pure oscillations, i.e. without rotating.

4.3.2 TEMPERATURE CONTROL

For a given power supply, the temperature of the sample depends on coil design, the size and electrical properties of the sample, and the gas flow rate and composition[53].

A 450 kc/s, 10 kω Tocco generator was coupled to a 7.5:1 step-down transformer in order to reduce power input to the coil to prevent overheating of the sample. Coupled with a coil of suitable design (4.3.1), it was possible to maintain the temperature of a levitated molten sample of iron or nickel (from 0.5 gm to 1 gm) at any given temperature from 1450°C to 1700°C and at very low gas flow rates, simply by adjusting the power input to the coil. Keeping the temperature constant, however, is contingent on having a non-fluctuating supply from the mains, a condition which

rarely existed except very late at night. As a result, most of the runs to obtain the final results were done from 10:00 pm to 4:00 am.

Since gas flow rate and composition determine the efficiency of heat removal from the levitated sample, there is also the possibility of temperature control using the gas. However, in this case, since high gas flow rates were not conducive to proper purification and, since high flow rates would also appear to affect the drop oscillations characteristics (3.3.2), this method was avoided as a means of temperature control as much as possible, being mainly used just to quench the droplets while they were still levitated. The atmospheric mixture of hydrogen and helium, being of high thermal conductivity, was very efficient at removing heat and hence allowed flow rates to be kept to a minimum.

Thus, under these conditions of low flow rates (1 l./hr , the temperature of a levitated specimen of iron or nickel could be controlled to within $\pm$ 5°C of the desired value in the range 1450-1750°C.

4.3.3 TEMPERATURE MEASUREMENT

A Milletron two-colour optical pyrometer and direct reading indicator were used to measure temperature of the iron samples while an Ircon Infrared Radiation Thermometer, Series 300 and its non-direct reading indicator were used for nickel temperature measurements. The reason for the use of the

Ircon pyrometer, which is not as accurate as the Milletron, was the inability to obtain a satisfactory calibration on the latter for use with nickel, although calibration procedures were similar for the two instruments. Full details of the calibration method is given by Kershaw[54] so it will suffice to mention that the calibration was performed against a standarized Pt/Pt-13% Rh thermocouple. Both pyrometers were calibrated shortly before the experiments were run to collect the final sets of data that were used to calculate surface tension. Calibration checks were frequently made by observing melting and freezing point temperatures of the levitated droplets.

The actual temperatures reported in the present study are estimated to be within $\pm$ 10°C for the Milletron pyrometer readings (Fe) and $\pm$ 15°C for the Ircon pyrometer readings (Ni).

4.3.4 MATERIALS PREPARATION

Samples weighing from 1 gm to 1/2 gm were cut from rods of three types of high purity iron; Ferrovac "E", National Physical Laboratory (NPL) and Battelle iron, and from electrolyte nickel (Inco). The analysis of the irons are given in Table I and of the nickel, in Table II.

The samples were cut with a fine jewellers saw from bar stock (1/4" diameter rod for Ferrovac "E" , NPL; 1-1/4 bar for Battelle and 2" x 2" x 1/4" plate for nickel), and then ultrasonically cleaned and degreased in acetone prior

to levitation. After melting, each sample, now a smooth spheroid,was placed in a solution of 50% HCl, 2% HF, 1% HNO_3, balance distilled water for approximately 5 minutes, after which the samples were rinsed, in turn, in distilled water and methanol. After levitation for a second time, to check for surface film, each sample was stored in its own labelled container,all of which were placed in a dessicator (labelled for size and type of material since all samples were virtually indistinguishable except for size). After cleaning in this manner, a vacuum fusion analysis of a random sample of specimens was made as shown in Table III. Due to the limits of accuracy ($\pm$ 10 ppm) of this technique, we can claim only that the oxygen level on the drop is < 10 ppm.

4.3.5 PHOTOGRAPHY

The camera used in this study was a Hycam rotating prism type high speed motion picture camera, model K2001E. This instrument is capable of running at frame rates from 100 to 9000 pictures per second using up to 100 feet of 16 mm film. The optical system is shown in Figure 11[55] and consists briefly of an objective lens followed by a segmented shutter which,by rotating,effects an opening and closing similar to that in a normal intermittenttype shutter. The images here, however, pass through an eight sided rotating prism and from there on to the moving film. The film sprocket, the prism and shutter are all on a single rotating shaft and with proper sychronization allows the film to be continuously

exposed to changing images. This type of action allows for precise timing and precise frame rate control which is essential for measurement work.

The frame rate is controlled electronically by a signal from a photodiode in the optical head of the camera. Unfortunately the frame rate cannot be set from the speed control panel to any greater accuracy than $\pm$ 5% at best. It is therefore, necessary to measure the speed of the filming by use of a timing light which, at a signal from an external pulse generator, exposes a small dot on the side of the film. The pulse generator was accurately calibrated with a frequency counter to put out 1000 $\pm$ .5 pulses per second. Thus, every one thousandth of a second a small blip will appear along the edge of the developed film. The actual measurement of the film speed will be discussed in 4.3.6.

The lens system used at all times for this work was a 50 mm lens with a 10 mm extension tube. The extension tube effectively increases the focal length of the lens but reduces, at the same time the depth of field, making focusing critical. The camera was supported by a solidly build tripod in order to avoid displacing the camera once it had been focused since it was necessary to prefocus the camera before loading the film.

The film used throughout the present study was Kodak TRI-X Reversal, Type 7278 with an ASA rating of 200 in daylight. With a frame rate of 1000 fps., chosen as the lower

limit of reasonable resolution of an estimated oscillation frequency of 40 cps, no artificial illumination was necessary for drops of molten iron and nickel. In fact, any illumination at all would have to be in the form of backlighting (i.e. silhouetting) since the drop surfaces, being such good reflectors and being curved, would reflect light only from a small point.

In the present set-up, the camera was tilted in order to obtain the top and side views along the diagonal of each frame so that magnification could be as great as possible. These blow-ups also give further indication of the critical nature of the focus, for it was impossible to focus simultaneously on the top and side views, since they were at different distances from the lens. The top view was focused on since it revealed the most information, the side view being mainly for a check on possible rotation of the drop.

During acceleration of the camera to full speed, more or less film is wasted depending on the full speed rating. For 1000 fps this amounts to about 15 feet. It was found convenient to place a title or experiment number on this otherwise wasted footage. This was done by placing a mirror in front of the camera which reflected a title into lens from an illuminated card above levitation chamber. After one second of running the mirror was flipped out of the way leaving the camera with several seconds of film (~5 seconds)

to be exposed at a constant frame rate.

4.3.6 FILM ANALYSIS

Film analysis consists of two separate measurements, one to determine the frame rate and the other to determine the oscillation frequency.

Frame rate measurements involve simply counting the number of frames passing a given point in a given time. Figure 12 is a schematic diagram of a typical piece of film. The time measurements are made directly from the small timing light blips, separated by one millisecond, along the side of the film. For each measurement approximately 20 milliseconds of film were used. If the distance D is the actual amount of film (in mm) which traversed the film gate during t milliseconds and if F is the actual length of one frame in mm, then the frame rate in frames per second is 1000 D/tF.

All measurements of length on the film were taken with vernier calipers measuring to the nearest twentieth of a millimetre. The length of one frame, F, was found consistently to be 7.5 ± 0.005 when measured on a considerable number (in groups of 10) of random frames on randomly selected pieces of film. This is hardly surprising considering that the high speed camera is a precision device and film for high speed must be made to exacting tolerances.

The length, D, was determined by counting integral numbers of frames and adding the fractional parts at either end as measured with the venier calipers. The error in D

is therefore ± 0.1 mm. The error in t, the number of milliseconds is small (± 0.05%, Sec. 4.3.5) but when combined with the error in frame rate determined from the measurements D and F taken from the film, the frame rate measurement error is significant.

Each frame rate was determined at three different places over the length of film, excluding the initial acceleration period, and over approximately twenty frames (i.e. twenty milliseconds at approximately one thousand fps) for each measurement. These three values were averaged to obtain the frame rate for that particular run. The error in the frame rate values given in Tables IV, V are the sum of the error in D, (0.1/150) x 100% (20 frames = 150 mm) the error in F, (0.005/7.5) x 100% and the error in t (0.05%). Thus, we have frame rate, FP ± 0.2%.

The second part of the film analysis consists of determining the number of frames of film that passed through the projector's film gate during a specified number of oscillations. An L.W. Photo, Inc., Photo-Optical Data Analyzer, Model 224-A was used for this purpose. This instrument is capable of projecting 16 mm film at speeds from one through twenty four frames per second forwards and backwards. A mechanical frame counter keeps track of the net number of frames passing through the projector's film gate and may be reset to zero at any stage. The film may also be advanced or reversed, frame by frame.

The film is projected onto a beaded glass screen upon which has been placed an 8-1/2" by 11" piece of translucent, heavy-lined graph paper, 20 x 20 lines to the inch. The projector and screen were placed relative to one another such that the drop image size at the screen is from 3"-5" in diameter. The higher limit was imposed by lack of image brightness above this size while the lower limit was fixed by difficulties in resolving the oscillation frequency for small images since the oscillations were quite small.

The procedure was very straight forward. The film was run through completely after setting the frame counter to zero. Periods of pure oscillation (as distinct from rotation or a mixture of the two, see Appendix A) were noted and then the film was backed up to these periods. Several groups of five to ten oscillations were then examined in more detail. The film was run until in the vicinity of an extremum of oscillation. The grid superimposed on the screen via the graph paper was used to detect the slight motion about the extremum position. The exact location of the extremum position was located by running the film backwards and forwards, continually narrowing the region about this point, until it was observed that advancing or reversing the film about the point by one frame caused the image to move in the same direction away from the extremum. This was taken then as the start of a frequency measurement and the

frame counter set equal to zero. The film was run slowly (6 or 8 fps) for a specified number of oscillations. Approaching the corresponding extremum to that used to start the series, an identical procedure to that described above was used to locate the exact position of this extremum. The entire procedure was then repeated, usually by running the film back over the same area, but relocating each extremum by one oscillation or so. Invaribly, however, both determinations returned the same values within one frame. The measurement error in this technique was considered to be $\pm$ 1.0 frames.

4.4 EXPERIMENTAL PROCEDURE

Prior to each set of experiments, the H.F. generator, the optical pyrometer and the titanium furnace were switched on and allowed to warm up to operational levels before proceeding.

A cleaned specimen of known origin (4.3.4) was taken from the storage dessicator and weighed to $\pm$ 0.0005 gms. This specimen was dropped through the sample addition hole (Figure 5) onto the raised quartz receptor and the hole then sealed with a rubber stopper. The apparatus was sealed as described in 4.21 and evacuated to 0.1 mm Hg, following which it was backfilled with the purified gas mixture (4.2.2) and re-evacuated to the same level. After refilling the chamber with the purified gas mixture to atmospheric pressure, the gas was allowed to pass through the system into the atmosphere. The flow rate was adjusted by means of a needle valve upstream from the chamber and was set by the rate at which it passed through the bubbler. The quartz tube seal was released and the oil bath moved up into position.

The sample was lowered into the levitation coil and levitated immediately the power to the coil was raised. Upon melting, the optical pyrometer was adjusted and the desired temperature reached by manipulating the power input to the coil. At this stage the droplet was completely

stable and the oscillations were visible as a stroboscopic image near the edge of the drop. This effect was very pronounced upon viewing through a red filter which increased the contrast by reducing the background light.

With temperature control established, the camera was set up. After swinging the prism into position over the top of the coil, the camera was focused on the top view of the drop as seen through the prism. The camera was then loaded with 100 feet of film and after checking the camera speed control and the specimen temperature, the camera was switched on. The run lasted approximately five seconds at 1000 frames per second and then the camera was automatically stopped when out of film. After removing the film, the temperature was altered to a new level, and the film taking repeated. This procedure continued until oscillations at four temperatures were recorded. The sample was then quenched by increasing the gas flow rate and directing it at the drop by moving the quartz tube right under the drop. Upon solidification and further cooling, the drop was dropped into the quartz receptor by shutting off the power to the coil. The drop was removed from the chamber after it returned to room temperature and reweighed. The weight measured first was used for the first two temperatures and the latter weight for the last two temperatures. The difference in weight was never greater than 0.001 gm. The

samples were returned to their storage vials in the dessicator.

After processing by a commercial film house, the films were analyzed as described in 4.3.6.

CHAPTER V

EXPERIMENTAL RESULTS

5.1 INTRODUCTION

The surface tension of pure liquid iron was investigated in the temperature range 1550-1650°C and the surface tension of pure liquid nickel in the temperature range 1475-1625°C using the oscillating drop technique in a purified atmosphere of 6% H_2 - balance He.

As well as taking measurements over a range of temperatures, the size of the droplets was varied from 0.5 gm to 1 gm, and for iron, three types of high purity iron were studied in the above ranges of drop size and temperature.

In this chapter, the experimental data are presented in tabular and graphical form and the temperature, drop size and material composition relationships (or lack of relationships) are statistically determined.

5.2 EXPERIMENTAL DATA

The experimentally determined values of frame rate and rate of oscillation of a drop of known weight and impurity level are given in Table IV, (iron-1550-1650°C) and V (nickel-1475-1625°C). The raw data is given in columns 3-6 in either table. The experimental numbers run from F-8 to F-34 for the iron series and from N-1 to N-8 for the nickel series, each number being associated with a specific drop weight and drop material. The second number in this experiment identification scheme refers to the temperature of that particular run. Hence, we have F-8-1550 and F-8-1580 referring to a film of a droplet of Battelle iron weighing 0.994 grams, half the film being exposed at 1550°C corresponding to F-8-1550 and the rest exposed at 1580°C, referred to by F-8-1580. This procedure was used frequently and involved simply stopping the camera half way through 100 feet of film, changing the drop temperature and restarting the camera. However, the same drop is not always referred to by a similar experiment number due to repeats of runs that did not turn out and due also to the fact that only two temperatures could be run on any one roll of film. Similar nomenclature applies to Table V.

The surface tension of each run was calculated in the following way. The number of frames (column 6) was divided by the frame rate (column 4) giving a time (seconds) for the

number of oscillations in column 5 to occur. This time was divided into the number of oscillations as per column 5 to give the drop oscillation frequency. Using (3.27), the value for surface tension of that particular experiment was calculated.

In Figures 14 and 15 the surface tension versus temperature relationships are plotted for iron (Table IV) and for nickel, (Table V), respectively. All three types of high purity iron were assumed to be of virtually the same purity, within the detectable limits available and hence, all the data for iron is regarded as coming from a homogeneous source. This will, in fact, be shown in Chapter 6 using a statistical technique (6.3.2). The points on both Figures 14 and 15 are coded with respect to different size categories.

The linear relationships between surface tension and temperature were obtained by linear regression analysis. The 95% confidence limits about the regression lines are also plotted from the values calculated in Tables B-I, B-II (see Appendix B). In addition, the 95% confidence limits of the slopes of the regression lines have been found. The statistical details are given in Appendix B, i.

5.3 EXPERIMENTAL ERRORS

The scatter in the values of surface tension as seen in Figures 14 and 15 is associated with the experimental errors in frame rate measurement, temperature measurement and control and oscillation frequency measurement. The frame rate was measured to within $\pm$ 0.2% (4.36) and the oscillation frequency to within $\pm$ 1 frames (in terms of frames for a given number of oscillations, column 6, Tables IV and V).

Recalling (3.27) we have,

$$\gamma = 3/8\ \pi\ m\ \omega^2 \qquad (3.27)$$

The fractional error in γ, $\Delta\gamma/\gamma$, resulting from the errors in mass measurement, Δm and in ω, $\Delta\omega$ (where $\Delta\omega$ is the sum of the errors in frame rate measurement, ΔS, and in number of frames for a given number of oscillations, ΔD) was found on differentiation of (3.27) to be

$$\frac{\Delta\gamma}{\gamma} = \frac{\Delta m}{m} + 2\ \left(\frac{\Delta S}{S} + \frac{\Delta D}{D} \right) \qquad (5.1)$$

for $\Delta m/m$, $\pm$ 0.1% (4.4), for $\Delta S/S$, $\pm$ 0.2%, and for $\Delta D/D$, $\pm$ 1.0% (4.3.6), the estimated error in surface tension for any individual measurement is $\pm$ 2.5%. It is to be noted that this error bound is not directly related to the 95% confidence limits since the 2.5% error bound deals with each measurement individually, whereas the 95% confidence interval deals with the "expected" value of surface tension as predicted by the regression equation.

It is also to be noted that in Figure 14, some five points lie outside the 95% confidence limits. This is readily explained on consideration of the fact that the 95% confidence interval implies that the regression line passes through the 2Σ limits about any point. The standard deviation, Σ, for the iron data is 5.9 dyn/cm and for the nickel data, it is 8.4 dyn/cm, (Appendix B). It is readily seen from an examination of Figures 14 and 15 for iron and nickel respectively that the regression line does pass within the 2Σ limits of every point lying in or outside the 95% confidence limits.

The uncertainty in temperature measurement is $\pm$ 10°C for iron and $\pm$ 15°C for nickel (4.3.3), the difference being due to different pyrometer techniques.

As indicated in Tables IV and V some of the data obtained was not plotted. There were two reasons for this. The first was simply that occasionally the film appeared to slip in the film gate of the camera during running and on projection these films showed a sequence of translating images moving up and down the screen. This made measurement of the oscillation frequency impossible. A majority of these situations were refilmed as noted. The cause of the film slippage was traced to loose idler wheel supports which moved occasionally under the stresses of high speed running. A second reason for discarding data was that some filmed runs appeared to exhibit no pure oscillations but rather a mixed oscillation involving rotation of the drop. This phenomenon

is discussed in detail in Appendix A and was characterized by consistently lower values of oscillation frequency. The cause of this rotation-oscillation interaction is thought to be some instability in the power imput to the H.F. generator which causes the field strength in the coil to fluctuate and, hence, to disturb the otherwise stable drop so that it began to rotate while oscillating. That the oscillation frequency is shifted is a direct consequence of rotational motion of the drop as one of the basic premises of the theory of Rayleigh (3.2.1) is irrotational motion.

CHAPTER 6.

DISCUSSION

6.1 Introduction

Some general experimental considerations are discussed including drop stability, the attainment of equilibrium, sample purity and film analysis.

The surface tensions of both iron and nickel are compared to previous work at 1550°C. A very limited amount of work has been done on the effects of temperature on surface tension measurements of these two metals at high temperatures, but indications are that other workers have also found a positive temperature coefficient. The effects of drop shape variations and deviations from the spherical equilibrium shape are discussed.

Finally drop oscillations are discussed generally with respect to the magnitude of the vibration, observed oscillation patterns, initial impulse to begin vibration and other parameters whose possible effects were discussed in 3.3.

6.2 Experimental Considerations

6.2.1 Drop Stability

Drop stability in a levitation melting system is dependent on both static and dynamic elements. Static stability is due to balanced electromagnetic and gravitational forces resulting in a stable location of the centre of mass with respect to the coil. On the other hand, dynamic stability is concerned with the internal oscillations set up by these same forces and surface tension about the stable centre of mass.

The static stability is influenced mainly by the design of the levitation coil (4.3.1). Hence with careful coil design and construction, the elimination of bulk drop rotation and translation was achieved and the equilibrium, non-oscillatory drop shape was considered to be stable. It was most critical to completely cut out the rotational degree of freedom for,if rotation occured,the oscillatory degree of freedom was non-operative.

Dynamic instabilities of this internal degree of freedom were observed during the course of the experiments to determine the surface tension of iron and nickel and this resulted in the rejection of some of the data as noted in Tables IV and V. Appendix A is an attempt to show the result of dynamic instabilities by comparing photographic enlargements of sequences of stable oscillations, no oscillations (but rather simple drop rotation) and unstable oscillation (hitherto

termed mixed oscillations). It would be, however, much more beneficial to observe the actual film while it is being projected at a slow speed, say 10 fps.

These unstable oscillations are a result of small fluctuations in power output from the high frequency generator due to variations in the power supply from the mains. A small decrease in power for example, will lower the position of minimum field strength in the coil (the null point), forcing the levitated drop to seek a new location at the new null point. The drop is thus in translation and will be affected as would any other conductor moving in a non-uniform electromagnetic field. All the while, however, the drop may be oscillating with a charateristic frequency and amplitude. As will be shown later (6.5), the directions of the axes of symmetry of oscillation are a function of the distribution of the electromagnetic field in the coil (Figure 19). Movement of the drop in the coil and altering the field strength would cause a slight adjustment in the relative orientations of these axes, disturbing the previously stable pattern of oscillations. Once disturbed, the droplet is no longer symmetrically located with respect to the electromagnetic field, as if it had been given a small downward push. The resulting instability as caused by the change in oscillation pattern was observed to initiate drop rotation as a result of the asymmetric displacement of the drop.

Rotation mixed with oscillation lowered the observed oscillation frequency and hence, invalidated that particular frequency measurement for the purposes of calculating surface tension.

It was observed, however, that usually these instabilities quickly died out and the drop resumed its characteristic oscillation frequency. This is thought to be mainly due to the high value of surface tension in these two systems, Fe and Ni, which may be expected to inhibit the growth of instabilities[60].

The cause of these instabilities, then is not easily eliminated since one has no control over the mains voltage. However, between the hours of 10:00 pm and 3:00 am approximately, fluctuations in line voltage are minimial, both in number and in magnitude and most of the valid experimental runs were obtained in this time period.

6.2.2 Attainment of Equilibrium

A levitated molten droplet of pure liquid metal is not in complete thermodynamic equilibrium with the bulk of gaseous phase since, as noted in 4.4, continuous vapourization is occuring. This is due to the existence of a cold spot in the system, namely the water cooled levitation coil, which acts as a sink for metal vapour condensation. The complete elimination of this sink in the present set-up is virtually impossible since the copper levitation coil cannot be

operated without water cooling. Nevertheless, it is still possible to establish that the levitated drop system is in mechanical equilibrium with its surroundings; i.e. there is no net force acting on the molten droplet. Also, it is likely that a good approximation to thermodynamic equilibrium between liquid metal and its vapor exists in the interface since mass transport away from the interface has been suggested to be the rate controlling step of vaporization[27].

Drop stability (6.2.1) is a necessary condition for mechanical equilibrium for it is accomplished only as a result of an exact balancing of the electromagnetic, gravitational and surface tension forces. Any rotation or precession of the drop is clear evidence of an imbalance in these forces and hence a visual examination of any film of a levitated drop is sufficient to establish the existance or non-existance of mechanical equilibrium.

Recalling equation 2.29 and using the results of 2.30 we have,

$$p^{\alpha} - p^{\beta} = \frac{2\gamma}{a} \qquad (6.1)$$

where p^{α} is the hydrostatic pressure exerted within the drop and p^{β} is the pressure exerted inwards on the drop, taking into account electromagnetic, gravitational and surface forces arising from continuous evaporation and adsorption.

This relation is, of course, the defining equation for surface tension under conditions of mechanical equilibrium.

No temperature dependance is implied in (6.1), as a direct consequence of the derivation of this relation in terms of the first law of thermodynamics, without the restrictions imposed by the second law of thermodynamics.

This definition of surface tension in terms of energy/unit area is very well suited for use with the Rayleigh equation, 3.27, since it implies nothing of the nature of surface tension, except that it is surface energy/unit area which is identical to concept used by Rayleigh and Lamb in their work[37].

6.2.3 Sample Purity

The analysis of the various types of iron and of electrolytic nickel (as received) are found in Tables I and II, respectively. Following the cleaning procedure outlined in 4.3.4, a representative random sampling of specimens was analyzed for oxygen content (Table III). However, with the oxygen analysis done by vacuum fusion in the available equipment (LECO) any analysis is only accurate to $\pm$ 10 ppm. Therefore, although the indications are that the oxygen content of a "clean" specimen was approximately five times lower than 10 ppm in all cases, one must assume that the oxygen level is 10 ppm.

This procedure was actually a check on both sample and chamber atmosphere cleanliness (with respect to oxygen), for an otherwise clean metal would pick up any oxygen from the gas mixture. Therefore, knowing that the maximum oxygen

content of the metal is 10 ppm, the corresponding maximum Po_2 of the gas mixture is easily estimated to be of the order of 10^{-14} atm. at 1550°C based on the reaction

$$\frac{1}{2}\,O_2\,(g) \rightarrow O_{(wt\ \%\ in\ Fe)} \qquad (6.2)$$

the standard free energy of reaction (cal) being [62]

$$\Delta G^\circ = -27{,}790 - 0.79\,T \qquad (6.3)$$

The Po_2 of the gas, however, was thought to be somewhat lower than this due to the inability of the gas, as purified, to oxidize a small levitated piece of aluminum (4.2.2). The oxygen level in the gas was therefore, somewhere between 10^{-14} and 10^{-30} atmospheres (the lowest possible Po_2 of the purified gas, 4.2.2) and the oxygen level in the levitated drops is therefore chiefly a function of the initial oxygen level. The effect of the various types of iron used on surface tension measurements is discussed in 6.3.2.

A similar investigation with sulphur was not considered necessary since additional sulphur would not have been picked up by a specimen either in specimen cleaning or from the purified gas, which contained no detectable sulphur. Thus the sulphur levels in the drops were taken as those given in Tables I and II.

6.2.4 Film Analysis

As shown in 5.3, the major contribution to experimental measurement errors arose from the film analysis involving the techniques of determining frame rate and the number of frames for a given number of oscillations.

The frame rate or film speed measurements could be improved if there were no variation in camera speed from one run to the next. The camera running speed is controlled through voltage regulation which is, unfortunately, a function of the mains voltage to which the camera is connected. The mains supply used here is 120 volts rather than the 550 volt supply to the H.F. generator and the former is used a great deal more in everyday local practice. During the daytime hours the load on the 120 volt supply reduces the voltage to as low as 108 volts and this figure fluctuates much more than the 550 volt supply. Hence one could never be sure of the voltage controlling the camera speed and this was reflected in the variation in frame rate from run to run.

The use of a constant voltage supply for the camera speed regulator would eliminate these variations and allow a large number of measurements of the same frame rate to be made. This would, in turn, give one the opportunity to make a statistical estimate of the measurement errors involved in frame rate determination.

By increasing the frame rate of the camera, say by a factor of three, the resolution of the oscillation frequency

might also be improved. The change in direction of the drop motion as it passes through an extremum position would take place more slowly and the determination of the number of frames per cycle could be more exact. One difficulty that might arise, however, is that, at slower projection rates (8 fps as projection speed for a film taken at 100 fps is the full 24 fps for a film taken at 3000 fps, based on the same number of drop oscillations) the distinction between stable and unstable oscillations is exceptionally difficult to observe.

6.3 Surface Tension of Pure Liquid Iron

6.3.1 The Effect of Temperature

The surface tension of pure liquid iron was measured at 1550°C, 1580°C, 1620°C and 1650°C and the results plotted as a function of temperature in Figure 14. A straight line was fitted to this data by linear regression analysis (Appendix B, part i). Therefore, the temperature dependance of the surface tension of liquid iron is expressed as

$$\gamma_{Fe} = 0.68t + 725.7 \qquad (6.4)$$

in the range 1550-1650°C. The 95% confidence limits about the slope (0.68) of this line are 0.58 and 0.78 (Appendix B, part i) and thus the surface tension of pure liquid iron increases with increasing temperature in this temperature range. The correlation coefficient for this regression line was found to be 0.97.

The positive temperature coefficient found here is somewhat surprising since, $\frac{\partial \gamma}{\partial T}$, has been shown to be (2.15),

$$\left(\frac{\partial \gamma}{\partial T}\right)_{x\alpha} = -\sigma + \sum_{i=1}^{x} \Gamma_i \left(S_i^{\alpha} - v_i^{\alpha} \left(\frac{\partial P}{\partial T}\right)_{x\alpha}\right) \qquad (2.37)$$

where σ is the superficial density of the entropy $\left(\frac{S^s}{A}\right)$ and Γ_i is the superficial number density of the molecules of species i ($N_1^s/A \equiv \frac{-d\gamma}{d\mu_i} \equiv \Gamma_i$). This relation, however, is based on the assumption of thermodynamic equilibrium. But

the oscillatory levitated drop system is known not to be in thermodynamic equilibrium (6.2.2) and hence 2.37 cannot be expected to be an exact description of the temperature dependance in the present case. We shall, nevertheless, attempt an explanation of the positive temperature coefficient based on the functional dependances indicated by 2.37.

The surface entropy term ($-\sigma$) in 2.37 might be expected to be negative even for systems such as studied here since surface entropy in general will increase in proporation to a given temperature rise.

The second part of the temperature dependance expression is related only to adsorption of the various species i=1, ..., x. It is apparent, then that adsorption phenomena may be the cause of the positive temperature coefficient. It is known that evaporation is increased with temperature rise and it is possible that at higher evaporation rates, the adsorption of trace amounts of surface elements which tend to lower the values of surface tension is inhibited. In other words, there is less chance, say, of an oxygen atom (or water molecule) from reaching the surface due to collision with atoms escaping from the surface while simultaneously there is a greater possibility of surface active atoms leaving the drop surface. It is also possible that some unknown but volatile species of a surface active nature is distilled off at higher temperatures, thus creating the appearance of a positive temperature coefficient for the surface tension of

liquid iron.

This same effect was observed by Kingery et al in the discussion of the work of Kozakevitch and Urbain[63] in the study of the surface tension of the iron-carbon eutectic in vacuum where the explanation of possible volatiles distilling off was substantiated by an apparent hysteresis in surface tension values. The surface tension increased on heating but on cooling did not decrease at the same rate (but rather more slowly), approaching the heating values only at lower temperatures.

It should also be noted that experiments on the effect of temperature on the surface tension of copper have also showed a positive temperature coefficient in the range 1100°C-1400°C[64, 65]. However, from 1400°C to 1600°C, the temperature coefficient was negative[65], having changed sign in the neighbourhood of 1400°C. These results, however, have yet to be explained.

We can, therefore, say nothing quantitative about our results for the effects of temperature, other than to suggest possible explanations and to observe that such a positive temperature coefficient is not unprecedented and may, in fact, follow the same pattern as does $\partial\gamma/\partial T$ for copper. That surface tension must eventually go to zero with increasing temperature is obvious since, at the critical point, surface tension ceases to exist. The work on copper[65] was done over a much higher temperature range above the melting point of

copper (1083-1600°C), the comparable range for iron being 1535°C to 2250°C (in terms of percentage above the melting in °K). The extension of the present data for iron in this range, then, is necessary before drawing any positive conclusion about the temperature dependance of the surface tension of pure liquid iron.

6.3.2 THE EFFECTS OF IMPURITIES

As mentioned in 6.2.3, the oxygen and sulphur levels as well as other impurity levels in a levitated drop of iron are essentially determined from the initial solute concentrations given in Table I. The oxygen and sulphur levels of the iron drops that would be in equilibrium with the purified gas mixture were below the limits of detection of the available analytical techniques. Therefore, as an upper bound on the oxygen content for this system a figure of 10 ppm was used, even though this is somewhat of a hypothetical value and possibly high by a factor 5 or more. Sulphur levels and those of other impurities were taken to be as given by the suppliers of the various types of high purity iron.

In descending order of overall impurity level we have, therefore, Ferrovac "E", NPL and Battelle irons, (Table I). Since surface active elements will have a cumulative effect in lowering the surface tension, the overall effects of impurities on the surface tension was investigated from the existing data by grouping the data according to origin at each temperature and applying analysis

of variance statistics to this arrangement of data. The exact techniques and figures are given in Appendix B, part ii.

As a result of this analysis, it was found that, with 95% confidence, there appears to be no significant effect on measured surface tension values involved in using one or another of the above types of iron.

6.3.3 THE EFFECTS OF DROP SHAPE

One of the basic assumptions involved in the derivation of Rayleigh's equation is that the oscillations take place about a spherical equilibrium shape. In the leviated drop system such a spherical equilibrium shape is not found, but it was observed that small droplets approached this ideal much more closely than larger ones. This is a gravitational effect and is shown in Figure 16 where the differences in shape for three drop sizes in the range of half a gram to one gram are compared to a true sphere. The size limits of half gram and one gram were due to difficulties in melting specimens smaller than half a gram and in levitating one larger than one gram.

Similar to the technique used in 6.3.2, the data was grouped according to drop size, at each temperature, the size grouping being less than 0.6 gms, between 0.6 and 0.9 gms and greater than 0.9 gms. Analysis of variance techniques were then used on this arrangement of the data. The results are given in Appendix B, part ii.

It was found with 95% confidence that there appeared to be no effect of altering the drop sphere on surface tension values in the size distribution from half a gram to one gram. This range corresponds to a 25% change in radius for a sphere and as seen in Figure 16, a fair departure from the spherical equilibrium shape for the actual non-spherical drops. It appears, therefore, a certain amount of leeway may be allowed for in applying the assumption of spherical equilibrium in the present system.

6.3.4 COMPARISON WITH PREVIOUS WORK

In comparing the values of surface tension for iron obtained by the oscillating drop technique to previously measured values, it is only possible to compare the figure obtained at 1550°C, since no work has been done on this system at higher temperatures. Previous work has been summarized in 2.3.1 and is now presented in tabular form along with the present work in Table VI (1550°C only).

It is seen that at 1550°C, the present work agrees very favourably with the most widely accepted previous work, that of Kozakevitch and Urbain[24]. They have obtained a value of 1788 dynes per cm. at 1550°C and this value was claimed to be within ± 1% of the true value of surface tension of pure liquid iron (i.e. iron without any oxygen or sulphur). The iron used by these authors was reported to contain from one to ten ppm of oxygen and no detectable sulphur. A plot of surface tension of the liquid iron-oxygen

system versus weight percent oxygen (Figure 17) shows that below 10 ppm oxygen, the surface tension of iron as a function of oxygen concentration is constant within the limits of experimental error. Thus, the three types of iron used in this work are equivalent to that used by Kozakevitch and Urbain[24]. Also, the Po_2 of the gases employed by Kozakevitch (purified hydrogen; $Po_2 < 10^{-15}$ atm) and that of the gas used here (purified 6% H_2, balance He; $Po_2 < 10^{-14}$ atm) were similar.

The basic difference, therefore, is in the method of measurement of surface tension where previous work was done with static measurements, notably the sessile drop technique, and the present work done with a dynamic method. That such close agreement has been reached in the measured values of surface tension of pure liquid iron between a well established technique and the rather radical method of oscillating drops is encouraging.

6.4 SURFACE TENSION OF PURE LIQUID NICKEL

6.4.1 THE EFFECT OF TEMPERATURE

The surface tension of liquid nickel was measured at 1475°C, 1525°C, 1575°C and 1625°C and the results plotted as a function of temperature in Figure 15. Using linear regression analysis again, a straight line was fitted to this data (Appendix B, part i). The temperature dependance of the surface tension of liquid nickel in the range 1475-1625°C is expressed as

$$\gamma_{Ni} = 0.21t + 1663.8 \qquad (6.5)$$

The correlation coefficient representing "goodness of fit" was found to be 0.94 which is statistically highly significant at the 95% confidence level. The 95% confidence limits about the slope of (6.5) are, however, 0.6 to -0.2 (Appendix B, part i). Thus, although a linear relationship may, in fact, exist in this temperature range, it is not possible to say with any degree of precision whether γ_{Ni} does really rise or fall with increasing temperature.

The same conclusion may be reached as in the case for iron (6.3.1) that a broader temperature range up to 2150°C should be studied before committing ourselves to an explanation of the positive and/or negative temperature coefficients of pure liquid nickel.

As the situation now stands, there appears to be less of an effect of temperature on the surface tension of liquid nickel in the given temperature range than on the surface tension of liquid iron.

6.4.2 THE EFFECT OF IMPURITIES

Since only one variety of high purity nickel was available for this study, the effects of varying the initial levels of the different impurities were not investigated. Nevertheless, since identical experimental conditions were used to clean and levitate the iron and nickel specimens, the comments made in 6.3.2 about the impurity level in any given specimen are valid for nickel. It can be said, therefore, that the maximum impurity levels of the various solutes in nickel was a function of the initial purity of the specimens as quoted in Table II. Again, the maximum oxygen content was assumed to be 10 ppm due to the limits of detection available.

6.4.3 THE EFFECTS OF DROP SHAPE

As was done for the surface tension measurements for iron, the nickel results were grouped according to size distribution at the four temperatures of measurement. Analysis of variance statistics were applied to this table (Appendix B, part ii) in the same manner as in 6.3.3. This analysis again showed that there appeared to be no effect of altering the drop shape on the surface tension values for nickel in the size distribution from half a gram to slightly less than one gram.

The absence of any detectable drop shape dependance for both iron and nickel surface tension values is an important result. This is the justification for using Rayleigh's relationship either in its simplest form (3.27) or in more complex terms (as per 3.3) since any of these equations is based on oscillations about the spherical equilibrium shape. It is especially significant in the light of work done on falling fluid droplets which generally could not be assumed to have a spherical equilibrium shape[47, 48, 49] (also 3.3.2).

6.4.4 COMPARISON WITH PREVIOUS WORK

As with the surface tension of liquid iron, the only comparison that may be made with the present work on nickel and previous work is at 1550°C. The latter work has been reviewed in 2.3.2 and, as noted there, there appears to be a great amount of discrepancy from one author to the next. However, due to general acceptance of the work by Kozakevitch and Urbain in the measurement of surface tension of liquid metals, we shall compare the present work to theirs[24]. The value they obtained at 1550°C for high purity liquid nickel in 1934 dyn/cm (other authors report lower values), to be compared to 1990 dyn/cm for the present work. This is a favourable agreement taking into consideration estimated accuracy limits of $\pm$ 2.5% for the present work and somewhere of the order of $\pm$ 1% for the former (actual accuracy not given).

It appears from the work of Kozakevitch and Urbain[24] that the oxygen and sulphur contents of the nickel used in their experiments was at a similarly low level as that used in this case. The value of 1934 dyn/cm is dependent on the value of the density of liquid nickel at 1550°C which is a disputable figure. It can, therefore, be stated that the present work is in reasonable agreement with previous work.

6.5 INTERNAL CONSISTENCY OF PRESENT WORK

In evaluating any new technique, the internal consistency of the measurements of surface tension by the oscillating drop method is most important. This is the only yardstick by which one may evaluate the worth of any given set of data. With the establishment of internal consistency (by which is meant the relationship of each piece of data to the other) comparison can be made with other independent sets of internally consistent data to show the existence of possible systematic errors.

In the present work with iron and nickel, it has been shown (6.3) that, although different drop sizes and different sources of high purity material (iron only) were used, these factors did not have any influence on the measured values of surface tension. Hence each experiment at a given temperature may be regarded as a duplicate of any of the others and therefore, what appear to be a number of independent experiments at first glance are, in fact, homogeneous data.

Probably the best estimate of internal consistency is the standard deviation of the mean of the data at any temperature. However, there is not enough data at any one temperature to properly apply this technique. A quantity which is useful, nevertheless, is the standard error of the estimate or the standard error about the regression line which is calculated considering the regression line as the

mean (Appendix B, part i). All points are used and a reliable estimate of the standard deviation at any temperature is found. It can be shown[57] that this estimate is larger than the standard deviation as conventionally found. The standard deviation for the iron data was found to be 5.9 dyn/cm and for the nickel data was found to be 8.4 dyn/cm.

The standard deviations for both sets of data are quite small and hence, regardless of the magnitude of the experimental error, this is a good indication of the existence of internal consistency in the measurements taken in these experiments.

6.6 DROP OSCILLATIONS

6.6.1 INTRODUCTION

In Chapter 3 an attempt was made to establish the validity of many of the assumptions stated in 3.2.1 by consideration of the oscillating levitated drop system as a whole. Many significant results were obtained in this manner especially in regards to the effects of drop and atmosphere viscosities, inertial effects and the influence of charge on the drop surface.

Several major assumptions, however, remained to be verified by experiment, specifically the assumptions of the spherical equilibrium drop shape and of small oscillations about this sphere. In 6.3.3 and 6.4.3 the effects on the oscillation frequency of changing the equilibrium drop shape from a nearly spherical shape to a pronounced egg shape (Figure 16) was studied. Within the limits of the experiments performed to date no significant effect on the oscillation frequency could be determined. However, on viewing the films of the various drop sizes it is apparent that the smaller drops (1/2 gm.) oscillated with a relatively larger amplitude and also appeared to be much less susceptible to minor fluctuations in field strength. Hence, not only was detection of the frequency made easier by the larger amplitude, but also measurements could be made over a larger number of oscillations.

The remainder of this section will be given, then, to a discussion of the magnitude of the deviation from the equilibrium shape during oscillation and to a more general discussion of the nature of the oscillations.

6.6.2 AMPLITUDE OF VIBRATION

There are two factors concerning the amplitude of vibration which should be discussed. These are the magnitude of the maximum deviation from the equilibrium shape and the difference in magnitude between large and small drops.

It has been estimated[68] that the maximum deviation from the equilibrium configuration should be no greater than ten percent of the diameter of the drop in order to conform with the assumption of small oscillations. This figure of ten percent is, however, a very rough approximation and cannot be established by a rigourous mathematical treatment. In the present case, it is suspected that ten percent is a low estimate due to the very high values of surface tension which supply very large restoring forces to counteract perturbation.

In Appendix A, a series of stable oscillations is shown as part of a comparison with a rotating drop and a series of unstable oscillations. The stable oscillations are typical of those of a small droplet (1/2 gm) and hence typical of a drop showing maximum amplitude of vibration (6.6.1). Figure 18 (a), (b) compares the top view of an equilibrium position and of an extremum position, respectively,

for such a case (Experiment number F-33). The diameters of the nearly spherical equilibrium shape (Figure 18 (a)) are 67 and 68 mm long while the major and minor axes of the extremum shape are 74 and 59 mm respectively. The average deviation, then, from the equilibrium position is 7.5 mm or eleven percent. Since this is, as stated above, the most extreme deviation observed, the original assumption of small oscillations is obeyed in this system.

The difference in amplitude between small and larger drops cannot be explained quantitatively at present. It is suspected, however, that an impulse of uncertain origin which triggers the oscillations imparts the same amount of energy to the small drop as to the larger. Hence, since the restoring force (surface tension, erg cm^{-2}) is a function of the drop surface area, the smaller drop tends to deviate from the equilibrium position to a greater extent. To date the actual onset of vibration has not been observed but it is quite probably associated with disturbances observed during sample melting since invariably a newly melted specimen was observed to oscillate. Also, after long periods of levitation, the oscillations appeared to vanish.

6.6.3 AXES OF VIBRATION

It is shown in Figure 19 (a) that the field distribution within a similarly designed levitation coil to that used here is such that a maximum force is exerted on the

levitated specimen in the vertical and horizontal planes, ie. the field strength is greatest in these planes. (If δ is the depth of penetration of a high frequency electromagnetic field where $\delta = 15\ f^{-\frac{1}{2}}$ cm and f is the frequency in cps, then when δ is small compared to the diameter of the drop, the mean hydromagnetic pressure is $B^2/8\pi$ where B is the maximum field strength[60]). This feature of levitation coils determines the axes of vibration for an oscillating levitated droplet.

Since the maximum force pushing in on the drop is exerted in the vertical or horizontal planes it is not surprising to observe that the drop oscillates along axes situated between these planes as shown in Figure 19 (b). It appeared that, in the cone traced out by rotation of these axes about the axis of symmetry of the coil, there was no preferred direction of oscillation. Thus, with respect to the stationary camera, the drop as observed via the top view, did not always oscillate in the same direction. This was due to the complete symmetry of the electromagnetic field surrounding the drop and it seems that the direction of the initial impulse starting the oscillations must determine the particular pair of axes of vibration, each pair being exactly equivalent to any other in that cone of rotation as described above.

CHAPTER VII

CONCLUDING REMARKS

7.1 SUMMARY

The assumption of mechanical equilibrium (i.e. no net forces acting on the system) lead to a definition of surface tension which appears to be compatible with the experimental measurement of surface tension in the levitation melting unit. Other methods and the general pitfalls of measuring surface tension of pure liquid metals at high temperatures were reviewed. The existing data from the literature on the surface tensions of pure liquid iron and nickel were also reported.

The theory of oscillating fluid drops was investigated with respect to the levitation melting set-up used in this study and it was established that the Rayleigh equation in its simplest form was sufficient to describe the oscillation of molten drops of levitated iron and nickel.

The surface tensions of pure liquid iron and nickel were then found by the measurement of the oscillation frequencies from the high speed film taken of the molten levitated drops in the temperature ranges from melting to approximately one hundred degrees centigrade above melting. Besides temperature, the variables of drop shape and material type (iron only) were also studied.

The surface tension of pure liquid iron as a function of temperature was found to be

$$\gamma_{Fe} = (0.68 \pm 0.10)\ t + 725.7 \text{ dyn cm}^{-1} \quad (1550\text{-}1650°C)$$

and for pure liquid nickel was found to be

$$\gamma_{Ni} = (0.21 \pm 0.43)\ t + 1663.8 \text{ dyn cm}^{-1} \quad (1475\text{-}1625°C)$$

where temperature t, is expressed in degrees centigrade. The only point of comparison for these values for the surface tensions of iron and nickel is at 1550°C and, within the limits of experimental error, reasonable agreement has been found with previously accepted work.

Statistical analyses of the data as functions of drop shape and material type (iron only) showed that, in the ranges of these variables studied, there was no significant effect of either on the values of surface tension at any temperature. The absence of any material type dependance is a clear indication of the ease with which drop purity, as regards to oxygen and sulphur levels, may be controlled in a levitation melting system.

The absence of drop shape dependance of surface tension in the range covered here has established the validity of the initial assumption of a spherical equilibrium drop shape. It was also verified, independently from drop

equilibrium shape considerations, that the assumption of small oscillations about the equilibrium was valid for the systems studied.

In conclusion then, it has been shown that the surface tension of pure iron and pure nickel can be successfully determined in a levitation melting system by the measurement of the frequency of the oscillating fluid droplet. The underlying assumptions of Rayleigh's equation relating natural oscillation frequency with surface tension were obeyed by such a system and no additions or alterations to the original equation were required. The values of surface tension obtained by this technique have been shown to possess both internal consistency and agreement with independent work. As with all surface tension measurement techniques, the control of specimen cleanliness was of the utmost importance and careful consideration was taken even of seemingly unnecessary details.

7.2 SUGGESTIONS FOR FUTURE WORK

It was not the purpose of this thesis to only establish a "better" and fast technique for the measurement of the surface tension of molten metals but simply to investigate the possibility of measuring surface tension in metallurgical systems in a convenient way. It is believed that surface tension as measured by the oscillating drop technique will be an important tool for the investigation of the initial rates of oxidation and sulphidation of liquid metals at high temperatures since surface tension values have been shown to vary very rapidly in the presence of very small quantities (up to 500 ppm) of oxygen and sulphur.

Before this work is undertaken, however, there are several matters concerning the technique which should be looked into. The first of these is the increase in accuracy of the measurements. It is suggested that, at higher film speeds (e.g. 3000 fps), the determination of the number of frames in "n" oscillations can be considerably improved. Although the absolute error in determining the start and finish of any given cycle may remain the same at higher frame rates, the relative error will be less by a factor of three. The absolute error may also be significantly reduced by a photographing against a grid, several frames in the neighbourhood of the estimated start/finish of a given cycle.

This should virtually eliminate error by the experimenter in choosing the oscillation end-point as he would be able to compare these frames simultaneously. This will be especially important at 3000 fps where the changes in shape about the extremum position are very small indeed.

It is also to be observed that pure iron and nickel have extremely high values of surface tension, among the highest of any known substance. The study of a metal such as copper with a surface tension in the range of 1300 dyn cm^{-1} would be very useful in terms of investigating drop shape effects. The lower the surface tension, the more elongated and less spherical the drop's shape becomes and the assumption of spherical equilibrium shape may no longer hold.

The temperature coefficients of surface tension of pure liquid iron and nickel should also be measured over a much larger range of temperatures above the melting point in order to establish with certainty the behaviour of surface tension of these metals with temperature. It also would be very interesting and, possibly, very rewarding, to study the surface tension of these liquid metals when supercooled. This condition is very easily achieved with pure metals in a levitation system and up to 400 centigrade degrees supercooling have been reported with pure iron.

BIBLIOGRAPHY

1. Flugge, S: (Editor) Encyclopedia of Physics V.X. Structure of Liquids, p. 77-78, Springer-Verlag (1960).

2. Gibbs, J.W: The Collected Works of J.W. Gibbs V.1, Longmans-Green (1928).

3. Flugge, S: op cit, 138-140.

4. Fowler, R.H: Proc. Roy. Soc. London, (1937), 159, 229.

5. Flugge, S: op cit, 145-157.

6. Kondo, S. J: Chem. Phys., (1956), 25, 662.

7. Flugge, S: op cit, 145-148.

8. Swalin, R.A: Thermodynamics of Solids, 143-147, Wiley (1962).

9. Flugge, S: op cit, 148-149.

10. ibid., 157-280.

11. ibid., 140-142.

12. ibid., 149-152.

13. White, D.W.G., Metals and Materials (1968), Review 124.

14. Semenchenko, V.K: Surface Phenomena in Metals and Alloys 43-115, Pergamon (1962).

15. Kozakevitch, P.P. and Urbain, G: J. Iron Steel Inst., (1957), 186, 167.

16. Hughel, T.J: (Editor) Liquids: Structure, Properties, Solid Interactions, 243-258, Elsevier (1965).

17. Thomson, W: Phil. Mag., (1871), 42, 362.

18. Sutherland, K.L: Austr. J. Chem., (1954), 7, 319.

19. Rayleigh, Lord: Proc. Roy. Soc. London, (1879), 29, 71.

20. Bohr, N: Phil. Trans. Roy. Soc., (1909), 209(A), 281.

21. Duckworth, H.E: Electricity and Magnetism, MacMillan, (1960).

22. Cade, R: Proc. Phys. Soc., (1964), 83, 997.

23. Peterson, A.W., Kedesy, H., Keck, P.H., and Schwartz, E: J. Appl. Phys., (1958), 29, 213.

24. Kozakevitch, P.P. and Urbain, G: Mem. Scient. Rev. Met. (1961), 48, 517.

25. White, D.W.G: Trans. A.I.M.E., (1966), 236, 796.

26. Timofeevicheva, D.A: Russian J. Phys. Chem., (1961), 35, 558.

27. Sunderland, M: Private Communication.

28. Kozakevitch, P.P. and Urbain, G: Mem. Scient. Rev. Met., (1961), 48, 401.

29. Kingery, W.D. and Humenik, M: J. Phys. Chem., (1953), 57, 359.

30. Kingery, W.D. and Halden, F.A: J. Phys. Chem., (1957), 59, 557.

31. Wan Tsin Tan, Karassev, R.A. and Samarin, A.M.: Izv. Ahad. Nauk S.S.S.R., Old. Tekh. Nauk, Metall. i Toplivo, (1960), 1, 30.

32. Eremenko, V.V., Ivashenko, Y.N., Nijenko, V.N., and Fessenko, V.V: Izv. Akad. Nauk S.S.S.R., Old Tekh. Nauk. Metall. i Toplivo, (1958), 7, 144.

33. Kingery, W.D. and Kurkjian, C.R: J. Phys. Chem., (1956), 60, 961.

34. Monma, K. and Suto, H: J. Japan. Inst. Metals, (1960), 24, 167.

35. Thomson, W: Phil. Trans. (1863), 3, 384.

36. Rayleigh, Lord: Theory of Sound V.2. 2nd. Ed. 371-375, Dover, (1945).

37. Lamb, H: Hydrodynamics 6th ed, 473, Cambridge, (1952).

38. Lamb, H: Proc. London Math. Soc. (1), (1881), 13, 51.

39. Chandrasekhar, S: Proc. London Math. Soc. (3), (1959), 9, 141.

40. Reid, W.H: Quart. Appl. Math., (1960), 18, 86.

41. Chomiak, J: Fluid Dynamic Trans., (1964), 1, 371.

42. Okress, E.C., Wroughton, P.M., Comentez, G., Brace, P.H. and Kelly, J.C.R: J. Appl. Phys. (1952), 5, 545.

43. Bronwell, A: Advanced Mathematics in Physics and Engineering, Addison-Wesley, (1958).

44. Goldstein, H: Classical Mechanics Addison-Wesley, (1951).

45. Sokolnikoff, I.S. and Redheffer, R.M: Mathematics of Physics and Modern Engineering 2nd ed. McGraw-Hill, (1961).

46. Levich, V.G: Physicochemical Hydrodynamics 653, Prentice Hall, (1962).

47. Subramanyam, S.V: J. Fluid. Mech., (1969), 37, 715.

48. Miller, C.A. and Scriven, L.E: J. Fluid Mech., (1968), 32, 417.

49. Taylor, T.D. and Acrivos, A: J. Fluid Mech., (1964), 18, 466.

50. Weast, R.C: (Editor) Handbook of Chemistry and Physics 50th ed. The Chemical Rubber Co., (1963).

51. Shiraishi, S.Y. and Ward, R.G: Can. Met. Quart., (1964), 1, 117.

52. El-Mehairy, A.E. and Ward, R.G: Trans. A.I.M.E., (1963), 227, 1226.

53. Peifer, W.A: J. Metals, (1965), 17, 487.

54. Kershaw, P: Ph.D. Thesis, McMaster University, 1968.

55. Anon, Hycam High Speed Motion Picture Camera Manual, Red Lake Laboratories, Inc., Santa Clara, California.

56. Rayleigh, Lord: Phil. Mag., (1882), 14, 184.

57. Johnson, N.L. and Leone, F.C: Statistics and Experimental Design Vol. 1, 388, Wiley, (1964).

58. Moon, P. and Spencer, D.E: Field Theory Handbook Springer-Verlag, (1961).

59. Levich, V.G: Physicochemical Hydrodynamics, Prentice Hall, (1962).

60. Colgate, S.A., Firth, H.P., and Halliday, F.O: Rev. Mod. Phys., (1960), 32, 744.

61. Darken, L.S: J.I.S.I., (1970), 208, 7.

62. Floridis, T.P. and Chipman, J: Trans. A.I.M.E., (1958), (212), 549.

63. Elliot, J.F: (Editor) Physical Chemistry of Iron and Steelmaking, Proc. Conf., Dedham Mass (1956).

64. Krause, W., Sauerwald, F. and Michalke, M: Zeits. F. anorg. u. allgem. Chem., (1929), 181, 353.

65. Pugachevich, P.P. and Lazarev, V.B: Russian J. Phys. Chem., (1960), 34, 1228.

66. Johnson, N.L. and Leone, F.C: Statistics and Experimental Design Vol. 1, Wiley, (1964).

67. Johnson, N.L. and Leone, F.C: Statistics and Experimental Design Vol. 2, Wiley, (1964).

68. LeClair, B., Private Communication.

69. Becker, G.,Hardero, F., and Kornfeld, H: Archiv Eisenhuttenw., (1949), 20, 363.

APPENDIX A

MODES OF DROP MOTION

A-1 INTRODUCTION

This appendix will serve the purpose of providing the reader with a visual distinction between stable oscillations (Figure A-1), rotation, (Figure A-2) and unstable or mixed oscillations (Figure A-3). This is, however, not completely adequate as we are considering moving images and these are best observed by viewing the film running at any speed at or above four frames per second. This projection rate is the approximate limit of one's persistence of vision. Hence, visual connection of successive images on the screen below this rate becomes difficult and little information about the stability of drop oscillations can be observed. The sequences shown here were photographed on 35mm film from the images of the top views of the drops on the original films projected onto a grid.

A-2 DISCUSSION

In Figure A-1 slightly more than one complete stable oscillation is shown. The stable oscillation is characterized by a complete lack of rotation of the elongated drop shape from one oscillation to the next and by the passing of the drop shape through a spherical (or nearly spherical) position (Frames 5, 14).

Figure A-2 shows pure rotation of a molten drop. Rotation is occuring in a clockwise direction and it is distinquished by the consistency of drop shape and size from frame to frame, the only change being in the orientation of this shape.

In contrast to the pure rotation and the stable oscillations, Figure A-3 shows the unstable or mixed oscillations. In this sequence noticeable rotation of consecutive images is observed (Frames 1, 2, 3) as well as changes in shape of the images (Frames 9-12) and in the size of the images (Frame 6 vs. 12). The droplet passes through a nearly spherical shape in frame 10 but adjacent frames show that the drop is also rotating. These signs, then, are indicative of rotation occuring while the droplet is oscillating and oscillations taking place in several different directions. The image size changes may also show that the droplet may have been translating vertically but this is unlikely since all the images appear to be in the same focus. Such films as represented by Figure A-3 are quite obviously highly unsuitable for oscillation frequency measurements.

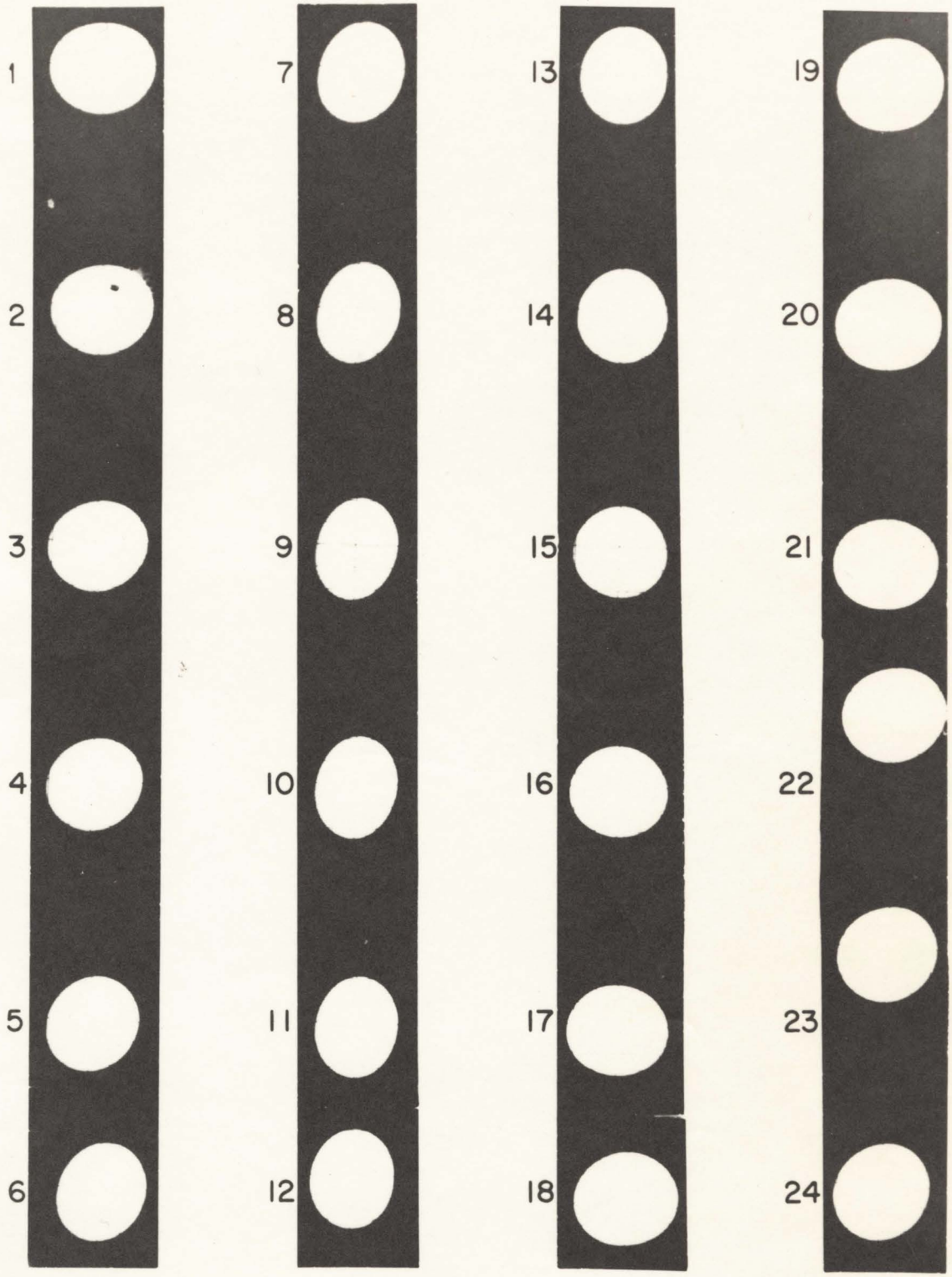

FIGURE A-1. EXAMPLE OF STABLE OSCILLATIONS. COMPLETE CYCLE FRAMES 1–19.

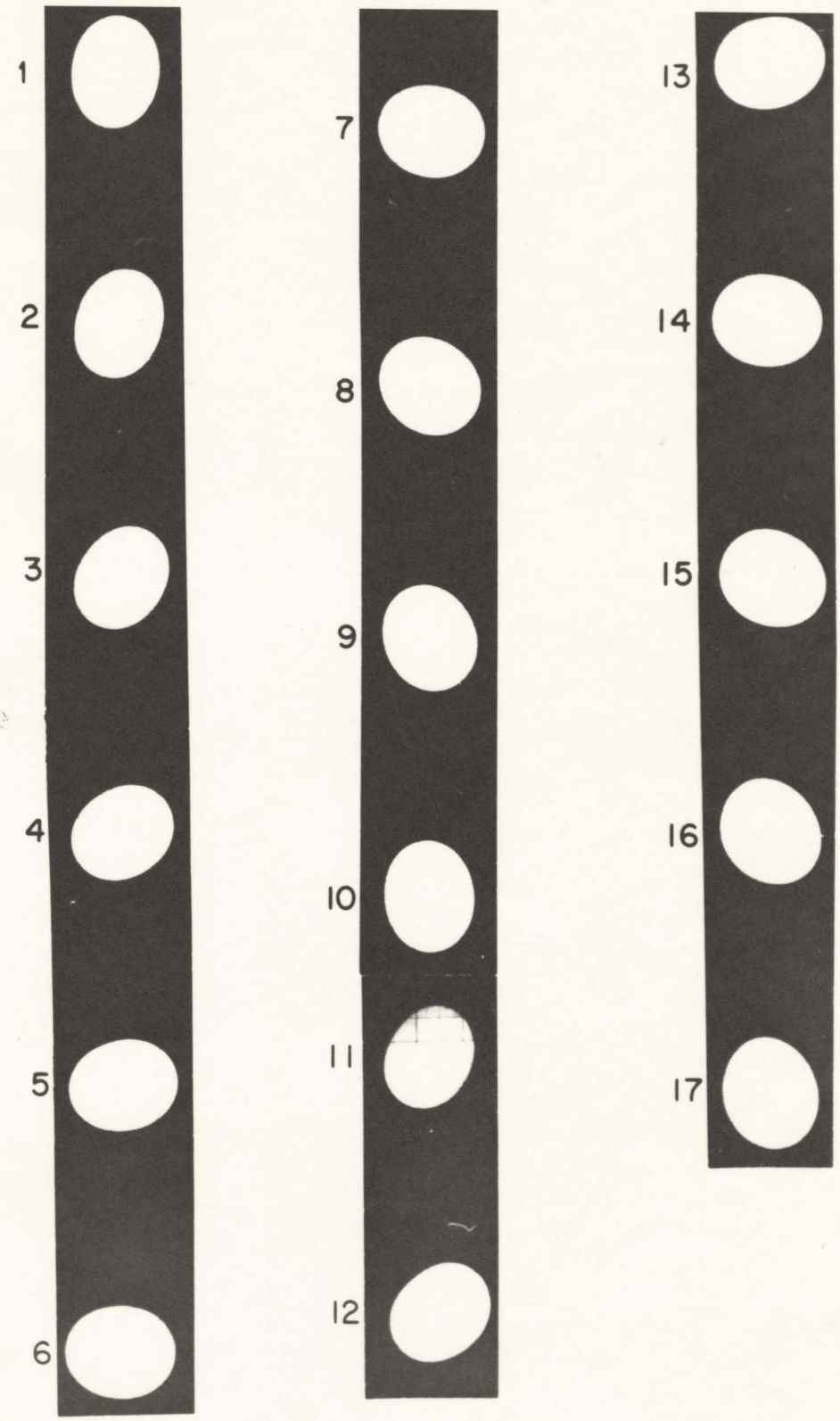

FIGURE A-2. EXAMPLE OF ROTATING DROP

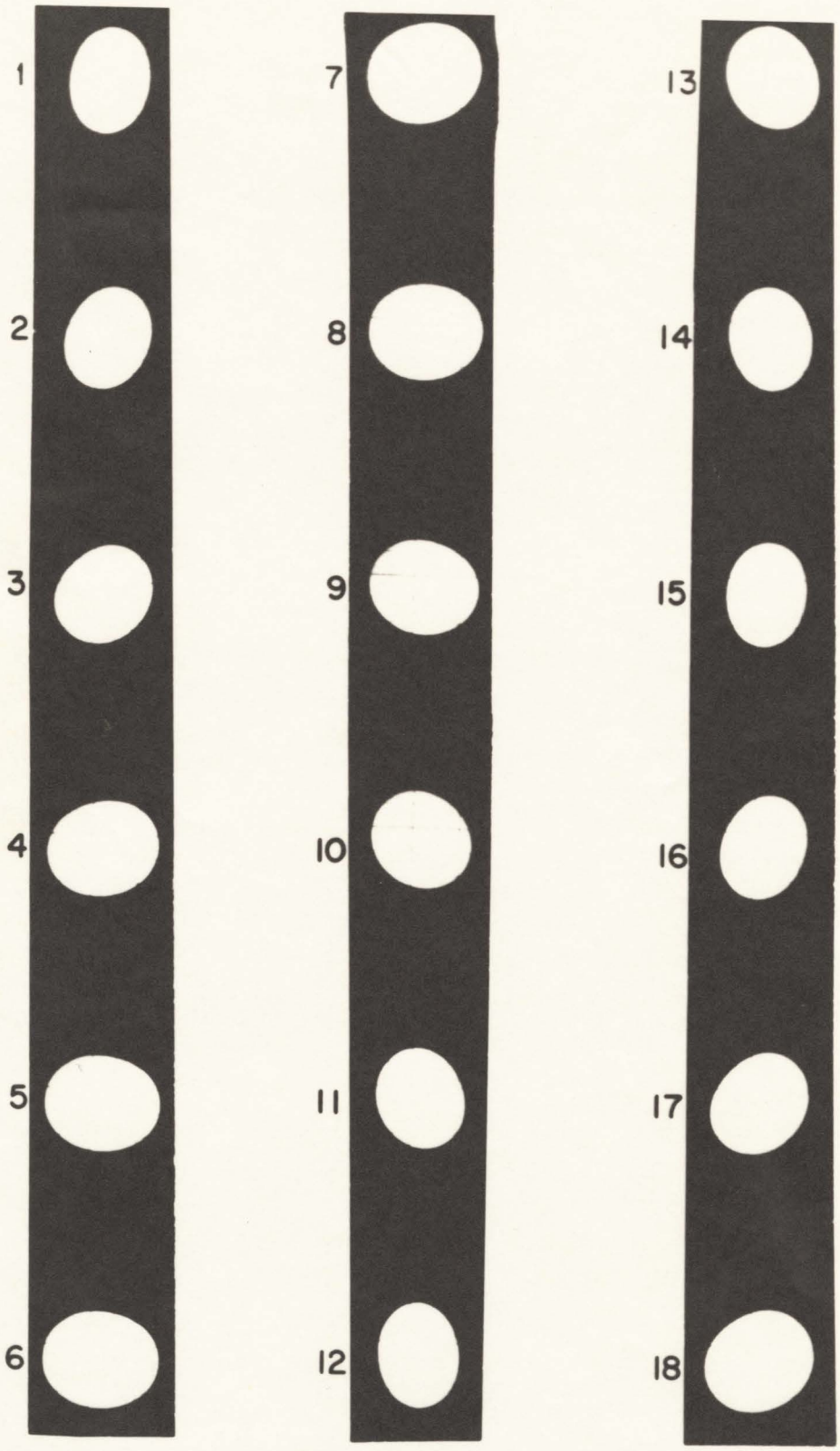

FIGURE A-3. EXAMPLE OF UNSTABLE OR MIXED OSCILLATION.

APPENDIX B

STATISTICAL TREATMENT OF EXPERIMENTAL DATA

B-i REGRESSION ANALYSIS AND CONFIDENCE INTERVALS

Of interest in this section is linear regression of the dependent variable, surface tension (γ), on the single dependent variable, temperature (T). The equation $\gamma = \alpha + \beta T$ represents a straight line with the γ-intercept (at $T = 0$) equal to α and slope equal to β. The method of calculating estimates of α and β is the method of least squares which will be described shortly. First, however, certain assumptions must be implied about the data which are to be regressed.

Apart from the basic assumption that the conditional expected value of γ, given T, is a linear function of T, we must assume that the values of T are controlled and observed without error. In the present set-up temperature is measured with an optical pyrometer and all such measurements are considered to be observed without error, i.e., although there is a limit $\pm$ 10-15% in accuracy, all recorded values of any given temperature vary in the same manner with respect to the true temperature.

It is also assumed that the conditional variance does not depend on the value of T. In other words, the values of γ at any T have equal or similar variances. This variance is normally not known precisely but it is considered[66] that unless deviations from this and the above assumptions are

very large, they are unlikely to have any substantial effect.

The most important and overriding assumptions that must be considered are that the data must be taken from the population about which inferences are to be made and that there are no extraneous variables affecting the relationship between γ and T. The former condition is fairly obviously obeyed in the present case for, only measurements of surface tension made by the author by the oscillating drop technique were used. The latter condition is also taken to be valid as to date there is no evidence of any effect of such miscellaneous factors as variation of results from one day's work to the next or variation in experimenter interpretation of results.

It can be shown[66] that the method of least squares gives estimate of α and β which are unbiased and have the smallest variances among all unbiased estimators which are linear functions of the observed values.

This method provides values of α and β which minimize the sums of squares of vertical distances from the line $\gamma=\alpha+\beta T$ such that if D is this sum, then

$$D = \sum_{j=1}^{n} [\gamma_j - (\alpha + \beta T_j)]^2 \qquad \text{(B-1)}$$

Minimizing D with respect to α and β and solving the resultant equations in terms of α and β, we obtain

$$\beta = \frac{n \sum_{j=1}^{n} T_j \gamma_j - \sum_{j=1}^{n} T_j \sum_{j=1}^{n} \gamma_j}{n \sum_{j=1}^{n} T_j^2 - \left(\sum_{j=1}^{n} T_j\right)^2} \qquad \text{(B-2)}$$

$$\alpha = \bar{\gamma} - \beta \bar{T} \qquad \text{(B-3)}$$

where $\bar{\gamma}$ and $\bar{T}$ are the means of γ and T, respectively.

Treating the data in Tables IV and V for iron and nickel respectively and using (B-2) and (B-3), we find

$$\gamma_{Fe} = 0.68t + 725.7 \qquad \text{(B-4)}$$

$$\gamma_{Ni} = 0.21t + 1663.8 \qquad \text{(B-5)}$$

(See Chapter 6, 6.3.1 and 6.4.1, respectively)

The correlation coefficient, r, is a measure of the linearity of the relationship between γ and T[66]. When $r = \pm 1$ perfect correlation exists and γ and T can be related absolutely by a linear mathematical equation. It can be shown[66] that

$$r = \frac{\Sigma (T_j - \bar{T})(\gamma_j - \bar{\gamma})}{[\Sigma (T_j - \bar{T})^2][\Sigma (\gamma_j - \bar{\gamma})^2]} \qquad \text{(B-6)}$$

For the iron data and regression equation (B-4), r = 0.97 and for the nickel data and regression equation (B-5), r = 0.94. Both of these correlation coefficients can be shown to be highly significant at the 99% confidence level[66] and hence, we can say that the values of surface tension, measured in their respective temperatures ranges, vary linearly with temperature.

Confidence intervals in general are regions in which the expected value of a given parameter, as statistically determined, may be considered to lie with a certain probability expressed in terms of a percentage. The 95% confidence interval about the slope of a regression line is given as[66]

$$\pm \frac{t_{n-2,\ 0.975}\ S}{\sqrt{\sum_{j=1}^{n} (T_j - \bar{T})^2}} \qquad \text{(B-7)}$$

where n is the number of pieces of data, $t_{n-2,\ 0.975}$ is the t distribution with n-2 degrees of freedom and S^2 is the unbiased estimate of the variance about the regression line and is equal to $\sqrt{\sum_{j=1}^{n} (\gamma_j - \alpha - \beta T_j)^2/(n-2)}$[66]. For iron it was found that S = 5.9 and for nickel, S = 8.4. Using these values for $t_{n-2,\ 0.975}$ as determined from prepared tables, the confidence intervals about the slopes of (B-4) and (B-5) were found to be:

B-4 (IRON) 0.68 ± 0.10

B-5 (NICKEL) 0.21 ± 0.43

To find the confidence interval about the regression line (the expected value of γ) for any value of T, the formula (B-8) is used[66]

$$(\alpha + \beta T) \pm t_{n-2,\ 0.975} \left(\frac{1}{n} + \frac{(T - \bar{T})^2}{\sum_{j=1}^{n} (T_j - \bar{T})^2}\right)^{\frac{1}{2}} S \qquad \text{(B-8)}$$

Tables B-I and B-II give the upper and lower confidence limits for iron and nickel respectively at various temperatures. (See Figures 14, 15 respectively)

B-ii ANALYSIS OF VARIANCE

Analysis of variance[67] techniques are widely used in the physical, engineering and social sciences to test the hypothesis that several independent samples have been drawn at random from a common population. The data is arranged in tabular form such that the columns represent the various samples and the rows represent the number of cases in each sample where there are n rows and p columns. In the present case, the columns will contain data grouped according to size distribution or material type (iron only). The rows will be the measurements in each sample taken at each temperature. The total number of measurements of the combined samples is N.

The method of analysis of variance is to obtain two independent estimates of the population variance and to compare the ratio of these estimates to a standard statistic. This test of significance is called the F test.

The estimates of population variances are found by partitioning the total sum of squares, TSS, which is based upon the deviations of the N values of γ from the mean of the combined samples. The partitions are the sum of squares within groups, WSS, based on the deviations of the various

measurements from the means of the samples from which they are taken and the sum of squares between groups, BSS, based upon the deviations of the means of the various samples from the mean of the combined samples. The degrees of freedom associated with the TSS are N-1 and they are partitioned between WSS and BSS as N-p and p-1, respectively[67]. It can be shown that WSS/N-p and BSS/p-1, called mean squares, are independent estimates of the population variance[67].

The mean square based on the within-group sum of squares measures the uncontrolled variation between bits of data treated alike while the mean square based on the between-groups sum of squares is a measure of the variation between groups of data treated differently, i.e., between the various experimental conditions being compared.

The ratio used in the F test is

$$F = \frac{\text{mean square between groups}}{\text{mean square within groups}} \qquad \text{(B-9)}$$

If the mean square in the numerator is significantly larger than that in the denominator, the hypothesis of random sampling from a common population will be rejected. This indicates that the means of the samples differ more than can be reasonably expected in random sampling from a common population. The ratio is compared, at a given level of confidence, to the standard F statistic distributed with p-1 and N-p degress of freedom.

Johnson and Leone[67] have given a computational short cut to calculate sums of squares which will be used in the following analyses for the study of the effects of specimen size variation for the surface tension of iron and nickel Tables B-IV and B-V, respectively, and the effects of variation of the type of high purity iron on the surface tension of iron, Table B-III.

As a preface to the mechanics of analysis of variance it is to be noted that when more than one measurement was made at a given temperature within a sample grouping (say Battelle iron or size less than 0.6 gm), then these measurements were averaged[67]. Also no interaction effects between variation of material and drop size were studied, but these were not considered to be related variables.

The results of the analyses of variance are discussed in Chapter 6; effect of material type for iron-6.3.2; effects of drop shape for iron-6.3.3; for nickel-6.4.3.

TEMPERATURE (T) (°C)	LOWER CONFIDENCE LIMIT dyn cm^{-1}	ESTIMATED γ dyn cm^{-1}	UPPER CONFIDENCE LIMIT dyn cm^{-1}
1550	1761	1780	1790
1560	1773	1787	1800
1570	1784	1793	1802
1580	1794	1800	1806
1590	1803	1807	1811
1600	1810	1814	1818
1610	1816	1821	1825
1620	1820	1827	1835
1630	1823	1834	1845
1640	1825	1841	1857
1650	1825	1848	1870

TABLE B-I. ESTIMATED VALUES OF γ (FROM (B-4)) AND 95% CONFIDENCE LIMITS FOR THE SURFACE TENSION OF LIQUID IRON AS A FUNCTION OF TEMPERATURE

TEMPERATURE (T) (°C)	LOWER CONFIDENCE LIMIT dyn cm^{-1}	ESTIMATED γ dyn cm^{-1}	UPPER CONFIDENCE LIMIT dyn cm^{-1}
1475	1934	1974	2013
1485	1942	1976	2009
1500	1953	1979	2005
1515	1961	1982	2002
1525	1966	1984	2002
1550	1974	1989	2005
1575	1976	1995	2013
1600	1974	2000	2026
1615	1970	2003	2036
1625	1966	2005	2044

TABLE B-II. ESTIMATED VALUES OF γ (FROM (B-5)) AND 95% CONFIDENCE LIMITS FOR THE SURFACE TENSION OF LIQUID NICKEL AS A FUNCTION OF TEMPERATURE

MATERIAL / TEMPERATURE	BATTELLE	FERROVAC "E"	NPL	ROW TOTALS
1550°C	1779.4	1785.2	1779.5	5344.1
1580°C	1789.8	1792.1	1798.2	5380.1
1620°C	1815.2	1825.6	1821.0	5461.8
1650°C	1848.2	1856.7	1850.4	5555.3
COLUMN TOTALS	7232.6	7259.6	7249.1	21741.3

GRAND TOTAL (G)

TABLE B-III. GROUPING OF IRON SURFACE TENSION DATA ACCORDING TO MATERIAL TYPE

number of rows (n) = 4 $\quad N = np = 12$
number of columns (p) = 3 $\quad G$ = Grand Total = 21741.3

(1) Correction factor = $G^2/N = 3.93903438 \times 10^7$

(2) Raw Sum of Squares = $\sum_n \sum_p \gamma_{ij}^2 = 3.939931903 \times 10^7$

(3) Total Sum of Squares (TSS) = (2) - (1) = 8975.2224

(4) Between Sum of Squares (BSS) = $\frac{7232.6^2}{4} + \frac{7259.6^2}{4} + \frac{7249.1^2}{4}$ - (1) = 92.6249

(5) Within Sum of Squares (WSS) = (3) - (4) = 8877.5975

Analysis of Variance (ANOVA)

SOURCES OF VARIATION	DEGREES OF FREEDOM (df)	SUM OF SQUARES (SS)	MEAN SUM OF SQUARES SS/df	VARIANCE RATIO BSS/df / WSS/df
BSS	(p-1) 2	92.6249	46.31245	<1
WSS	N-p 9	8877.5975	986.3997	
TSS	N-1 11	152.9725		

But F (2,9) = 5.14 at the 95% confidence level and this is much greater than the variance ratio. Therefore the hypothesis that the column means are equal is not rejected and we can say there appears to be no effect in varying the type of high purity iron on surface tension values.

DROP SIZE / TEMPERATURE	<0.6gm	0.6<x<0.9	>0.9gm	ROW TOTALS
1550°C	1786.7	1775.2	1781.2	5343.1
1580°C	*	1791.0	1798.2	3589.2
1620°C	1819.7	1820.9	1826.4	5467.0
1650°C	1852.5	1847.1	1853.7	5553.3
COLUMN TOTALS	5458.9	7234.2	7259.5	19952.6

*missing number only of importance in finding BSS

TABLE B-IV. GROUPING OF IRON SURFACE TENSION DATA ACCORDING TO SIZE DISTRIBUTION

number of rows (n) = 4 N = np = 12
number of columns (p) = 3 Grand Total (G) = 19952.6

(1) Correction factor = $G^2/N = 3.1619147697 \times 10^7$

(2) Raw Sum of Squares = $\sum_{n}\sum_{p}\gamma_{ij}^{2} = 3.620068626 \times 10^7$

(3) Total Sum of Squares (TSS) = (2) - (1) = 9209.29

(4) Between Sum of Squares (BSS) = $\frac{5458.9^2}{3} + \frac{7234.2^2}{4} + \frac{7259.5^2}{4}$ - (1) = 216.9058

(5) Within Sum of Squares (WSS) = (3) - (4) = 8992.2842

Analysis of Variance (ANOVA)

SOURCES OF VARIATION	DEGREES OF FREEDOM (df)	SUM OF SQUARES (SS)	MEAN SUM OF SQUARES (SS/df)	VARIANCE RATIO (BSS/df/WSS/df)
BSS	(p-1) 2	216.9058	108.4529	<1
WSS	N-p 9	8992.2842	999.1427	
TSS	N-1 11	9209.29		

But f (2,9) at the 95% confidence level is 5.14 and this is much greater than the variance ratio. Therefore, the hypothesis that the column means are equal is not rejected and we can say that there appears to be no effect in varying the drop size (in this range) on the surface tension of iron.

DROP SIZE / TEMPERATURE	0.8gm	0.65gm	0.55gm	ROW TOTALS
1475°C	1979.5	1976.7	1970.6	5926.8
1525°C	1979.5	1993.1	1983.5	5956.1
1575°C	1996.6	2000.2	1997.0	5993.8
1625°C	2007.2	2011.3	2001.4	6019.9
COLUMN TOTALS	7962.8	7981.3	7952.5	23896.6

TABLE B-V. GROUP OF NICKEL SURFACE TENSION DATA ACCORDING TO SIZE DISTRIBUTION

number of rows (n) = 4 N = np = 12
number of columns (p) = 3 Grand Total (G) = 23896.6

(1) Correction factor = $G^2/N = 4.758729096 \times 10^7$

(2) Raw Sum of Squares = $\sum_n \sum_p \gamma_{ij}^2 = 4.758916970 \times 10^7$

(3) Total Sum of Squares (TSS) = (2) - (1) = 1878.74

(4) Between Sum of Squares (BSS) = $\frac{7962.8^2}{4} + \frac{7981.3^2}{4} + \frac{7952.5^2}{4}$

$- (1) = 106.4816$

(5) Within Sum of Squares (WSS) = (3) - (4) = 1772.2584

Analysis of Variance (ANOVA)

SOURCES OF VARIATION	DEGREES OF FREEDOM (df)	SUM OF SQUARES (SS)	MEAN SUM OF SQUARES (SS/df)	VARIANCE RATIO (BSS/df/WSS/df)
BSS	(p-1) 2	106.4816	53.24	<1
WSS	(N-p) 9	1772.2584	195.8065	
TSS	(N-1) 11	1878.74		

But F (2,9) = 5.14 at the 95% confidence level and thus is much greater than the variance ratio. Therefore, the hypothesis that the column means are equal is not rejected and we can say that there appears to be no effect in varying the drop size on the surface tension of nickel in this range.

IMPURITY	CONCENTRATION (ppm)		
	FERROVAC "E"	NATIONAL PHYSICAL LABORATORY	BATTELLE
C	70	180	8
Co	70		7
Cr	100		10
Cu	100		2
H	60		<1
Mn	10		1
Mo	100		<1
N	30	6	<1
Ni	100		6
O		6	1.5
P	30	20	3
S	60	30	<1
Si		30	<2
V	40		<1
W	100		

TABLE 1. ANALYSES OF HIGH PURITY IRONS SUPPLIED BY MANUFACTURERS

IMPURITY	CONCENTRATION (ppm)	IMPURITY	CONCENTRATION (ppm)
As	0.3	Mn	<0.4
Ag	<0.4	Mo	<1
Al	<3	Pb	<4
Ba	1	S	<2
Bi	5	Si	<6
B	5	Sn	<1.5
C	56	Ta	<50
Ca	2	Ti	<1
Cb	<17	V	<1
Cd	<5	W	<50
Co	12	Zn	3.5
Cr	<0.6	Zr	<17
Cu	2	H_2	2.8
Fe	2	N_2	4
Mg	<0.6	O_2	30

TABLE II. ANALYSIS OF ELECTOLYTIC NICKEL AS SUPPLIED BY MANUFACTURER

MATERIAL	LECO* READING	SAMPLE WEIGHT (grams)	CONCENTRATION (ppm)
NPL	1.8	0.843	2
FERROVAC "E"	1.4	0.885	1
BATTELLE	3.3	0.970	2
NPL	2.7	0.784	2
NICKEL	1.4	0.623	2

*LECO - Inert Gas Fusion Equipment

TABLE III. OXYGEN ANALYSIS OF RANDOM SPECIMENS AFTER CLEANING PROCESS

EXPER-MENT* NUMBER	TEMPERATURE °C ± 10	WEIGHT GRAMS ±0.001	FRAME-RATE SEC^{-4} ±10	NUMBER OF (N) OSCILL-ATIONS	NUMBER OF FRAMES ±1	TIME FOR N OSCILL-ATIONS (SECS)	FREQUEN-CY CYCLES SEC^{-1}	SURFACE TENSION (1.178xwt xFREQ^2) $dynes\ cm^{-1}$
F-8-B**	1550	0.994	1111.3	5	***142.5	0.12823	38.99	1780
F-13-B	1550	0.660	1097.3	10	229.5	0.20961	47.71	1777
F-13-B	1580	0.660	1098.9	5	114.5	0.10420	47.78	1790
F-14-B	1620	0.595	1099.1	5	108	0.09826	50.89	1815
F-14-B	1650	0.595	1097.6	4	85.5	0.77897	51.35	1848
F-16-B	1550	0.561	1096.5	4	84.5	0.07706	51.91	1781
F-18-F	1550	1.049	1137.9	5	150	0.13182	37.93	1778
F-19-F	1580	1.048	1116.0	5	146.5	0.13127	38.10	1792
F-25-N	1550	1.117	1090.5	5	148	0.13572	36.84	1786
F-25-N	1580	1.117	1096.2	5	148	0.13501	37.03	1804

* Non-sequential experiment numbers due to unsuitability of missing films for frequency measurement (see Appendix A).
** Last letter in experiment number refers to iron source-B, Battelle; F, Ferrovac"E"; N, NPL.
*** Non integer number of frames due to averaging of two measurement over same region.

TABLE IV. EXPERIMENTAL DATA AND RESULTANT SURFACE TENSION VALUES FOR THREE TYPES OF HIGH PURITY IRON IN THE RANGE 1550-1650°C.

EXPERIMENT* NUMBER	TEMPERATURE °C ± 10	WEIGHT GRAMS ±0.001	FRAME-RATE SEC^{-4} ±10	NUMBER OF (N) OSCILLATIONS	NUMBER OF FRAMES ±1	TIME FOR N OSCILLATIONS (SECS)	FREQUENCY CYCLES SEC^{-1}	SURFACE TENSION (1.178xwt x$FREQ^2$) dynes cm^{-1}
F-26-N	1620	1.116	1088.3	5	146	0.13415	37.27	1826
F-26-N	1650	1.116	1089.1	5	145	0.13314	37.55	1854
F-27-N	1550	0.741	1086.3	5	120.5	0.11093	45.07	1773
F-27-N	1580	0.741	1091.9	5	120.5	0.11036	45.31	1792
F-28-N	1620	0.741	1085.6	5	119	0.10962	45.61	1816
F-28-N	1650	0.741	1090.2	5	118.5	0.10870	46.00	1847
F-31-F	1620	1.045	1028.5	5	133.5	0.12980	38.52	1827
F-32-F	1550	0.578	1031.4	5	100.5	0.09744	51.31	1793
F-32-F	1620	0.578	1030.0	5	99.5	0.09660	51.76	1824
F-33-F	1650	0.578	1028.8	5	98.5	0.09574	52.22	1857
F-34-F	1620	0.715	1028.9	5	110.5	0.10739	46.56	1826

TABLE IV. CONT'D EXPERIMENTAL DATA AND RESULTANT SURFACE TENSION VALUES FOR THREE TYPES OF HIGH PURITY IRON IN THE RANGE 1550-1650°C

EXPERIMENT* NUMBER	TEMPERATURE °C ± 15	WEIGHT GRAMS ±0.001	FRAME-RATE FRAMES SEC^{-1} ±10	NUMBER OF (N) OSCILLATIONS	NUMBER OF FRAMES ±1	TIME FOR N OSCILLATIONS (SECS)	FREQUENCY CYCLES SEC^{-1}	SURFACE TENSION ($1.178 \times wt \times FREQ^2$) dynes cm^{-1}
N-1	1475	0.835	1022.7	10	228	0.22294	44.86	1980
N-1	1525	0.835	1018.3	5	113.5**	0.11146	44.86	1980
N-2	1575	0.834	1018.9	10	226	0.22181	45.08	1997
N-2	1625	0.834	1021.5	5	112.5	0.11062	45.20	2007
N-3	1475	0.651	1015.4	5	100	0.09848	50.77	1977
N-3	1525	0.651	1014.5	5	99.5	0.09808	50.98	1993
N-4	1575	0.650	1017.0	5	99.5	0.09784	51.11	2000
N-4	1625	0.650	1014.8	5	99	0.09756	51.25	2011
N-7	1475	0.549	1015.7	5	92	0.09058	55.20	1971
N-7	1525	0.549	1013.4	5	91.5	0.09029	55.38	1984
N-8	1575	0.548	1017.9	5	91.5	0.08989	55.62	1997
N-8	1625	0.548	1013.4	5	91	0.08980	55.68	2001

* Non-sequential experiment numbers due to unsuitability of missing films for frequency measurement (see Appendix A).

** Non-integer number of frames due to averaging of two measurements over same region.

TABLE V. EXPERIMENTAL DATA AND RESULTANT SURFACE TENSION VALUES FOR ELECTROLYTIC NICKEL IN THE RANGE 1475-1625°C

AUTHOR	TEMPERATURE (°C)	SURFACE TENSION (dyn cm^{-1})
Becker et al[69]	1550	1380
Kingery and Hamenik[29]	1550	1230 to 1560
Kingery and Halden[30]	1570	1717
Samarin et al[31]	1550	1865
Kozakevitch and Urbain[28]	1550	1788
Present Work	1550°C	1780

TABLE VI COMPARISON OF PREVIOUS MEASUREMENTS OF THE SURFACE TENSION OF PURE LIQUID IRON WITH PRESENT WORK

AUTHOR	TEMPERATURE (°C)	SURFACE TENSION (dyn cm^{-1})
Eremenko et al[32]	1520	1490 to 1770
Kozakevitch and Urbain[24]	1550	1934
Monma and Suto[28]	1600	1600
Present Work	1550°C	1989

TABLE VII COMPARISON OF PREVIOUS MEASUREMENTS OF THE SURFACE TENSION OF PURE LIQUID NICKEL WITH PRESENT WORK

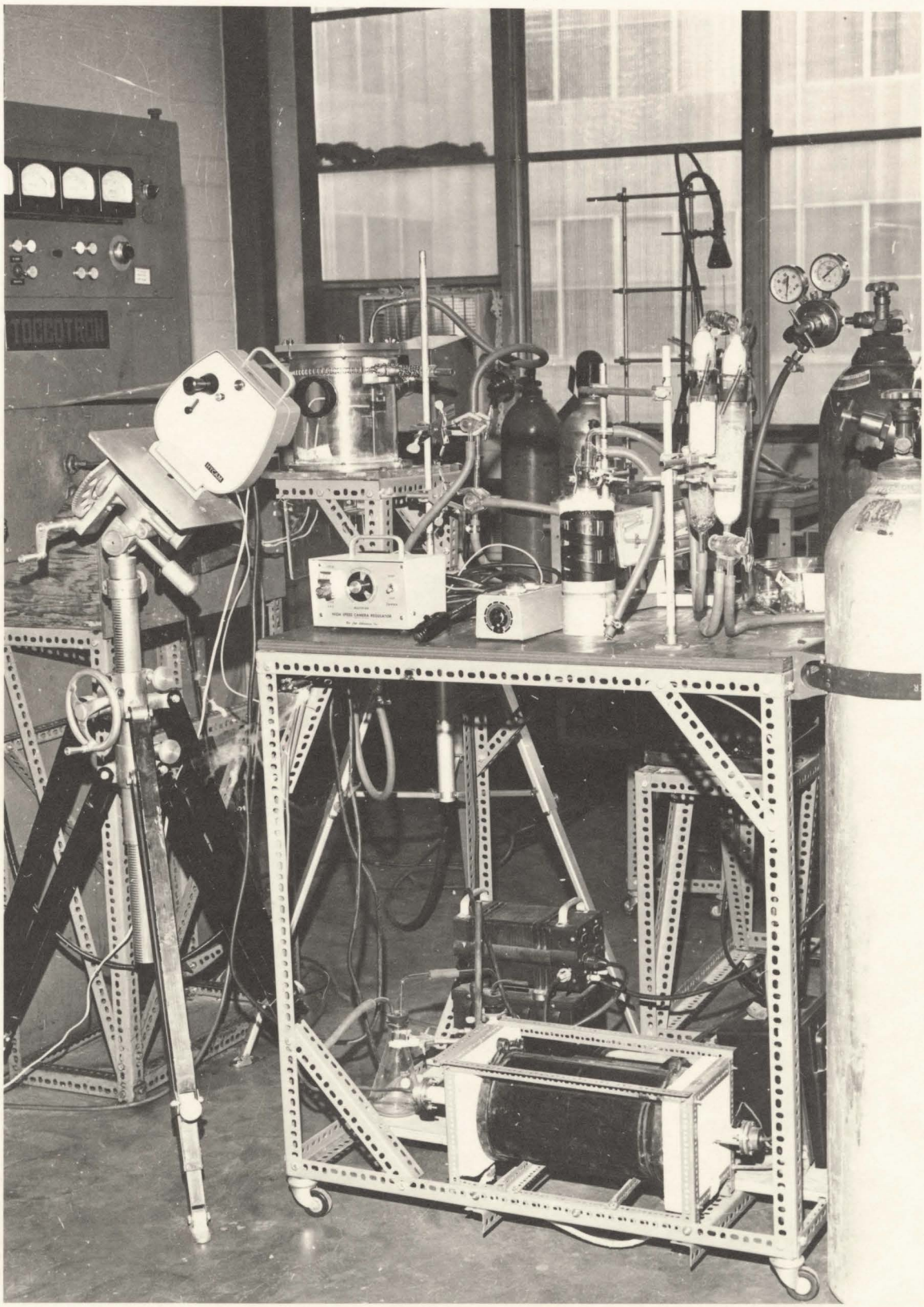

Figure 4. Overall View of the Apparatus Used for High Speed Photography of Oscillating Levitated Drops

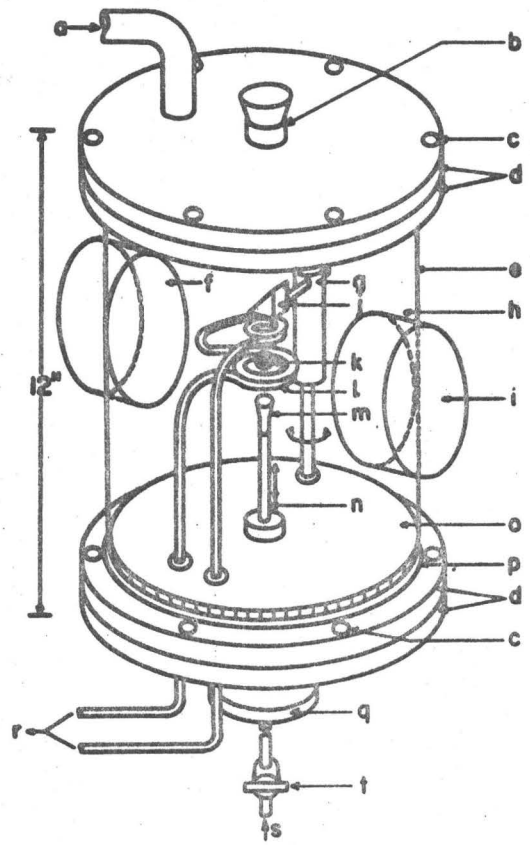

Figure 5. Apparatus For Levitation and Photography of Liquid Metal Drops

a) Gas Exhaust and Vacuum
b) Specimen Insertion Hole
c) Securing bolts
d) ½" Plexiglas Cover and Flange
e) ¼" Plexiglas Cylinder
f) ¼" Plexiglas Pyrometry Port
g) Prism Holder and Swivel
h) ¼" Plexiglas Photography Port
i) Plate Glass Window
j) Prism
k) Liquid Metal Drop
l) 1/8" Copper Tubing Levitation Coil
m) Quartz Receptor For Quenched Drop and Gas Nozzle
n) Sliding Metal Tube
o) Asbestos Plate
p) 1/8" "O" Ring
q) Oil Bath Seal
r) Leads To HF. Generator
s) Purified Gas Entrance
t) Vacuum Stop Cork

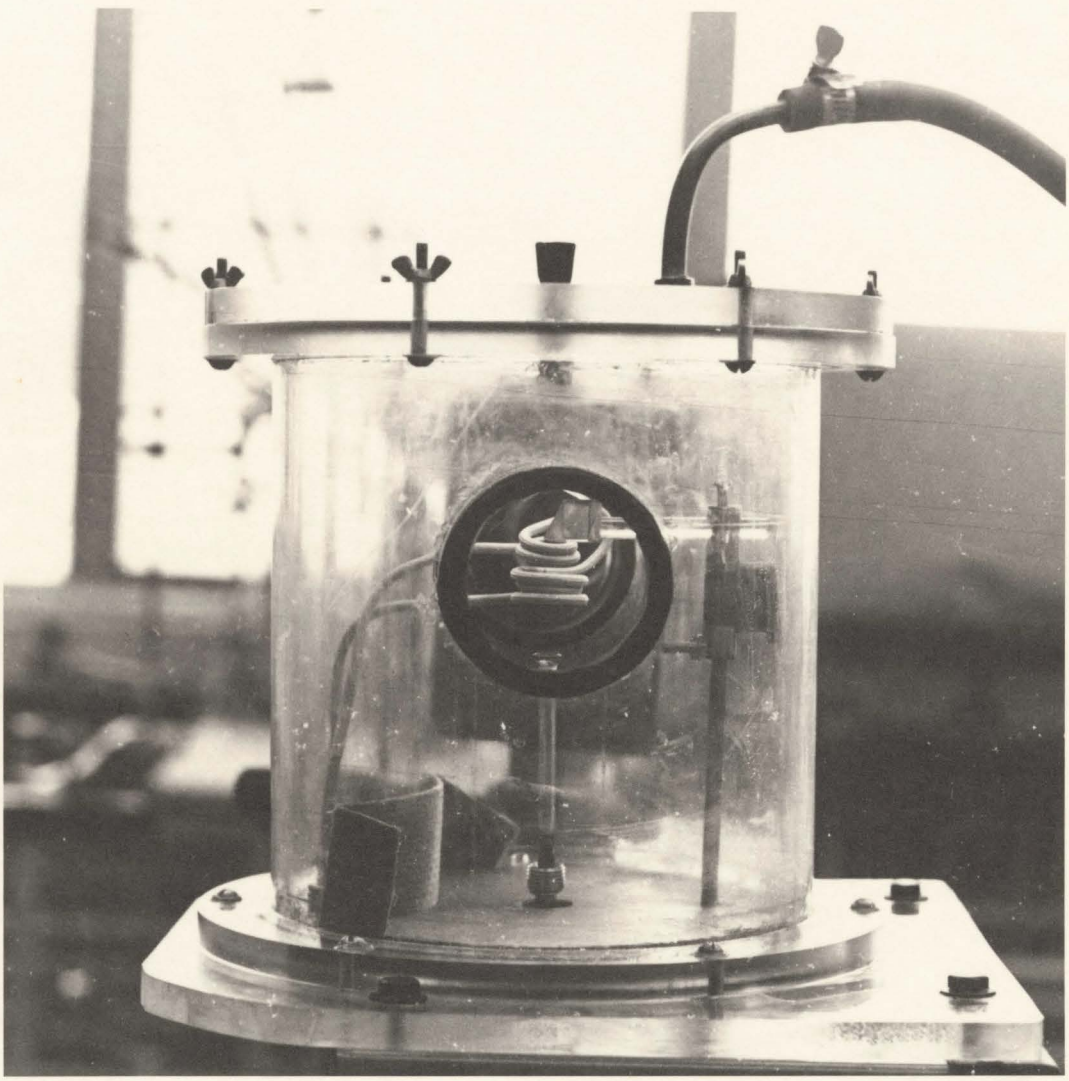

Figure 6. Close-up of Levitation Chamber

PURIFICATION TRAIN FOR HYDROGEN AND HELIUM FOR LOW FLOW RATES.

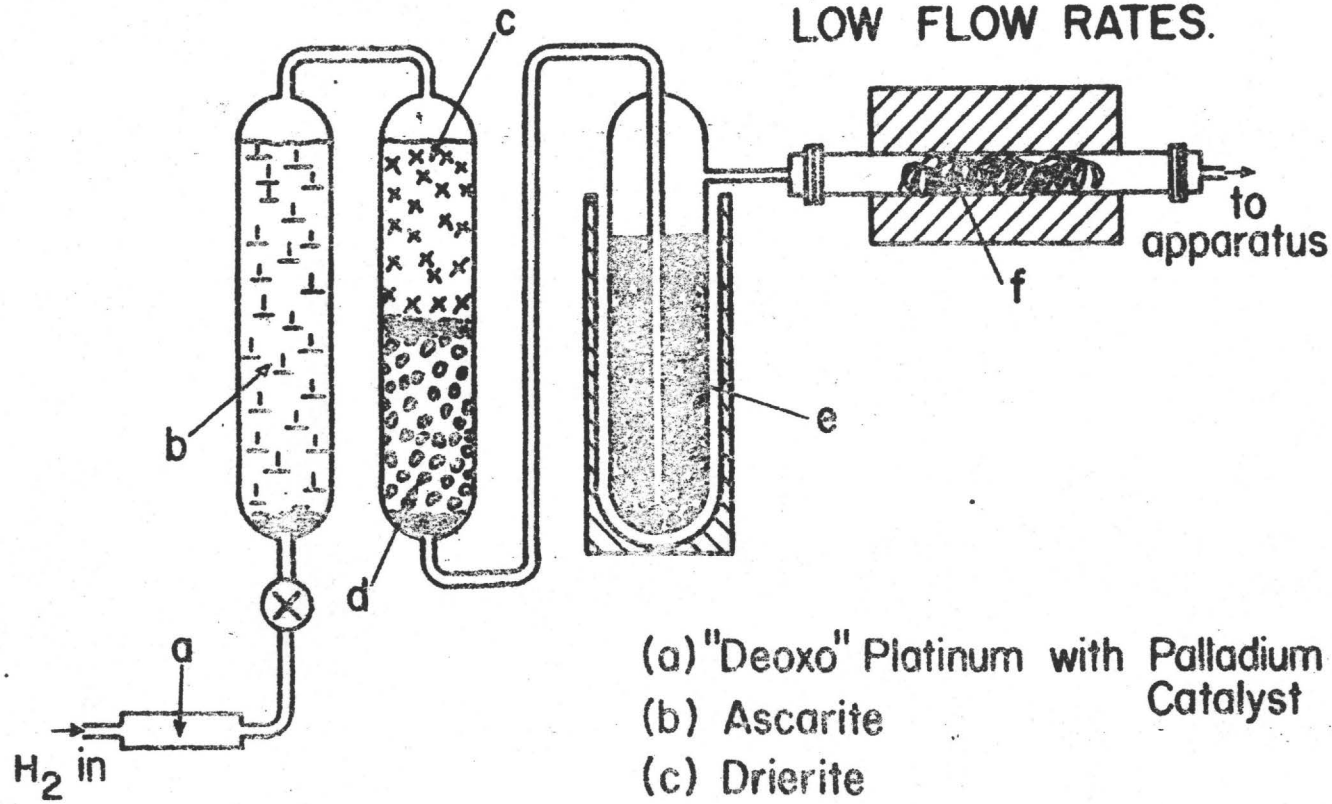

FIG. 7

(a) "Deoxo" Platinum with Palladium Catalyst
(b) Ascarite
(c) Drierite
(d) Silica Gel
(e) Activated Charcoal in Liquid N_2
(f) Titanium at 900° C.

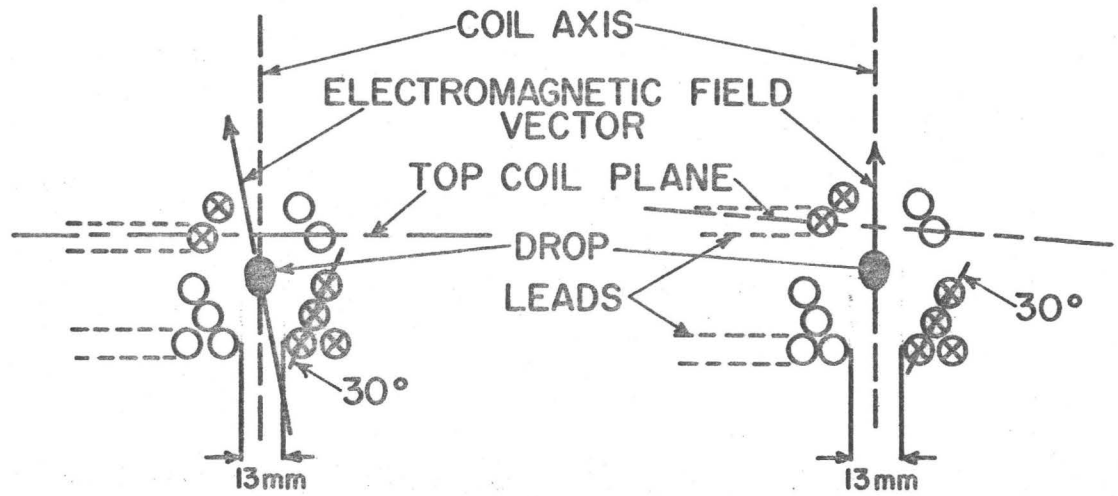

FIG. 8(a) COIL WITH PRECESSING DROP.

FIG. 8 (b) COIL WITH STABLE DROP.

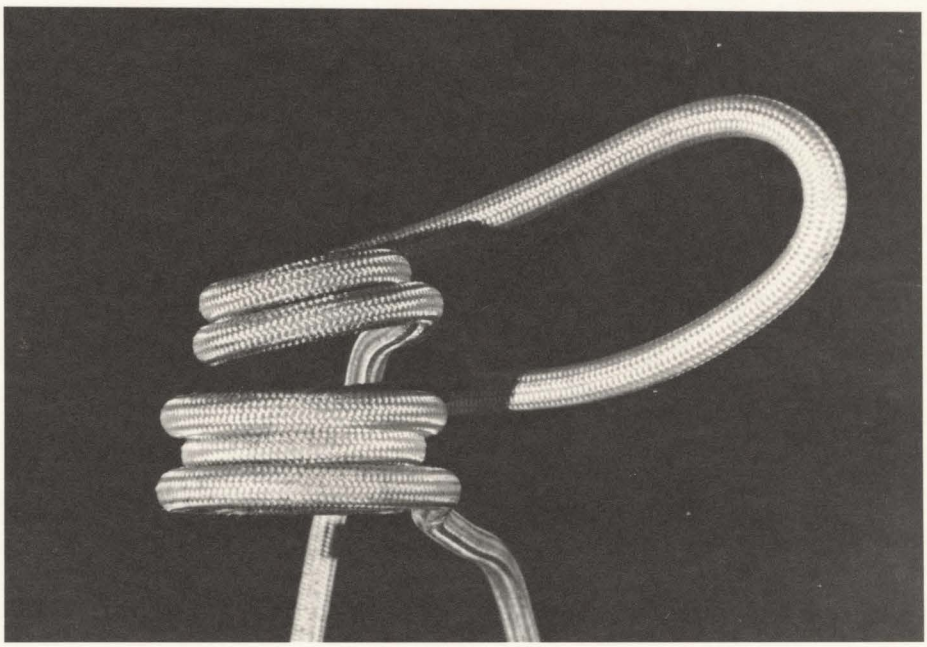

Figure 9. Coil Used for Stable Levitation of Iron and Nickel

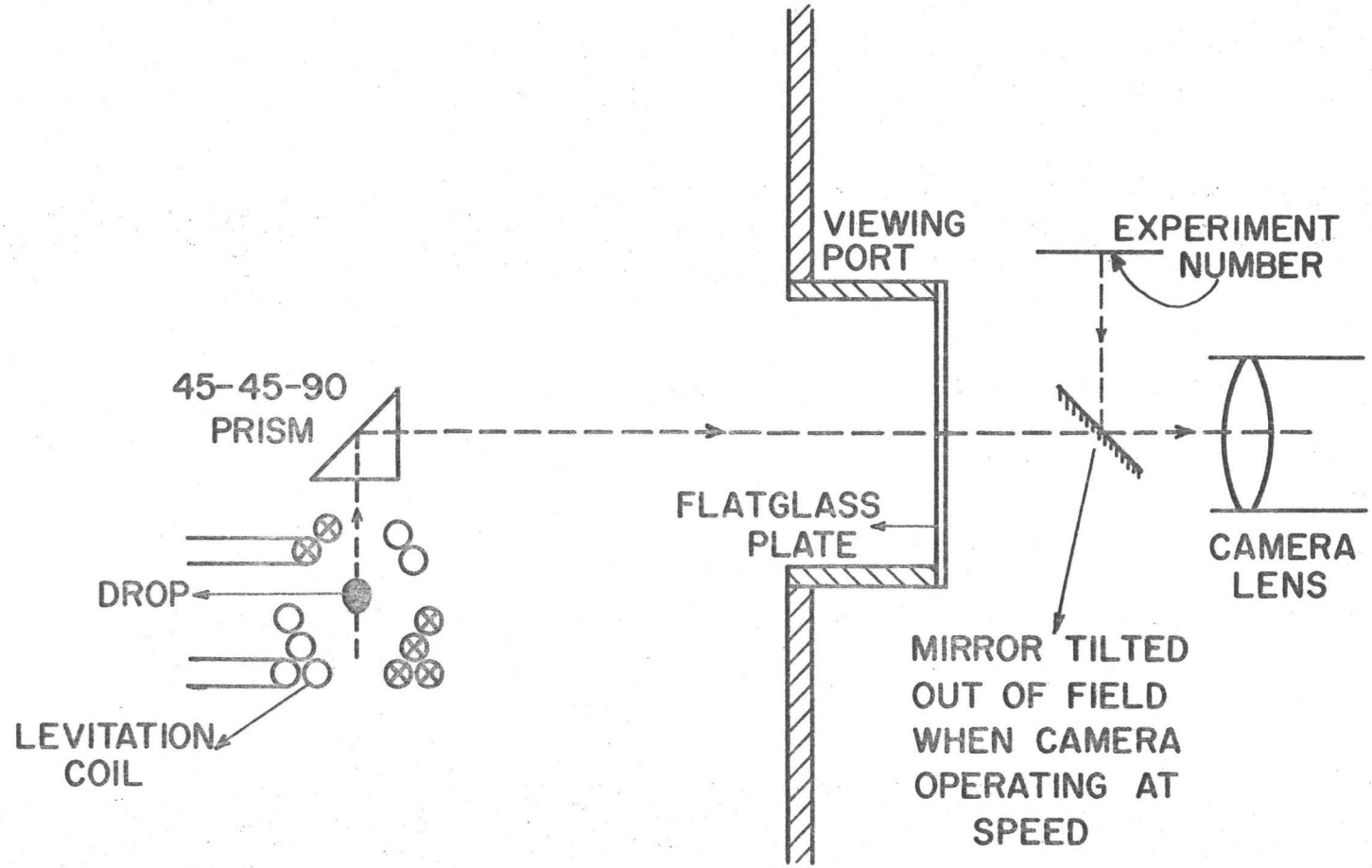

FIG. 10. OPTICAL ARRANGEMENT FOR PHOTOGRAPHY OF LEVITATED DROPS.

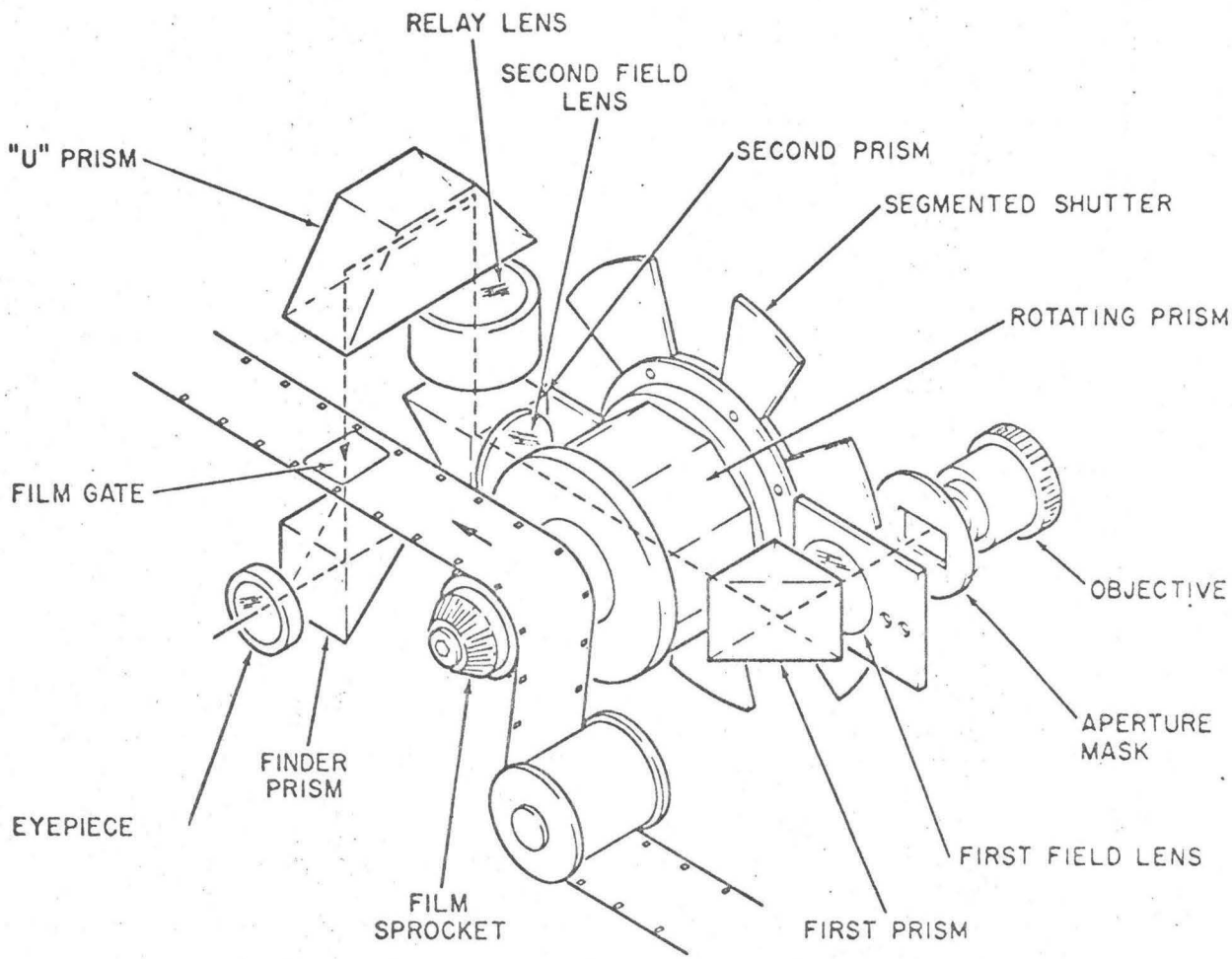

Fig. 11. HIGH SPEED CAMERA OPTICS.[55]

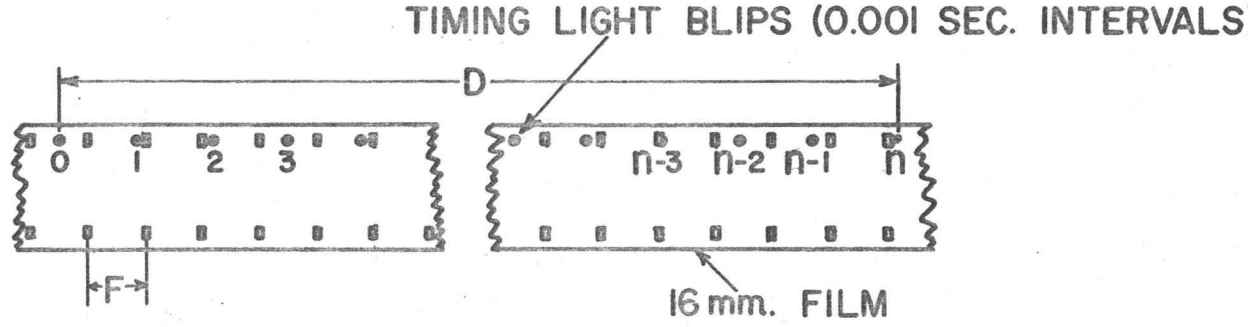

FIGURE 12. FRAME RATE DETERMINATION

WHERE D IS THE AMOUNT OF FILM (cm) PASSING A GIVEN POINT IN n MILLISECONDS AND F IS THE LENGTH OF ONE FRAME OF 16 mm. FILM (mm).

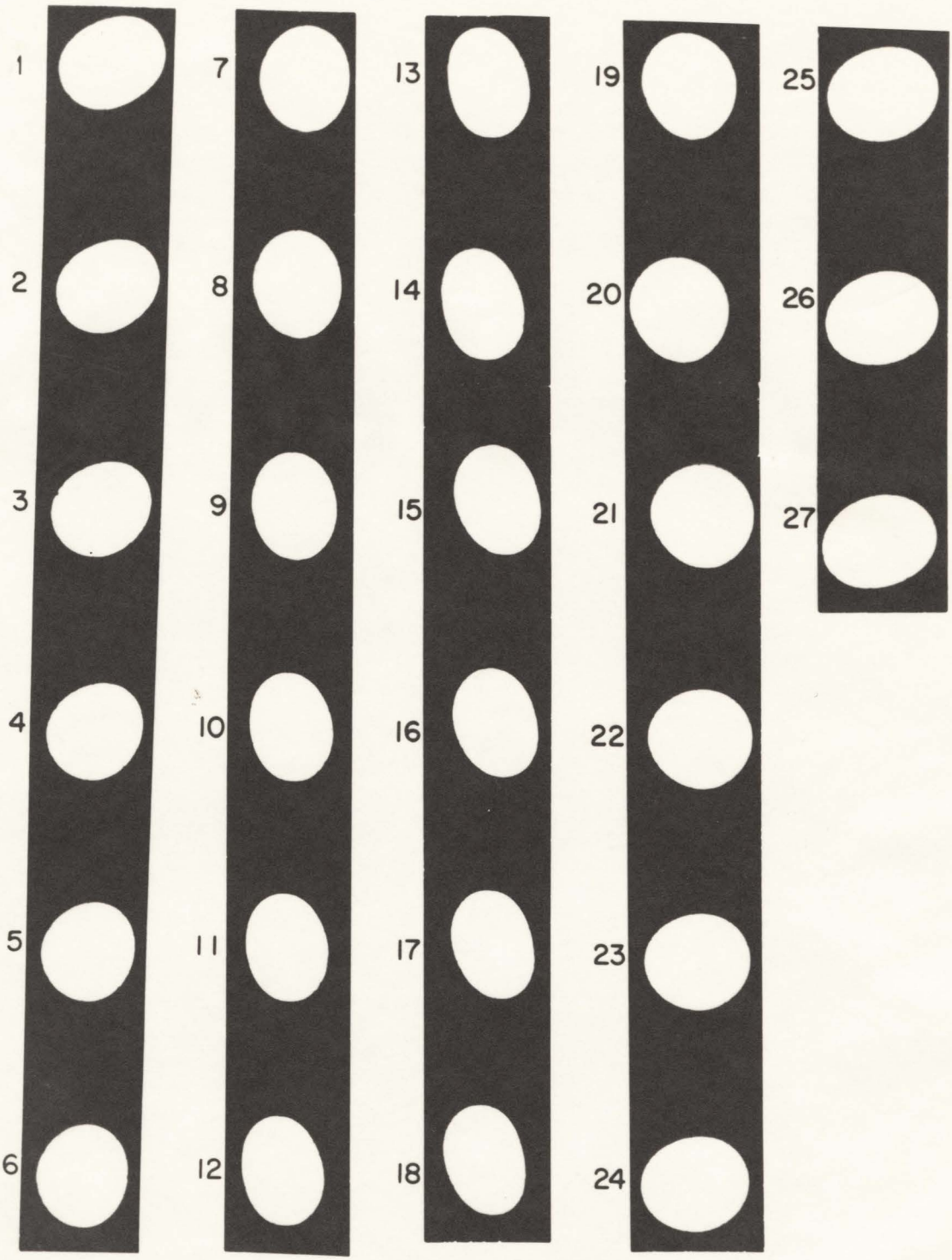

FIGURE 13. MOTION OF A DROPLET ABOUT AN EXTREMUM POSITION -(FRAME 13). TAKEN EVERY SECOND FRAME FROM FILM AT 3000 F.P.S.

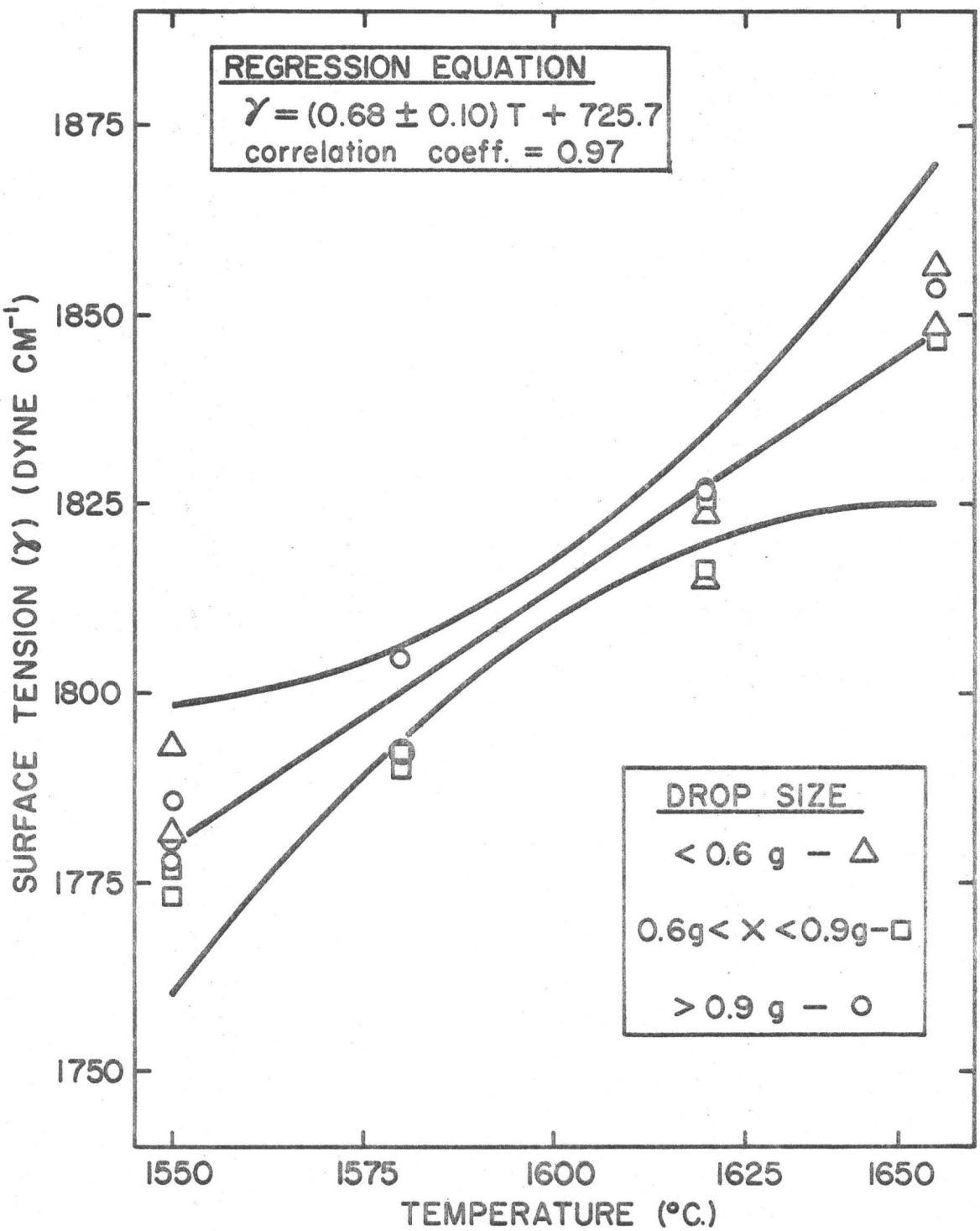

FIGURE 14. SURFACE TENSION OF IRON VS. TEMPERATURE WITH 95% CONFIDENCE INTERVALS.

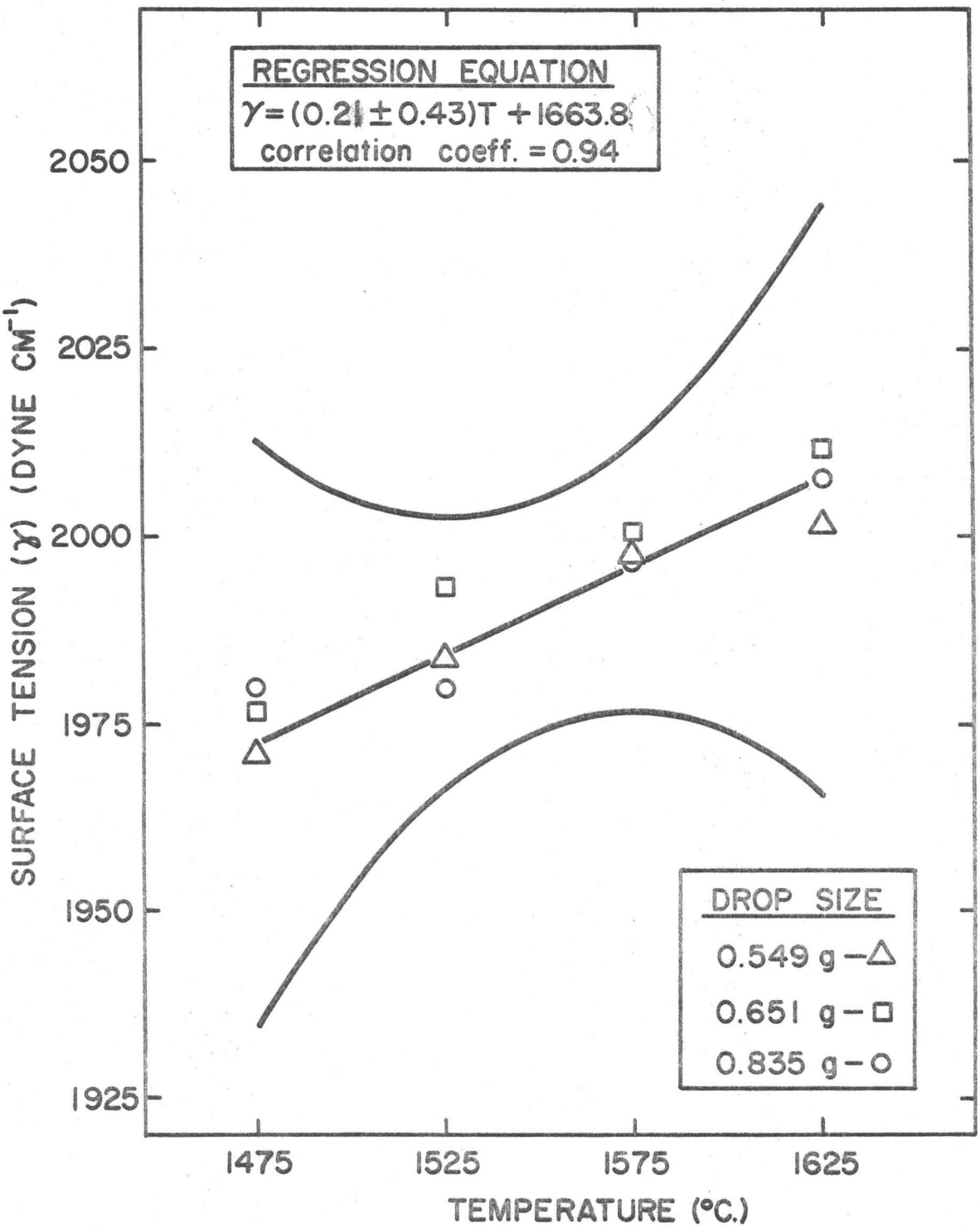

FIGURE 15. SURFACE TENSION OF NICKEL VS. TEMPERATURE WITH 95 % CONFIDENCE INTERVALS.

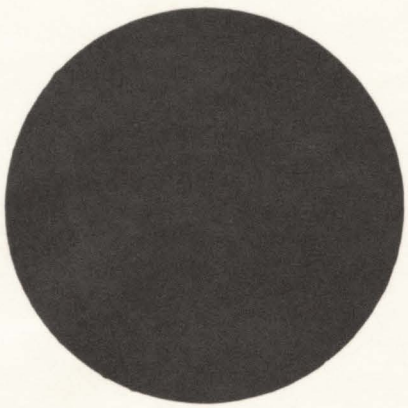

0.250" DIAMETER
BALL BEARING

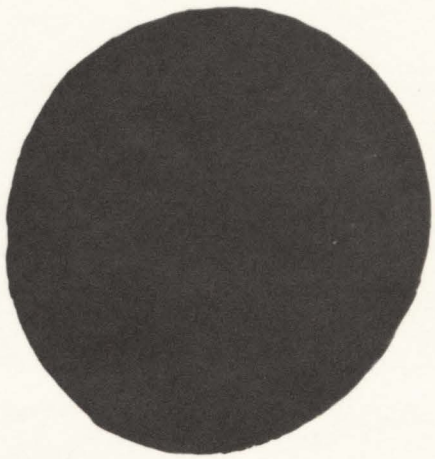

0.58 GRAMS

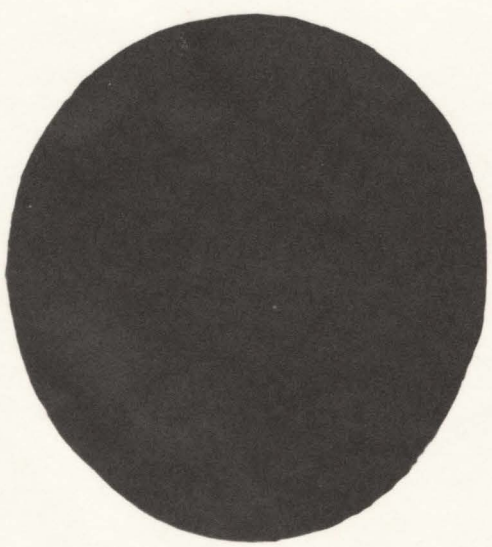

0.72 GRAMS

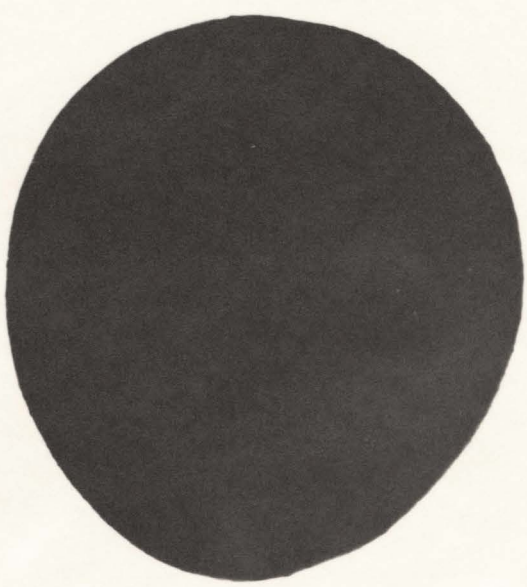

0.99 GRAMS

FIGURE 16. DROP SHAPE CHANGES WITH SIZE.
PHOTOS OF FROZEN IRON DROPS (13X)

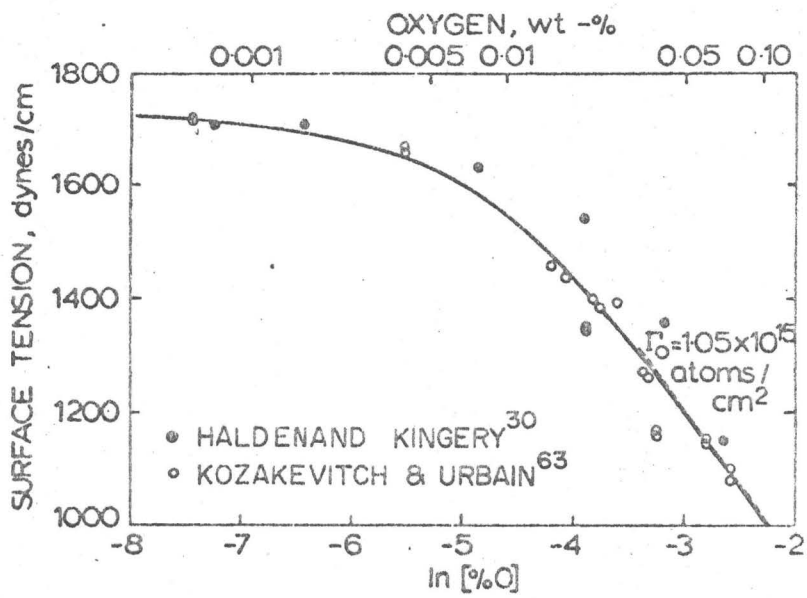

FIGURE 17. SURFACE TENSION OF LIQUID IRON-OXYGEN ALLOYS AT 1550 °C.[61]

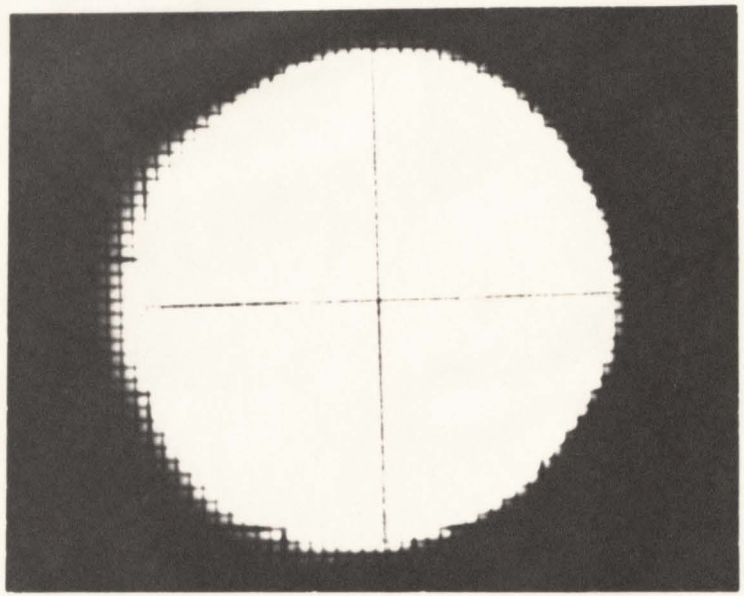

FIGURE 18(a)

EQUILIBRIUM POSITION-TOP VIEW

DIAMETERS -67, 68 mm.

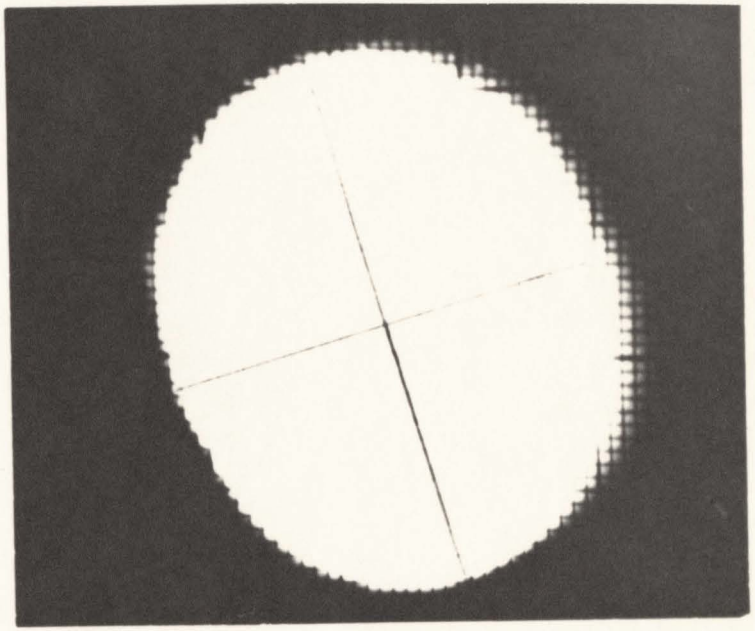

FIGURE 18(b)

EXTREMUM POSITION-TOP VIEW

MAJOR, MINOR AXIS - 74, 59 mm.

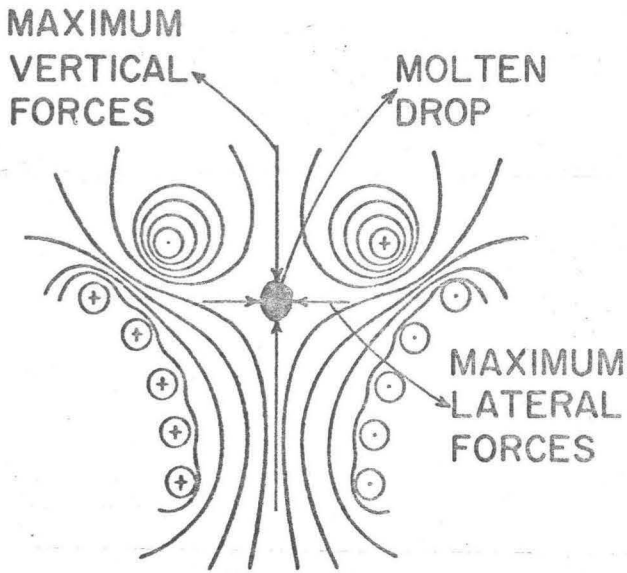

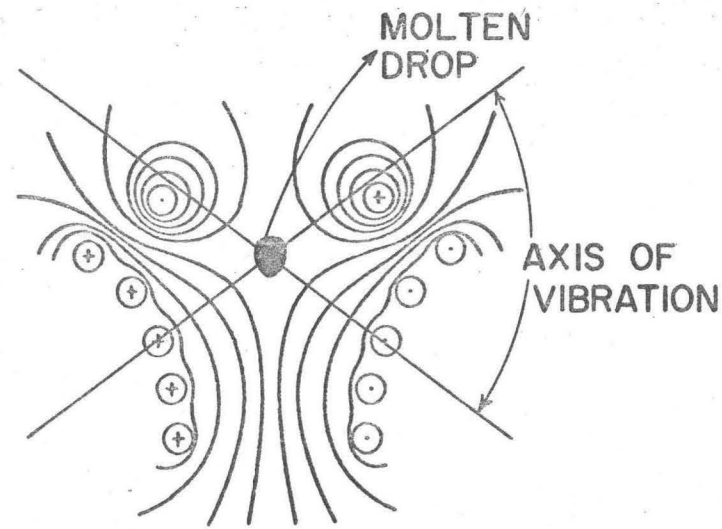

FIGURE 19(a)

FIGURE 19(b)

TYPICAL DISTRIBUTION OF ELECTROMAGNETIC FIELD WITHIN A LEVITATION COIL.[53]
SHOWING (a) THAT MAXIMUM FORCES ARE EXERTED IN THE VERTICAL AND HORIZONTAL PLANES.
(b) THE RESULTANT AXIS OF VIBRATION DUE TO (a).